

إلى قارئ هذا الكتاب ، تحية طيبة وبعد ...

لقد أصبحنا نعيش في عالم يعج بالأبحاث والكتب والمعلومات، وأصبح العلم معياراً حقيقياً لتفاضل الأمم والدول والمؤسسات والأشخاص على حدٍ سواء، وقد أمسى بدوره حلاً شبيه وحيداً لأكثر مشاكل العالم حدة وخطورة، فالبيئة تبحث عن حلول، وصحة الإنسان تبحث عن حلول، والموارد التي تشكل حاجة أساسية للإنسان تبحث عن حلول كذلك، والطاقة والغذاء والماء جميعها تحديات يقف العلم في وجهها الآن ويحاول أن يجد الحلول لها. فأين نحن من هذا العلم؟ وأين هو منا؟

نسعى في موقع عالم الإلكترونيات www.4electron.com لأن نوفر بين أيدي كل من حمل على عاتقه مسيرة درب تملؤه التحديات ما نستطيع من أدوات تساعد في هذا الدرب، من مواضيع علمية، ومراجع أجنبية بأحدث إصداراتها، وساحات لتبادل الآراء والأفكار العلمية والمرتبطة بحياتنا الهندسية، وشروح لأهم برمجيات الحاسب التي تتداخل مع تطبيقات الحياة الأكاديمية والعملية، ولكننا نتوقع في نفس الوقت أن نجد بين الطلاب والمهندسين والباحثين من يسعى مثلنا لتحقيق النفع والفائدة للجميع، ويحلم أن يكون عضواً في مجتمع يساهم بتحقيق بيئة خصبة للمواهب والإبداعات والتألق، فهل تحلم بذلك؟

حاول أن تساهم بفكرة، بومضة من خواطر تفكيرك العلمي، بفائدة رأيتها في إحدى المواضيع العلمية، بجانب مضيء لمحتة خلف ثنانيا مفهوم هندسي ما. تأكد بأنك ستلتمس الفائدة في كل خطوة تخطوها، وترى غيرك يخطوها معك ...

أخي القارئ، نرجو أن يكون هذا الكتاب مقدمة لمشاركتك في عالمنا العلمي التعاوني، وسيكون موقعكم عالم الإلكترونيات www.4electron.com بكل الإمكانيات المتوفرة لديه جاهزاً على الدوام لأن يحقق البيئة والواقع الذي يبحث عنه كل باحث أو طالب في علوم الهندسة، ويسعى فيه للإفادة كل ساعة ، فأهلاً وسهلاً بكم .

مع تحيات إدارة الموقع وفريق عمله



www.4electron.com

Topics in Modern Quantum Optics

Lectures presented at *The 17th Symposium on Theoretical Physics - APPLIED FIELD THEORY*, Seoul National University, Seoul, Korea, 1998.

Bo-Sture Skagerstam¹

Department of Physics, The Norwegian University of Science and Technology, N-7491 Trondheim, Norway

Abstract

Recent experimental developments in electronic and optical technology have made it possible to experimentally realize in space and time well localized *single photon* quantum-mechanical states. In these lectures we will first remind ourselves about some basic quantum mechanics and then discuss in what sense quantum-mechanical single-photon interference has been observed experimentally. A relativistic quantum-mechanical description of single-photon states will then be outlined. Within such a single-photon scheme a derivation of the Berry-phase for photons will be given. In the second set of lectures we will discuss the highly idealized system of a single two-level atom interacting with a single-mode of the second quantized electro-magnetic field as e.g. realized in terms of the micromaser system. This system possesses a variety of dynamical phase transitions parameterized by the flux of atoms and the time-of-flight of the atom within the cavity as well as other parameters of the system. These phases may be revealed to an observer outside the cavity using the long-time correlation length in the atomic beam. It is explained that some of the phase transitions are not reflected in the average excitation level of the outgoing atom, which is one of the commonly used observable. The correlation length is directly related to the leading eigenvalue of a certain probability conserving time-evolution operator, which one can study in order to elucidate the phase structure. It is found that as a function of the time-of-flight the transition from the thermal to the maser phase is characterized by a sharp peak in the correlation length. For longer times-of-flight there is a transition to a phase where the correlation length grows exponentially with the atomic flux. Finally, we present a detailed numerical and analytical treatment of the different phases and discuss the physics behind them in terms of the physical parameters at hand.

¹email: boskag@phys.ntnu.no. Research supported in part by the Research Council of Norway.

Contents

1	Introduction	1
2	Basic Quantum Mechanics	1
2.1	Coherent States	2
2.2	Semi-Coherent or Displaced Coherent States	4
3	Photon-Detection Theory	6
3.1	Quantum Interference of Single Photons	7
3.2	Applications in High-Energy Physics	8
4	Relativistic Quantum Mechanics of Single Photons	8
4.1	Position Operators for Massless Particles	10
4.2	Wess-Zumino Actions and Topological Spin	14
4.3	The Berry Phase for Single Photons	18
4.4	Localization of Single-Photon States	20
4.5	Various Comments	22
5	Resonant Cavities and the Micromaser System	24
6	Basic Micromaser Theory	25
6.1	The Jaynes–Cummings Model	26
6.2	Mixed States	29
6.3	The Lossless Cavity	34
6.4	The Dissipative Cavity	35
6.5	The Discrete Master Equation	35
7	Statistical Correlations	37
7.1	Atomic Beam Observables	37
7.2	Cavity Observables	39
7.3	Monte Carlo Determination of Correlation Lengths	41
7.4	Numerical Calculation of Correlation Lengths	42
8	Analytic Preliminaries	45
8.1	Continuous Master Equation	45
8.2	Relation to the Discrete Case	47
8.3	The Eigenvalue Problem	47
8.4	Effective Potential	50
8.5	Semicontinuous Formulation	50
8.6	Extrema of the Continuous Potential	52
9	The Phase Structure of the Micromaser System	55
9.1	Empty Cavity	55
9.2	Thermal Phase: $0 \leq \theta < 1$	56
9.3	First Critical Point: $\theta = 1$	57
9.4	Maser Phase: $1 < \theta < \theta_1 \simeq 4.603$	58
9.5	Mean Field Calculation	60

9.6	The First Critical Phase: $4.603 \simeq \theta_1 < \theta < \theta_2 \simeq 7.790$	62
10	Effects of Velocity Fluctuations	67
10.1	Revivals and Prerevivals	68
10.2	Phase Diagram	70
11	Finite-Flux Effects	72
11.1	Trapping States	72
11.2	Thermal Cavity Revivals	73
12	Conclusions	75
13	Acknowledgment	77
A	Jaynes–Cummings With Damping	78
B	Sum Rule for the Correlation Lengths	80
C	Damping Matrix	82

1 Introduction

“Truth and clarity are complementary.”

N. Bohr

In the first part of these lectures we will focus our attention on some aspects of the notion of a photon in modern quantum optics and a relativistic description of single, localized, photons. In the second part we will discuss in great detail the “standard model” of quantum optics, i.e. the Jaynes-Cummings model describing the interaction of a two-mode system with a single mode of the second-quantized electro-magnetic field and its realization in resonant cavities in terms of in particular the micro-maser system. Most of the material presented in these lectures has appeared in one form or another elsewhere. Material for the first set of lectures can be found in Refs.[1, 2] and for the second part of the lectures we refer to Refs.[3, 4].

The lectures are organized as follows. In Section 2 we discuss some basic quantum mechanics and the notion of coherent and semi-coherent states. Elements from the photon-detection theory of Glauber is discussed in Section 3 as well as the experimental verification of quantum-mechanical single-photon interference. Some applications of the ideas of photon-detection theory in high-energy physics are also briefly mentioned. In Section 4 we outline a relativistic and quantum-mechanical theory of single photons. The Berry phase for single photons is then derived within such a quantum-mechanical scheme. We also discuss properties of single-photon wave-packets which by construction have positive energy. In Section 6 we present the standard theoretical framework for the micromaser and introduce the notion of a correlation length in the outgoing atomic beam as was first introduced in Refs.[3, 4]. A general discussion of long-time correlations is given in Section 7, where we also show how one can determine the correlation length numerically. Before entering the analytic investigation of the phase structure we introduce some useful concepts in Section 8 and discuss the eigenvalue problem for the correlation length. In Section 9 details of the different phases are analyzed. In Section 10 we discuss effects related to the finite spread in atomic velocities. The phase boundaries are defined in the limit of an infinite flux of atoms, but there are several interesting effects related to finite fluxes as well. We discuss these issues in Section 11. Final remarks and a summary is given in Section 12.

2 Basic Quantum Mechanics

*“Quantum mechanics, that mysterious, confusing
discipline, which none of us really understands,
but which we know how to use”*

M. Gell-Mann

Quantum mechanics, we believe, is the fundamental framework for the description of all known natural physical phenomena. Still we are, however, often very

often puzzled about the role of concepts from the domain of classical physics within the quantum-mechanical language. The interpretation of the theoretical framework of quantum mechanics is, of course, directly connected to the “classical picture” of physical phenomena. We often talk about quantization of the *classical observables* in particular so with regard to classical dynamical systems in the Hamiltonian formulation as has so beautifully been discussed by Dirac [5] and others (see e.g. Ref.[6]).

2.1 Coherent States

The concept of coherent states is very useful in trying to orient the inquiring mind in this jungle of conceptually difficult issues when connecting classical pictures of physical phenomena with the fundamental notion of quantum-mechanical probability-amplitudes and probabilities. We will not try to make a general enough definition of the concept of coherent states (for such an attempt see e.g. the introduction of Ref.[7]). There are, however, many excellent text-books [8, 9, 10], recent reviews [11] and other expositions of the subject [7] to which we will refer to for details and/or other aspects of the subject under consideration. To our knowledge, the modern notion of coherent states actually goes back to the pioneering work by Lee, Low and Pines in 1953 [12] on a quantum-mechanical variational principle. These authors studied electrons in low-lying conduction bands. This is a strong-coupling problem due to interactions with the longitudinal optical modes of lattice vibrations and in Ref.[12] a variational calculation was performed using coherent states. The concept of coherent states as we use in the context of quantum optics goes back Klauder [13], Glauber [14] and Sudarshan [15]. We will refer to these states as Glauber-Klauder coherent states.

As is well-known, coherent states appear in a very natural way when considering the classical limit or the infrared properties of quantum field theories like quantum electrodynamics (QED)[16]-[21] or in analysis of the infrared properties of quantum gravity [22, 23]. In the conventional and extremely successful application of perturbative quantum field theory in the description of elementary processes in Nature when gravitons are not taken into account, the number-operator Fock-space representation is the natural Hilbert space. The realization of the canonical commutation relations of the quantum fields leads, of course, in general to mathematical difficulties when interactions are taken into account. Over the years we have, however, in practice learned how to deal with some of these mathematical difficulties.

In presenting the theory of the second-quantized electro-magnetic field on an elementary level, it is tempting to exhibit an apparent “paradox” of Erhenfest theorem in quantum mechanics and the existence of the classical Maxwell’s equations: any average of the electro-magnetic field-strengths in the physically natural number-operator basis is zero and hence these averages will not obey the classical equations of motion. The solution of this apparent paradox is, as is by now well established: the classical fields in Maxwell’s equations corresponds to *quantum states* with an

arbitrary number of photons. In classical physics, we may neglect the quantum structure of the charged sources. Let $\mathbf{j}(\mathbf{x}, t)$ be such a classical current, like the classical current in a coil, and $\mathbf{A}(\mathbf{x}, t)$ the second-quantized radiation field (in e.g. the radiation gauge). In the long wave-length limit of the radiation field a classical current should be an appropriate approximation at least for theories like quantum electrodynamics. The interaction Hamiltonian $\mathcal{H}_I(t)$ then takes the form

$$\mathcal{H}_I(t) = - \int d^3x \mathbf{j}(\mathbf{x}, t) \cdot \mathbf{A}(\mathbf{x}, t) \quad , \quad (2.1)$$

and the quantum states in the interaction picture, $|t\rangle_I$, obey the time-dependent Schrödinger equation, i.e. using natural units ($\hbar = c = 1$)

$$i \frac{d}{dt} |t\rangle_I = \mathcal{H}_I(t) |t\rangle_I \quad . \quad (2.2)$$

For reasons of simplicity, we will consider only one specific mode of the electromagnetic field described in terms of a canonical creation operator (a^*) and an annihilation operator (a). The general case then easily follows by considering a system of such independent modes (see e.g. Ref.[24]). It is therefore sufficient to consider the following single-mode interaction Hamiltonian:

$$\mathcal{H}_I(t) = -f(t) \left(a \exp[-i\omega t] + a^* \exp[i\omega t] \right) \quad , \quad (2.3)$$

where the real-valued function $f(t)$ describes the in general time-dependent classical current. The “free” part \mathcal{H}_0 of the total Hamiltonian in natural units then is

$$\mathcal{H}_0 = \omega(a^*a + 1/2) \quad . \quad (2.4)$$

In terms of canonical “momentum” (p) and “position” (x) field-quadrature degrees of freedom defined by

$$\begin{aligned} a &= \sqrt{\frac{\omega}{2}} x + i \frac{1}{\sqrt{2\omega}} p \quad , \\ a^* &= \sqrt{\frac{\omega}{2}} x - i \frac{1}{\sqrt{2\omega}} p \quad , \end{aligned} \quad (2.5)$$

we therefore see that we are formally considering an harmonic oscillator in the presence of a time-dependent external force. The explicit solution to Eq.(2.2) is easily found. We can write

$$|t\rangle_I = T \exp \left(-i \int_{t_0}^t \mathcal{H}_I(t') dt' \right) |t_0\rangle_I = \exp[i\phi(t)] \exp[iA(t)] |t_0\rangle_I \quad , \quad (2.6)$$

where the non-trivial time-ordering procedure is expressed in terms of

$$A(t) = - \int_{t_0}^t dt' \mathcal{H}_I(t') \quad , \quad (2.7)$$

and the c-number phase $\phi(t)$ as given by

$$\phi(t) = \frac{i}{2} \int_{t_0}^t dt' [A(t'), \mathcal{H}_I(t')] \quad . \quad (2.8)$$

The form of this solution is valid for *any* interaction Hamiltonian which is at most linear in creation and annihilation operators (see e.g. Ref.[25]). We now define the unitary operator

$$U(z) = \exp[za^* - z^*a] \quad . \quad (2.9)$$

Canonical coherent states $|z; \phi_0\rangle$, depending on the (complex) parameter z and the fiducial normalized state number-operator eigenstate $|\phi_0\rangle$, are defined by

$$|z; \phi_0\rangle = U(z)|\phi_0\rangle \quad , \quad (2.10)$$

such that

$$1 = \int \frac{d^2z}{\pi} |z\rangle\langle z| = \int \frac{d^2z}{\pi} |z; \phi_0\rangle\langle z; \phi_0| \quad . \quad (2.11)$$

Here the canonical coherent-state $|z\rangle$ corresponds to the choice $|z; 0\rangle$, i.e. to an initial Fock vacuum state. We then see that, up to a phase, the solution Eq.(2.6) is a canonical coherent-state if the initial state is the vacuum state. It can be verified that the expectation value of the second-quantized electro-magnetic field in the state $|t\rangle_I$ obeys the classical Maxwell equations of motion for *any* fiducial Fock-space state $|t_0\rangle_I = |\phi_0\rangle$. Therefore the corresponding complex, and in general time-dependent, parameters z constitute an explicit mapping between classical phase-space dynamical variables and a pure quantum-mechanical state. In more general terms, quantum-mechanical models can actually be constructed which demonstrates that by the process of phase-decoherence one is naturally lead to such a correspondence between points in classical phase-space and coherent states (see e.g. Ref.[26]).

2.2 Semi-Coherent or Displaced Coherent States

If the fiducial state $|\phi_0\rangle$ is a number operator eigenstate $|m\rangle$, where m is an integer, the corresponding coherent-state $|z; m\rangle$ have recently been discussed in detail in the literature and is referred to as a *semi-coherent state* [27, 28] or a *displaced number-operator state* [29]. For some recent considerations see e.g. Refs.[30, 31] and in the context of resonant micro-cavities see Refs.[32, 33]. We will now argue that a classical current can be used to amplify the information contained in the pure fiducial vector $|\phi_0\rangle$. In Section 6 we will give further discussions on this topic. For a given initial fiducial Fock-state vector $|m\rangle$, it is a rather trivial exercise to calculate the probability $P(n)$ to find n photons in the final state, i.e. (see e.g. Ref.[34])

$$P(n) = \lim_{t \rightarrow \infty} |\langle n|t\rangle_I|^2 \quad , \quad (2.12)$$

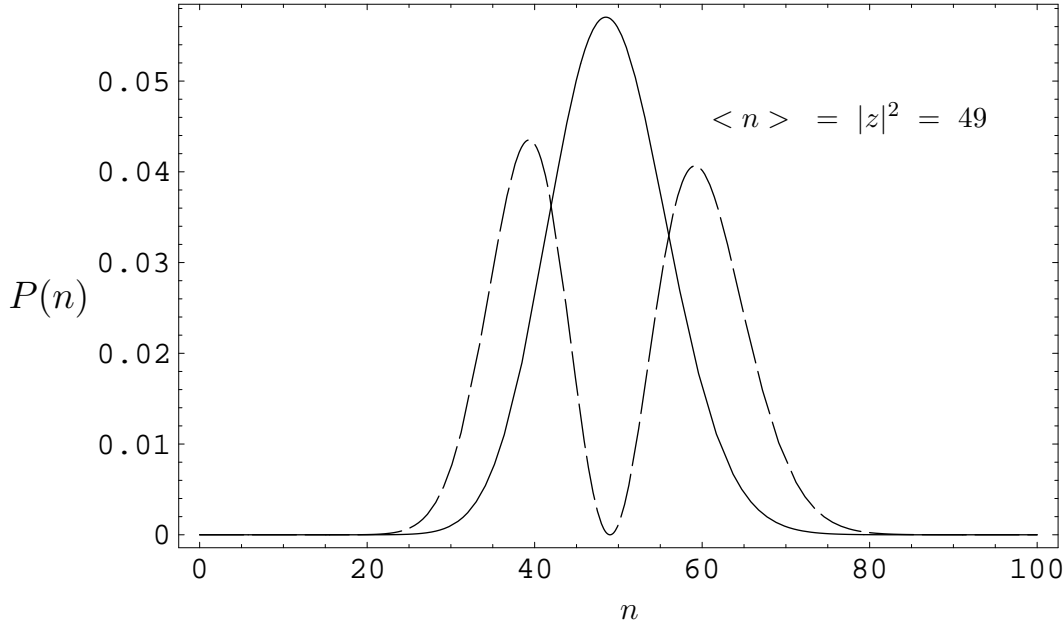


Figure 1: Photon number distribution of coherent (with an initial vacuum state $|t = 0\rangle = |0\rangle$ - solid curve) and semi-coherent states (with an initial one-photon state $|t = 0\rangle = |1\rangle$ - dashed curve).

which then depends on the Fourier transform $z = f(\omega) = \int_{-\infty}^{\infty} dt f(t) \exp(-i\omega t)$. In Figure 1, the solid curve gives $P(n)$ for $|\phi_0\rangle = |0\rangle$, where we, for the purpose of illustration, have chosen the Fourier transform of $f(t)$ such that the mean value of the Poisson number-distribution of photons is $|f(\omega)|^2 = 49$. The distribution $P(n)$ then characterizes a *classical state* of the radiation field. The dashed curve in Figure 1 corresponds to $|\phi_0\rangle = |1\rangle$, and we observe the characteristic oscillations. It may be a slight surprise that the minor change of the initial state by *one* photon completely changes the final distribution $P(n)$ of photons, i.e. *one* photon among a large number of photons (in the present case 49) makes a difference. If $|\phi_0\rangle = |m\rangle$ one finds in the same way that the $P(n)$ -distribution will have m zeros. If we sum the distribution $P(n)$ over the initial-state quantum number m we, of course, obtain unity as a consequence of the unitarity of the time-evolution. Unitarity is actually the simple quantum-mechanical reason why oscillations in $P(n)$ must be present. We also observe that two canonical coherent states $|t\rangle_I$ are orthogonal if the initial-state fiducial vectors are orthogonal. It is in the sense of oscillations in $P(n)$, as described above, that a classical current can amplify a quantum-mechanical pure state $|\phi_0\rangle$ to a coherent-state with a large number of coherent photons. This effect is, of course, due to the boson character of photons.

It has, furthermore, been shown that one-photon states localized in space and

time can be generated in the laboratory (see e.g. [35]-[45]). It would be interesting if such a state could be amplified by means of a classical source in resonance with the typical frequency of the photon. It has been argued by Knight et al. [29] that an imperfect photon-detection by allowing for dissipation of field-energy does not necessarily destroy the appearance of the oscillations in the probability distribution $P(n)$ of photons in the displaced number-operator eigenstates. It would, of course, be an interesting and striking verification of quantum coherence if the oscillations in the $P(n)$ -distribution could be observed experimentally.

3 Photon-Detection Theory

*“If it was so, it might be; And if it were so,
it would be. But as it isn’t, it ain’t.”*

Lewis Carroll

The quantum-mechanical description of optical coherence was developed in a series of beautiful papers by Glauber [14]. Here we will only touch upon some elementary considerations of photo-detection theory. Consider an experimental situation where a beam of particles, in our case a beam of photons, hits an ideal beam-splitter. Two photon-multipliers measures the corresponding intensities at times t and $t + \tau$ of the two beams generated by the beam-splitter. The quantum state describing the detection of one photon at time t and another one at time $t + \tau$ is then of the form $E^+(t + \tau)E^+(t)|i\rangle$, where $|i\rangle$ describes the initial state and where $E^+(t)$ denotes a positive-frequency component of the second-quantized electric field. The quantum-mechanical amplitude for the detection of a final state $|f\rangle$ then is $\langle f|E^+(t + \tau)E^+(t)|i\rangle$. The total detection-probability, obtained by summing over all final states, is then proportional to the *second-order correlation function* $g^{(2)}(\tau)$ given by

$$g^{(2)}(\tau) = \sum_f \frac{|\langle f|E^+(t + \tau)E^+(t)|i\rangle|^2}{(\langle i|E^-(t)E^+(t)|i\rangle)^2} = \frac{\langle i|E^-(t)E^-(t + \tau)E^+(t + \tau)E^+(t)|i\rangle}{(\langle i|E^-(t)E^+(t)|i\rangle)^2} . \quad (3.1)$$

Here the normalization factor is just proportional to the intensity of the source, i.e. $\sum_f |\langle f|E^+(t)|i\rangle|^2 = (\langle i|E^-(t)E^+(t)|i\rangle)^2$. A classical treatment of the radiation field would then lead to

$$g^{(2)}(0) = 1 + \frac{1}{\langle I \rangle^2} \int dIP(I)(I - \langle I \rangle)^2 , \quad (3.2)$$

where I is the intensity of the radiation field and $P(I)$ is a quasi-probability distribution (i.e. not in general an a priori positive definite function). What we call classical coherent light can then be described in terms of Glauber-Klauder coherent states. These states leads to $P(I) = \delta(I - \langle I \rangle)$. As long as $P(I)$ is a positive definite function, there is a complete equivalence between the classical theory of optical coherence

and the quantum field-theoretical description [15]. Incoherent light, as thermal light, leads to a second-order correlation function $g^{(2)}(\tau)$ which is larger than one. This feature is referred to as *photon bunching* (see e.g. Ref.[46]). *Quantum-mechanical light* is, however, described by a second-order correlation function which may be smaller than one. If the beam consists of N photons, all with the same quantum numbers, we easily find that

$$g^{(2)}(0) = 1 - \frac{1}{N} < 1 \quad . \quad (3.3)$$

Another way to express this form of *photon anti-bunching* is to say that in this case the quasi-probability $P(I)$ distribution cannot be positive, i.e. it cannot be interpreted as a probability (for an account of the early history of anti-bunching see e.g. Ref.[47, 48]).

3.1 Quantum Interference of Single Photons

A one-photon beam must, in particular, have the property that $g^{(2)}(0) = 0$, which simply corresponds to maximal photon anti-bunching. One would, perhaps, expect that a sufficiently attenuated classical source of radiation, like the light from a pulsed photo-diode or a laser, would exhibit photon maximal anti-bunching in a beam splitter. This sort of reasoning is, in one way or another, explicitly assumed in many of the beautiful tests of “single-photon” interference in quantum mechanics. It has, however, been argued by Aspect and Grangier [49] that this reasoning is *incorrect*. Aspect and Grangier actually measured the second-order correlation function $g^{(2)}(\tau)$ by making use of a beam-splitter and found this to be greater or equal to one even for an attenuation of a classical light source below the one-photon level. The conclusion, we guess, is that the radiation emitted from e.g. a monochromatic laser always behaves in classical manner, i.e. even for such a strongly attenuated source below the one-photon flux limit the corresponding radiation has no non-classical features (under certain circumstances one can, of course, arrange for such an attenuated light source with a very low probability for more than one-photon at a time (see e.g. Refs.[50, 51]) but, nevertheless, the source can still be described in terms of classical electro-magnetic fields). As already mentioned in the introduction, it is, however, possible to generate photon beams which exhibit complete photon anti-bunching. This has first been shown in the beautiful experimental work by Aspect and Grangier [49] and by Mandel and collaborators [35]. Roger, Grangier and Aspect in their beautiful study also verified that the one-photon states obtained exhibit one-photon interference in accordance with the rules of quantum mechanics as we, of course, expect. In the experiment by e.g. the Rochester group [35] beams of one-photon states, localized in *both* space and time, were generated. A quantum-mechanical description of such relativistic one-photon states will now be the subject for Chapter 4.

3.2 Applications in High-Energy Physics

Many of the concepts from photon-detection theory has applications in the context of high-energy physics. The use of photon-detection theory as mentioned in Section 3 goes historically back to Hanbury-Brown and Twiss [52] in which case the second-order correlation function was used in order to extract information on the size of distant stars. The same idea has been applied in high-energy physics. The two-particle correlation function $C_2(\mathbf{p}_1, \mathbf{p}_2)$, where \mathbf{p}_1 and \mathbf{p}_2 are three-momenta of the (boson) particles considered, is in this case given by the ratio of two-particle probabilities $P(\mathbf{p}_1, \mathbf{p}_2)$ and the product of the one-particle probabilities $P(\mathbf{p}_1)$ and $P(\mathbf{p}_2)$, i.e. $C_2(\mathbf{p}_1, \mathbf{p}_2) = P(\mathbf{p}_1, \mathbf{p}_2)/P(\mathbf{p}_1)P(\mathbf{p}_2)$. For a source of pions where any phase-coherence is averaged out, corresponding to what is called a chaotic source, there is an enhanced emission probability as compared to a non-chaotic source over a range of momenta such that $R|\mathbf{p}_1 - \mathbf{p}_2| \simeq 1$, where R represents an average of the size of the pion source. For pions formed in a coherent-state one finds that $C_2(\mathbf{p}_1, \mathbf{p}_2) = 1$. The width of the experimentally determined correlation function of pions with different momenta, i.e. $C_2(\mathbf{p}_1, \mathbf{p}_2)$, can therefore give information about the size of the pion-source. A lot of experimental data has been compiled over the years and the subject has recently been discussed in detail by e.g. Boal et al. [53]. A recent experimental analysis has been considered by the OPAL collaboration in the case of like-sign charged track pairs at a center-off-mass energy close to the Z^0 peak. 146624 multi-hadronic Z^0 candidates were used leading to an estimate of the radius of the pion source to be close to one fermi [54]. Similarly the NA44 experiment at CERN have studied $\pi^+\pi^+$ -correlations from 227000 reconstructed pairs in $S + Pb$ collisions at 200 GeV/c per nucleon leading to a space-time averaged pion-source radius of the order of a few fermi [55]. The impressive experimental data and its interpretation has been confronted by simulations using relativistic molecular dynamics [56]. In heavy-ion physics the measurement of the second-order correlation function of pions is of special interest since it can give us information about the spatial extent of the quark-gluon plasma phase, if it is formed. It has been suggested that one may make use of photons instead of pions when studying possible signals from the quark-gluon plasma. In particular, it has been suggested [57] that the correlation of high transverse-momentum photons is sensitive to the details of the space-time evolution of the high density quark-gluon plasma.

4 Relativistic Quantum Mechanics of Single Photons

“Because the word photon is used in so many ways, it is a source of much confusion. The reader always has to figure out what the writer has in mind.”

P. Meystre and M. Sargent III

The concept of a photon has a long and intriguing history in physics. It is, e.g., in this context interesting to notice a remark by A. Einstein; “*All these fifty years of pondering have not brought me any closer to answering the question: What are light quanta?*” [58]. Linguistic considerations do not appear to enlighten our conceptual understanding of this fundamental concept either [59]. Recently, it has even been suggested that one should not make use of the concept of a photon at all [60]. As we have remarked above, *single* photons can, however, be generated in the laboratory and the wave-function of single photons can actually be measured [61]. The decay of a *single* photon quantum-mechanical state in a resonant cavity has also recently been studied experimentally [62].

A related concept is that of localization of relativistic elementary systems, which also has a long and intriguing history (see e.g. Refs. [63]-[69]). Observations of physical phenomena takes place in space and time. The notion of *localizability* of particles, elementary or not, then refers to the empirical fact that particles, at a given instance of time, appear to be localizable in the physical space.

In the realm of non-relativistic quantum mechanics the concept of localizability of particles is built into the theory at a very fundamental level and is expressed in terms of the fundamental canonical commutation relation between a position operator and the corresponding generator of translations, i.e. the canonical momentum of a particle. In relativistic theories the concept of localizability of physical systems is deeply connected to our notion of space-time, the arena of physical phenomena, as a 4-dimensional continuum. In the context of the classical theory of general relativity the localization of light rays in space-time is e.g. a fundamental ingredient. In fact, it has been argued [70] that the Riemannian metric is basically determined by basic properties of light propagation.

In a fundamental paper by Newton and Wigner [63] it was argued that in the context of relativistic quantum mechanics a notion of point-like localization of a single particle can be, uniquely, determined by kinematics. Wightman [64] extended this notion to localization to finite domains of space and it was, rigorously, shown that massive particles are always localizable if they are elementary, i.e. if they are described in terms of irreducible representations of the Poincaré group [71]. Massless elementary systems with non-zero helicity, like a gluon, graviton, neutrino or a photon, are *not* localizable in the sense of Wightman. The axioms used by Wightman can, of course, be weakened. It was actually shown by Jauch, Piron and Amrein [65] that in such a sense the photon is *weakly localizable*. As will be argued below, the notion of weak localizability essentially corresponds to allowing for non-commuting observables in order to characterize the localization of massless and spinning particles in general.

Localization of relativistic particles, at a fixed time, as alluded to above, has been shown to be incompatible with a natural notion of (Einstein-) causality [72]. If relativistic elementary system has an exponentially small tail outside a finite domain of localization at $t = 0$, then, according to the hypothesis of a weaker form of causality, this should remain true at later times, i.e. the tail should only be

shifted further out to infinity. As was shown by Hegerfeldt [73], even this notion of causality is incompatible with the notion of a positive and bounded observable whose expectation value gives the probability to find a particle inside a finite domain of space at a given instant of time. It has been argued that the use of local observables in the context of relativistic quantum field theories does not lead to such apparent difficulties with Einstein causality [74].

We will now reconsider some of these questions related to the concept of localizability in terms of a quantum mechanical description of a massless particle with given helicity λ [75, 76, 77] (for a related construction see Ref.[78]). The one-particle states we are considering are, of course, nothing else than the positive energy one-particle states of quantum field theory. We simply endow such states with a set of appropriately defined quantum-mechanical observables and, in terms of these, we construct the generators of the Poincaré group. We will then show how one can extend this description to include both positive and negative helicities, i.e. including reducible representations of the Poincaré group. We are then in the position to e.g. study the motion of a linearly polarized photon in the framework of relativistic quantum mechanics and the appearance of non-trivial phases of wave-functions.

4.1 Position Operators for Massless Particles

It is easy to show that the components of the position operators for a massless particle must be non-commuting¹ if the helicity $\lambda \neq 0$. If J_k are the generators of rotations and p_k the diagonal momentum operators, $k = 1, 2, 3$, then we should have $\mathbf{J} \cdot \mathbf{p} = \pm\lambda$ for a massless particle like the photon (see e.g. Ref.[79]). Here $\mathbf{J} = (J_1, J_2, J_3)$ and $\mathbf{p} = (p_1, p_2, p_3)$. In terms of natural units ($\hbar = c = 1$) we then have that

$$[J_k, p_l] = i\epsilon_{klm}p_m \quad . \quad (4.1)$$

If a canonical position operator \mathbf{x} exists with components x_k such that

$$[x_k, x_l] = 0 \quad , \quad (4.2)$$

$$[x_k, p_l] = i\delta_{kl} \quad , \quad (4.3)$$

$$[J_k, x_l] = i\epsilon_{klm}x_m \quad , \quad (4.4)$$

then we can define generators of orbital angular momentum in the conventional way, i.e.

$$L_k = \epsilon_{klm}x_l p_m \quad . \quad (4.5)$$

Generators of spin are then defined by

$$S_k = J_k - L_k \quad . \quad (4.6)$$

They fulfill the correct algebra, i.e.

$$[S_k, S_l] = i\epsilon_{klm}S_m \quad , \quad (4.7)$$

¹This argument has, as far as we know, first been suggested by N. Mukunda.

and they, furthermore, commute with \mathbf{x} and \mathbf{p} . Then, however, the spectrum of $\mathbf{S} \cdot \mathbf{p}$ is $\lambda, \lambda - 1, \dots, -\lambda$, which contradicts the requirement $\mathbf{J} \cdot \mathbf{p} = \pm\lambda$ since, by construction, $\mathbf{J} \cdot \mathbf{p} = \mathbf{S} \cdot \mathbf{p}$.

As has been discussed in detail in the literature, the non-zero commutator of the components of the position operator for a massless particle primarily emerges due to the non-trivial topology of the momentum space [75, 76, 77]. The irreducible representations of the Poincaré group for massless particles [71] can be constructed from a knowledge of the little group G of a light-like momentum four-vector $p = (p^0, \mathbf{p})$. This group is the Euclidean group $E(2)$. Physically, we are interested in possible finite-dimensional representations of the covering of this little group. We therefore restrict ourselves to the compact subgroup, i.e. we represent the $E(2)$ -translations trivially and consider $G = SO(2) = U(1)$. Since the origin in the momentum space is excluded for massless particles one is therefore led to consider appropriate G -bundles over S^2 since the energy of the particle can be kept fixed. Such G -bundles are classified by mappings from the equator to G , i.e. by the first homotopy group $\Pi_1(U(1)) = \mathbf{Z}$, where it turns out that each integer corresponds to twice the helicity of the particle. A massless particle with helicity λ and *sharp momentum* is thus described in terms of a non-trivial line bundle characterized by $\Pi_1(U(1)) = \{2\lambda\}$ [80].

This consideration can easily be extended to higher space-time dimensions [77]. If D is the number of space-time dimensions, the corresponding G -bundles are classified by the homotopy groups $\Pi_{D-3}(Spin(D-2))$. These homotopy groups are in general non-trivial. It is a remarkable fact that the only trivial homotopy groups of this form in higher space-time dimensions correspond to $D = 5$ and $D = 9$ due to the existence of quaternions and the Cayley numbers (see e.g. Ref. [81]). In these space-time dimensions, and for $D = 3$, it then turns that one can explicitly construct canonical *and* commuting position operators for massless particles [77]. The mathematical fact that the spheres S^1 , S^3 and S^7 are parallelizable can then be expressed in terms of the existence of canonical *and* commuting position operators for massless spinning particles in $D = 3$, $D = 5$ and $D = 9$ space-time dimensions.

In terms of a canonical momentum p_i and coordinates x_j satisfying the canonical commutation relation Eq.(4.3) we can easily derive the commutator of two components of the position operator \mathbf{x} by making use of a simple consistency argument as follows. If the massless particle has a given helicity λ , then the generators of angular momentum is given by:

$$J_k = \epsilon_{klm} x_l p_m + \lambda \frac{p_k}{|\mathbf{p}|} \quad . \quad (4.8)$$

The canonical momentum then transforms as a vector under rotations, i.e.

$$[J_k, p_l] = i\epsilon_{klm} p_m \quad , \quad (4.9)$$

without any condition on the commutator of two components of the position operator \mathbf{x} . The position operator will, however, not transform like a vector unless the

following commutator is postulated

$$i[x_k, x_l] = \lambda \epsilon_{klm} \frac{p_m}{|\mathbf{p}|^3} \quad , \quad (4.10)$$

where we notice that commutator formally corresponds to a point-like Dirac magnetic monopole [82] localized at the origin in momentum space with strength $4\pi\lambda$. The energy p^0 of the massless particle is, of course, given by $\omega = |\mathbf{p}|$. In terms of a singular $U(1)$ connection $\mathcal{A}_l \equiv \mathcal{A}_l(\mathbf{p})$ we can write

$$x_k = i\partial_k - \mathcal{A}_k \quad , \quad (4.11)$$

where $\partial_k = \partial/\partial p_k$ and

$$\partial_k \mathcal{A}_l - \partial_l \mathcal{A}_k = \lambda \epsilon_{klm} \frac{p_m}{|\mathbf{p}|^3} \quad . \quad (4.12)$$

Out of the observables x_k and the energy ω one can easily construct the generators (at time $t = 0$) of Lorentz boosts, i.e.

$$K_m = (x_m \omega + \omega x_m)/2 \quad , \quad (4.13)$$

and verify that J_l and K_m lead to a realization of the Lie algebra of the Lorentz group, i.e.

$$[J_k, J_l] = i\epsilon_{klm} J_m \quad , \quad (4.14)$$

$$[J_k, K_l] = i\epsilon_{klm} K_m \quad , \quad (4.15)$$

$$[K_k, K_l] = -i\epsilon_{klm} J_m \quad . \quad (4.16)$$

The components of the Pauli-Plebanski operator W_μ are given by

$$W^\mu = (W^0, \mathbf{W}) = (\mathbf{J} \cdot \mathbf{p}, \mathbf{J}p^0 + \mathbf{K} \times \mathbf{p}) = \lambda p^\mu \quad , \quad (4.17)$$

i.e. we also obtain an irreducible representation of the Poincaré group. The additional non-zero commutators are

$$[K_k, \omega] = ip_k \quad , \quad (4.18)$$

$$[K_k, p_l] = i\delta_{kl}\omega \quad . \quad (4.19)$$

At $t \equiv x^0(\tau) \neq 0$ the Lorentz boost generators K_m as given by Eq.(4.13) are extended to

$$K_m = (x_m \omega + \omega x_m)/2 - tp_m \quad . \quad (4.20)$$

In the Heisenberg picture, the quantum equation of motion of an observable $\mathcal{O}(t)$ is obtained by using

$$\frac{d\mathcal{O}(t)}{dt} = \frac{\partial \mathcal{O}(t)}{\partial t} + i[H, \mathcal{O}(t)] \quad , \quad (4.21)$$

where the Hamiltonian H is given by the ω . One then finds that all generators of the Poincaré group are conserved as they should. The equation of motion for $\mathbf{x}(t)$ is

$$\frac{d}{dt}\mathbf{x}(t) = \frac{\mathbf{p}}{\omega} \quad , \quad (4.22)$$

which is an expected equation of motion for a massless particle.

The non-commuting components x_k of the position operator \mathbf{x} transform as the components of a vector under spatial rotations. Under Lorentz boost we find in addition that

$$i[K_k, x_l] = \frac{1}{2} \left(x_k \frac{p_l}{\omega} + \frac{p_l}{\omega} x_k \right) - t\delta_{kl} + \lambda\epsilon_{klm} \frac{p_m}{|\mathbf{p}|^2} \quad . \quad (4.23)$$

The first two terms in Eq.(4.23) corresponds to the correct limit for $\lambda = 0$ since the proper-time condition $x^0(\tau) \approx \tau$ is not Lorentz invariant (see e.g. [6], Section 2-9). The last term in Eq.(4.23) is due to the non-zero commutator Eq.(4.10). This anomalous term can be dealt with by introducing an appropriate two-cocycle for finite transformations consisting of translations generated by the position operator \mathbf{x} , rotations generated by \mathbf{J} and Lorentz boost generated by \mathbf{K} . For pure translations this two-cocycle will be explicitly constructed in Section 4.3.

The algebra discussed above can be extended in a rather straightforward manner to incorporate both positive and negative helicities needed in order to describe linearly polarized light. As we now will see this extension corresponds to a replacement of the Dirac monopole at the origin in momentum space with a $SU(2)$ Wu-Yang [83] monopole. The procedure below follows a rather standard method of imbedding the singular $U(1)$ connection \mathcal{A}_l into a *regular* $SU(2)$ connection. Let us specifically consider a massless, spin-one particle. The Hilbert space, \mathcal{H} , of one-particle transverse wave-functions $\phi_\alpha(\mathbf{p})$, $\alpha = 1, 2, 3$ is defined in terms of a scalar product

$$(\phi, \psi) = \int d^3p \phi_\alpha^*(\mathbf{p}) \psi_\alpha(\mathbf{p}) \quad , \quad (4.24)$$

where $\phi_\alpha^*(\mathbf{p})$ denotes the complex conjugated $\phi_\alpha(\mathbf{p})$. In terms of a Wu-Yang connection $\mathcal{A}_k^a \equiv \mathcal{A}_k^a(\mathbf{p})$, i.e.

$$\mathcal{A}_k^a(\mathbf{p}) = \epsilon_{alk} \frac{p_l}{|\mathbf{p}|^2} \quad , \quad (4.25)$$

Eq.(4.11) is extended to

$$x_k = i\partial_k - \mathcal{A}_k^a(\mathbf{p}) S_a \quad , \quad (4.26)$$

where

$$(S_a)_{kl} = -i\epsilon_{akl} \quad (4.27)$$

are the spin-one generators. By means of a singular gauge-transformation the Wu-Yang connection can be transformed into the singular $U(1)$ -connection \mathcal{A}_l times the third component of the spin generators S_3 (see e.g. Ref.[89]). This position operator defined by Eq.(4.26) is compatible with the transversality condition on the

one-particle wave-functions, i.e. $x_k \phi_\alpha(\mathbf{p})$ is transverse. With suitable conditions on the one-particle wave-functions, the position operator \mathbf{x} therefore has a well-defined action on \mathcal{H} . Furthermore,

$$i[x_k, x_l] = \mathcal{F}_{kl}^a S^a = \epsilon_{klm} \frac{p_m}{|\mathbf{p}|^3} \hat{\mathbf{p}} \cdot \mathbf{S} \quad , \quad (4.28)$$

where

$$\mathcal{F}_{kl}^a = \partial_k \mathcal{A}_l^a - \partial_l \mathcal{A}_k^a - \epsilon_{abc} \mathcal{A}_k^b \mathcal{A}_l^c = \epsilon_{klm} \frac{p_m p_a}{|\mathbf{p}|^4} \quad , \quad (4.29)$$

is the non-Abelian $SU(2)$ field strength tensor and $\hat{\mathbf{p}}$ is a unit vector in the direction of the particle momentum \mathbf{p} . The generators of angular momentum are now defined as follows

$$J_k = \epsilon_{klm} x_l p_m + \frac{p_k}{|\mathbf{p}|} \hat{\mathbf{p}} \cdot \mathbf{S} \quad . \quad (4.30)$$

The helicity operator $\Sigma \equiv \hat{\mathbf{p}} \cdot \mathbf{S}$ is covariantly constant, i.e.

$$\partial_k \Sigma + i[A_k, \Sigma] = 0 \quad , \quad (4.31)$$

where $A_k \equiv \mathcal{A}_k^a(\mathbf{p}) S_a$. The position operator \mathbf{x} therefore commutes with $\hat{\mathbf{p}} \cdot \mathbf{S}$. One can therefore verify in a straightforward manner that the observables p_k, ω, J_l and $K_m = (x_m \omega + \omega x_m)/2$ close to the Poincaré group. At $t \neq 0$ the Lorentz boost generators K_m are defined as in Eq.(4.20) and Eq.(4.23) is extended to

$$i[K_k, x_l] = \frac{1}{2} \left(x_k \frac{p_l}{\omega} + \frac{p_l}{\omega} x_k \right) - t \delta_{kl} + i\omega [x_k, x_l] \quad . \quad (4.32)$$

For helicities $\hat{\mathbf{p}} \cdot \mathbf{S} = \pm \lambda$ one extends the previous considerations by considering \mathbf{S} in the spin $|\lambda|$ -representation. Eqs.(4.28), (4.30) and (4.32) are then valid in general. A reducible representation for the generators of the Poincaré group for an arbitrary spin has therefore been constructed for a massless particle. We observe that the helicity operator Σ can be interpreted as a generalized “magnetic charge”, and since Σ is covariantly conserved one can use the general theory of topological quantum numbers [84] and derive the quantization condition

$$\exp(i4\pi\Sigma) = 1 \quad , \quad (4.33)$$

i.e. the helicity is properly quantized. In the next section we will present an alternative way to derive helicity quantization.

4.2 Wess-Zumino Actions and Topological Spin

Coadjoint orbits on a group G has a geometrical structure which naturally admits a symplectic two-form (see e.g. [85, 86, 87]) which can be used to construct topological Lagrangians, i.e. Lagrangians constructed by means of Wess-Zumino terms [88] (for a general account see e.g. Refs.[89, 90]). Let us illustrate the basic ideas for a

non-relativistic spin and $G = SU(2)$. Let \mathcal{K} be an element of the Lie algebra \mathcal{G} of G in the fundamental representation. Without loss of generality we can write $\mathcal{K} = \lambda_\alpha \sigma_\alpha = \lambda \sigma_3$, where $\sigma_\alpha, \alpha = 1, 2, 3$ denotes the three Pauli spin matrices. Let H be the little group of \mathcal{K} . Then the coset space G/H is isomorphic to S^2 and defines an adjoint orbit (for semi-simple Lie groups adjoint and coadjoint representations are equivalent due to the existence of the non-degenerate Cartan-Killing form). The action for the spin degrees of freedom is then expressed in terms of the group G itself, i.e.

$$S_P = -i \int \langle \mathcal{K}, g^{-1}(\tau) dg(\tau) / d\tau \rangle d\tau \quad , \quad (4.34)$$

where $\langle A, B \rangle$ denotes the trace-operation of two Lie-algebra elements A and B in \mathcal{G} and where

$$g(\tau) = \exp(i\sigma_\alpha \xi_\alpha(\tau)) \quad (4.35)$$

defines the (proper-)time dependent dynamical group element. We observe that S_P has a gauge-invariance, i.e. the transformation

$$g(\tau) \longrightarrow g(\tau) \exp(i\theta(\tau)\sigma_3) \quad (4.36)$$

only change the Lagrangian density $\langle \mathcal{K}, g^{-1}(\tau) dg(\tau) / d\tau \rangle$ by a total time derivative. The gauge-invariant components of spin, $S_k(\tau)$, are defined in terms of \mathcal{K} by the relation

$$S(\tau) \equiv S_k(\tau) \sigma_k = \lambda g(\tau) \sigma_3 g^{-1}(\tau) \quad , \quad (4.37)$$

such that

$$S^2 \equiv S_k(\tau) S_k(\tau) = \lambda^2 \quad . \quad (4.38)$$

By adding a non-relativistic particle kinetic term as well as a conventional magnetic moment interaction term to the action S_P , one can verify that the components $S_k(\tau)$ obey the correct classical equations of motion for spin-precession [75, 89].

Let $M = \{\sigma, \tau | \sigma \in [0, 1]\}$ and $(\sigma, \tau) \rightarrow g(\sigma, \tau)$ parameterize τ -dependent paths in G such that $g(0, \tau) = g_0$ is an arbitrary reference element and $g(1, \tau) = g(\tau)$. The Wess-Zumino term in this case is given by

$$\omega_{WZ} = -id \langle \mathcal{K}, g^{-1}(\sigma, \tau) dg(\sigma, \tau) \rangle = i \langle \mathcal{K}, (g^{-1}(\sigma, \tau) dg(\sigma, \tau))^2 \rangle \quad , \quad (4.39)$$

where d denotes exterior differentiation and where now

$$g(\sigma, \tau) = \exp(i\sigma_\alpha \xi_\alpha(\sigma, \tau)) \quad . \quad (4.40)$$

Apart from boundary terms which do not contribute to the equations of motion, we then have that

$$S_P = S_{WZ} \equiv \int_M \omega_{WZ} = -i \int_{\partial M} \langle \mathcal{K}, g^{-1}(\tau) dg(\tau) \rangle \quad , \quad (4.41)$$

where the one-dimensional boundary ∂M of M , parameterized by τ , can play the role of (proper-) time. ω_{WZ} is now gauge-invariant under a larger $U(1)$ symmetry, i.e. Eq.(4.36) is now extended to

$$g(\sigma, \tau) \longrightarrow g(\sigma, \tau) \exp(i\theta(\sigma, \tau)\sigma_3) \quad . \quad (4.42)$$

ω_{WZ} is therefore a closed but not exact two-form defined on the coset space G/H . A canonical analysis then shows that there are no gauge-invariant dynamical degrees of freedom in the interior of M . The Wess-Zumino action Eq.(4.41) is the topological action for spin degrees of freedom.

As for the quantization of the theory described by the action Eq.(4.41), one may use methods from geometrical quantization and especially the Borel-Weil-Bott theory of representations of compact Lie groups [85, 89]. One then finds that λ is half an integer, i.e. $|\lambda|$ corresponds to the spin. This quantization of λ also naturally emerges by demanding that the action Eq.(4.41) is well-defined in quantum mechanics for periodic motion as recently was discussed by e.g. Klauder [91], i.e.

$$4\pi\lambda = \int_{S^2} \omega_{WZ} = 2\pi n \quad , \quad (4.43)$$

where n is an integer. The symplectic two-form ω_{WZ} must then belong to an integer class cohomology. This geometrical approach is in principal straightforward, but it requires explicit coordinates on G/H . An alternative approach, as used in [75, 89], is a canonical Dirac analysis and quantization [6]. This procedure leads to the condition $\lambda^2 = s(s+1)$, where s is half an integer. The fact that one can arrive at different answers for λ illustrates a certain lack of uniqueness in the quantization procedure of the action Eq.(4.41). The quantum theories obtained describes, however, the same physical system namely one irreducible representation of the group G .

The action Eq.(4.41) was first proposed in [92]. The action can be derived quite naturally in terms of a coherent state path integral (for a review see e.g. Ref.[7]) using spin coherent states. It is interesting to notice that structure of the action Eq.(4.41) actually appears in such a language already in a paper by Klauder on continuous representation theory [93].

A classical action which after quantization leads to a description of a massless particle in terms of an irreducible representations of the Poincaré group can be constructed in a similar fashion [75]. Since the Poincaré group is non-compact the geometrical analysis referred to above for non-relativistic spin must be extended and one should consider coadjoint orbits instead of adjoint orbits (D=3 appears to be an exceptional case due to the existence of a non-degenerate bilinear form on the D=3 Poincaré group Lie algebra [94]. In this case there is a topological action for irreducible representations of the form Eq.(4.41) [95]). The point-particle action in D=4 then takes the form

$$S = \int d\tau \left(p_\mu(\tau) \dot{x}^\mu(\tau) + \frac{i}{2} \text{Tr}[\mathcal{K} \Lambda^{-1}(\tau) \frac{d}{d\tau} \Lambda(\tau)] \right) \quad . \quad (4.44)$$

Here $[\sigma_{\alpha\beta}]_{\mu\nu} = -i(\eta_{\alpha\mu}\eta_{\beta\nu} - \eta_{\alpha\nu}\eta_{\beta\mu})$ are the Lorentz group generators in the spin-one representation and $\eta_{\mu\nu} = (-1, 1, 1, 1)$ is the Minkowski metric. The trace operation has a conventional meaning, i.e. $\text{Tr}[\mathcal{M}] = \mathcal{M}^\alpha{}_\alpha$. The Lorentz group Lie-algebra element \mathcal{K} is here chosen to be $\lambda\sigma_{12}$. The τ -dependence of the Lorentz group element

$\Lambda_{\mu\nu}(\tau)$ is defined by

$$\Lambda_{\mu\nu}(\tau) = \left[\exp \left(i \sigma_{\alpha\beta} \xi^{\alpha\beta}(\tau) \right) \right]_{\mu\nu} . \quad (4.45)$$

The momentum variable $p_\mu(\tau)$ is defined by

$$p_\mu(\tau) = \Lambda_{\mu\nu}(\tau) k^\nu , \quad (4.46)$$

where the constant reference momentum k^ν is given by

$$k^\nu = (\omega, 0, 0, |\mathbf{k}|) , \quad (4.47)$$

where $\omega = |\mathbf{k}|$. The momentum $p_\mu(\tau)$ is then light-like by construction. The action Eq.(4.44) leads to the equations of motion

$$\frac{d}{d\tau} p_\mu(\tau) = 0 , \quad (4.48)$$

and

$$\frac{d}{d\tau} \left\{ x_\mu(\tau) p_\nu(\tau) - x_\nu(\tau) p_\mu(\tau) + S_{\mu\nu}(\tau) \right\} = 0 . \quad (4.49)$$

Here we have defined gauge-invariant spin degrees of freedom $S_{\mu\nu}(\tau)$ by

$$S_{\mu\nu}(\tau) = \frac{1}{2} \text{Tr} [\Lambda(\tau) \mathcal{K} \Lambda^{-1}(\tau) \sigma_{\mu\nu}] \quad (4.50)$$

in analogy with Eq.(4.37). These spin degrees of freedom satisfy the relations

$$p_\mu(\tau) S^{\mu\nu}(\tau) = 0 , \quad (4.51)$$

and

$$\frac{1}{2} S_{\mu\nu}(\tau) S^{\mu\nu}(\tau) = \lambda^2 . \quad (4.52)$$

Inclusion of external electro-magnetic and gravitational fields leads to the classical Bargmann-Michel-Telegdi [96] and Papapetrou [97] equations of motion respectively [75]. Since the equations derived are expressed in terms of *bosonic* variables these equations of motion admit a straightforward classical interpretation. (An alternative *bosonic* or *fermionic* treatment of internal degrees of freedom which also leads to Wongs equations of motion [98] in the presence of in general non-Abelian external gauge fields can be found in Ref.[99].)

Canonical quantization of the system described by *bosonic* degrees of freedom and the action Eq.(4.44) leads to a realization of the Poincaré Lie algebra with generators p_μ and $J_{\mu\nu}$ where

$$J_{\mu\nu} = x_\mu p_\nu - x_\nu p_\mu + S_{\mu\nu} . \quad (4.53)$$

The four vectors x_μ and p_ν commute with the spin generators $S_{\mu\nu}$ and are canonical, i.e.

$$[x_\mu, x_\nu] = [p_\mu, p_\nu] = 0 \quad , \quad (4.54)$$

$$[x_\mu, p_\nu] = i\eta_{\mu\nu} \quad . \quad (4.55)$$

The spin generators $S_{\mu\nu}$ fulfill the conventional algebra

$$[S_{\mu\nu}, S_{\lambda\rho}] = i(\eta_{\mu\lambda}S_{\nu\rho} + \eta_{\nu\rho}S_{\mu\lambda} - \eta_{\mu\rho}S_{\nu\lambda} - \eta_{\nu\lambda}S_{\mu\rho}) \quad . \quad (4.56)$$

The mass-shell condition $p^2 = 0$ as well as the constraints Eq.(4.51) and Eq.(4.52) are all first-class constraints [6]. In the proper-time gauge $x^0(\tau) \approx \tau$ one obtains the system described in Section 4.1, i.e. we obtain an irreducible representation of the Poincaré group with helicity λ [75]. For half-integer helicity, i.e. for fermions, one can verify in a straightforward manner that the wave-functions obtained change with a minus-sign under a 2π rotation [75, 77, 89] as they should.

4.3 The Berry Phase for Single Photons

We have constructed a set of $O(3)$ -covariant position operators of massless particles and a reducible representation of the Poincaré group corresponding to a combination of positive and negative helicities. It is interesting to notice that the construction above leads to observable effects. Let us specifically consider photons and the motion of photons along e.g. an optical fibre. Berry has argued [100] that a spin in an adiabatically changing magnetic field leads to the appearance of an observable phase factor, called the Berry phase. It was suggested in Ref.[101] that a similar geometric phase could appear for photons. We will now, within the framework of the *relativistic quantum mechanics* of a single massless particle as discussed above, give a *derivation* of this geometrical phase. The Berry phase for a *single* photon can e.g. be obtained as follows. We consider the motion of a photon with fixed energy moving e.g. along an optical fibre. We assume that as the photon moves in the fibre, the momentum vector traces out a closed loop in momentum space on the constant energy surface, i.e. on a two-sphere S^2 . This simply means that the initial and final momentum vectors of the photon are the same. We therefore consider a wave-function $|\mathbf{p}\rangle$ which is diagonal in momentum. We also define the translation operator $U(\mathbf{a}) = \exp(i\mathbf{a}\cdot\mathbf{x})$. It is straightforward to show, using Eq.(4.10), that

$$U(\mathbf{a})U(\mathbf{b})|\mathbf{p}\rangle = \exp(i\gamma[\mathbf{a}, \mathbf{b}; \mathbf{p}])|\mathbf{p} + \mathbf{a} + \mathbf{b}\rangle \quad , \quad (4.57)$$

where the two-cocycle phase $\gamma[\mathbf{a}, \mathbf{b}; \mathbf{p}]$ is equal to the flux of the magnetic monopole in momentum space through the simplex spanned by the vectors \mathbf{a} and \mathbf{b} localized at the point \mathbf{p} , i.e.

$$\gamma[\mathbf{a}, \mathbf{b}; \mathbf{p}] = \lambda \int_0^1 \int_0^1 d\xi_1 d\xi_2 a_k b_l \epsilon_{lkm} B_m(\mathbf{p} + \xi_1 \mathbf{a} + \xi_2 \mathbf{b}) \quad , \quad (4.58)$$

where $B_m(\mathbf{p}) = p_m/|\mathbf{p}|^3$. The non-trivial phase appears because the second de Rham cohomology group of S^2 is non-trivial. The two-cocycle phase $\gamma[\mathbf{a}, \mathbf{b}; \mathbf{p}]$ is therefore not a coboundary and hence it cannot be removed by a redefinition of $U(\mathbf{a})$. This result has a close analogy in the theory of magnetic monopoles [102]. The anomalous commutator Eq.(4.10) therefore leads to a ray-representation of the translations in momentum space.

A closed loop in momentum space, starting and ending at \mathbf{p} , can then be obtained by using a sequence of infinitesimal translations $U(\delta\mathbf{a})|\mathbf{p}\rangle = |\mathbf{p} + \delta\mathbf{a}\rangle$ such that $\delta\mathbf{a}$ is orthogonal to argument of the wave-function on which it acts (this defines the adiabatic transport of the system). The momentum vector \mathbf{p} then traces out a closed curve on the constant energy surface S^2 in momentum space. The total phase of these translations then gives a phase γ which is the λ times the solid angle of the closed curve the momentum vector traces out on the constant energy surface. This phase does not depend on Plancks constant. This is precisely the Berry phase for the photon with a given helicity λ . In the original experiment by Tomita and Chiao [103] one considers a beam of linearly polarized photons (a single-photon experiment is considered in Ref.[104]). The same line of arguments above but making use Eq.(4.28) instead of Eq.(4.10) leads to the desired change of polarization as the photon moves along the optical fibre.

A somewhat alternative derivation of the Berry phase for photons is based on observation that the covariantly conserved helicity operator Σ can be interpreted as a generalized “magnetic charge”. Let Γ denote a closed path in momentum space parameterized by $\sigma \in [0, 1]$ such that $\mathbf{p}(\sigma = 0) = \mathbf{p}(\sigma = 1) = \mathbf{p}_0$ is fixed. The parallel transport of a one-particle state $\phi_\alpha(\mathbf{p})$ along the path Γ is then determined by a path-ordered exponential, i.e.

$$\phi_\alpha(\mathbf{p}_0) \longrightarrow \left[P \exp \left(i \int_\Gamma A_k(\mathbf{p}(\sigma)) \frac{dp_k(\sigma)}{d\sigma} d\sigma \right) \right]_{\alpha\beta} \phi_\beta(\mathbf{p}_0) \quad , \quad (4.59)$$

where $A_k(\mathbf{p}(\sigma)) \equiv \mathcal{A}_k^a(\mathbf{p}(\sigma))S_a$. By making use of a non-Abelian version of Stokes theorem [84] one can then show that

$$P \exp \left(i \int_\Gamma A_k(\mathbf{p}(\sigma)) \frac{dp_k(\sigma)}{d\sigma} d\sigma \right) = \exp (i\Sigma\Omega[\Gamma]) \quad , \quad (4.60)$$

where $\Omega[\Gamma]$ is the solid angle subtended by the path Γ on the two-sphere S^2 . This result leads again to the desired change of linear polarization as the photon moves along the path described by Γ . Eq.(4.60) also directly leads to helicity quantization, as alluded to already in Section 4.1, by considering a sequence of loops which converges to a point and at the same time has covered a solid angle of 4π . This derivation does not require that $|\mathbf{p}(\sigma)|$ is constant along the path.

In the experiment of Ref.[103] the photon flux is large. In order to strictly apply our results under such conditions one can consider a second quantized version of the theory we have presented following e.g. the discussion of Amrein [65]. By making

use of coherent states of the electro-magnetic field in a standard and straightforward manner (see e.g. Ref.[7]) one then realize that our considerations survive. This is so since the coherent states are parameterized in terms of the one-particle states. By construction the coherent states then inherits the transformation properties of the one-particle states discussed above. It is, of course, of vital importance that the Berry phase of single-photon states has experimentally been observed [104].

4.4 Localization of Single-Photon States

In this section we will see that the fact that a one-photon state has *positive* energy, generically makes a localized one-photon wave-packet de-localized in space in the course of its time-evolution. We will, for reasons of simplicity, restrict ourselves to a one-dimensional motion, i.e. we have assume that the transverse dimensions of the propagating localized one-photon state are much large than the longitudinal scale. We will also neglect the effect of photon polarization. Details of a more general treatment can be found in Ref.[105]. In one dimension we have seen above that the conventional notion of a position operator makes sense for a single photon. We can therefore consider wave-packets not only in momentum space but also in the longitudinal co-ordinate space in a conventional quantum-mechanical manner. One can easily address the same issue in terms of photon-detection theory but in the end no essential differences will emerge. In the Schödinger picture we are then considering the following initial value problem ($c = \hbar = 1$)

$$\begin{aligned} i\frac{\partial\psi(x,t)}{\partial t} &= \sqrt{-\frac{d^2}{dx^2}}\psi(x,t) \quad , \\ \psi(x,0) &= \exp(-x^2/2a^2)\exp(ik_0x) \quad , \end{aligned} \quad (4.61)$$

which describes the unitary time-evolution of a single-photon wave-packet localized within the distance a and with mean-momentum $\langle p \rangle = k_0$. The *non-local* pseudo-differential operator $\sqrt{-d^2/dx^2}$ is defined in terms of Fourier-transform techniques, i.e.

$$\sqrt{-\frac{d^2}{dx^2}}\psi(x) = \int_{-\infty}^{\infty} dyK(x-y)\psi(y) \quad , \quad (4.62)$$

where the kernel $K(x)$ is given by

$$K(x) = \frac{1}{2\pi} \int_{-\infty}^{\infty} dk|k|\exp(ikx) \quad . \quad (4.63)$$

The co-ordinate wave function at any finite time can now easily be written down and the probability density is shown in Figure 2 in the case of a non-zero average momentum of the photon. The form of the soliton-like peaks is preserved for sufficiently large times. In the limit of $ak_0 = 0$ one gets two soliton-like identical peaks propagating in opposite directions. The structure of these peaks are actually very similar to the directed localized energy pulses in Maxwells theory [106] or to the

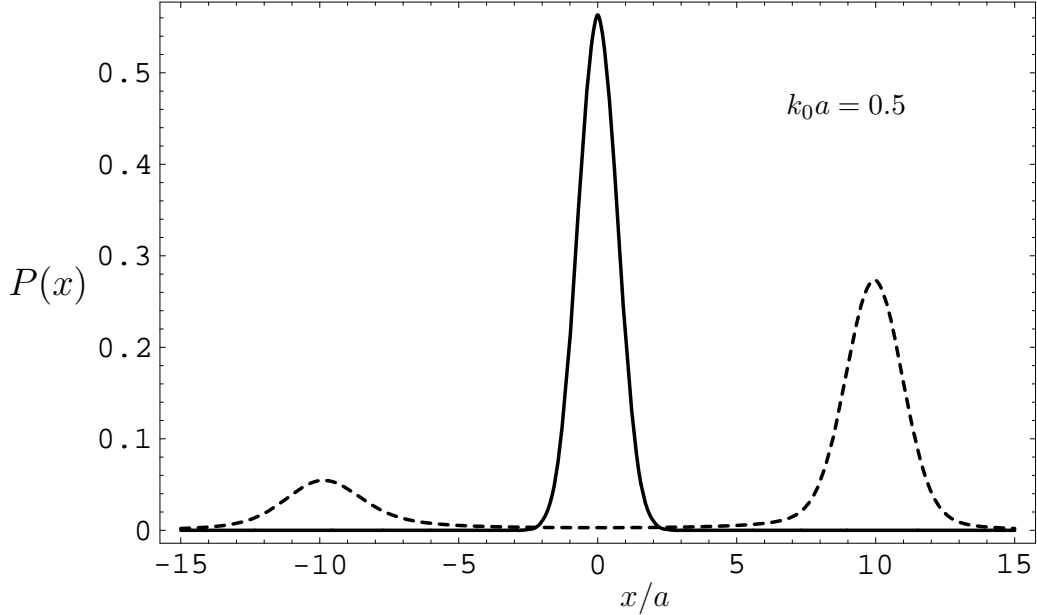


Figure 2: Probability density-distribution $P(x) = |\psi(x, t)|^2$ for a one-dimensional Gaussian single-photon wave-packet with $k_0 a = 0.5$ at $t = 0$ (solid curve) and at $t/a = 10$ (dashed curve).

pulse splitting processes in non-linear dispersive media (see e.g. Ref.[107]) but the physics is, of course, completely different.

Since the wave-equation Eq.(4.61) leads to the second-order wave-equation in one-dimension the physics so obtained can, of course, be described in terms of solutions to the one-dimensional d'Alembert wave-equation of Maxwell's theory of electromagnetism. The quantum-mechanical wave-function above in momentum space is then simply used to parameterize a coherent state. The average of a second-quantized electro-magnetic free field operator in such a coherent state will then be a solution of this wave-equation. The solution to the d'Alembertian wave-equation can then be written in terms of the general d'Alembertian formula, i.e.

$$\psi_{cl}(x, t) = \frac{1}{2}(\psi(x+t, 0) + \psi(x-t, 0)) + \frac{1}{2i} \int_{x-t}^{x+t} dy \int_{-\infty}^{\infty} dz K(y-z) \psi(z, 0) \quad , \quad (4.64)$$

where the last term corresponds to the initial value of the time-derivative of the classical electro-magnetic field. The fact this term is non-locally connected to the initial value of the classical electro-magnetic field is perhaps somewhat unusual. By construction $\psi_{cl}(x, t) = \psi(x, t)$. The physical interpretation of the two functions $\psi(x, t)$ and $\psi_{cl}(x, t)$ are, of course, very different. In the quantum-mechanical case the detection of the photon destroys the coherence properties of the wave-packet

$\psi(x, t)$ entirely. In the classical case the detection of a single photon can still preserve the coherence properties of the classical field $\psi_{cl}(x, t)$ since there are infinitely many photons present in the corresponding coherent state.

4.5 Various Comments

In the analysis of Wightman, corresponding to commuting position variables, the natural mathematical tool turned out to be systems of imprimitivity for the representations of the three-dimensional Euclidean group. In the case of non-commuting position operators we have also seen that notions from differential geometry are important. It is interesting to see that such a broad range of mathematical methods enters into the study of the notion of localizability of physical systems.

We have, in particular, argued that Abelian as well as non-Abelian magnetic monopole field configurations reveal themselves in a description of localizability of massless spinning particles. Concerning the physical existence of magnetic monopoles Dirac remarked in 1981 [108] that *“I am inclined now to believe that monopoles do not exist. So many years have gone by without any encouragement from the experimental side”*. The “monopoles” we are considering are, however, only mathematical objects in the momentum space of the massless particles. Their existence, we have argued, is then only indirectly revealed to us by the properties of e.g. the photons moving along optical fibres.

Localized states of massless particles will necessarily develop non-exponential tails in space as a consequence of the Hegerfeldts theorem [73]. Various number operators representing the number of massless, spinning particles localized in a finite volume V at time t has been discussed in the literature. The non-commuting position observables we have discussed for photons correspond to the point-like limit of the weak localizability of Jauch, Piron and Amrein [65]. This is so since our construction, as we have seen in Section 4.1, corresponds to an explicit enforcement of the transversality condition of the one-particle wave-functions.

In a finite volume, photon number operators appropriate for weak localization [65] do not agree with the photon number operator introduced by Mandel [109] for sufficiently small wavelengths as compared to the linear dimension of the localization volume. It would be interesting to see if there are measurable differences. A necessary ingredient in answering such a question would be the experimental realization of a localized one-photon state. It is interesting to notice that such states can be generated in the laboratory [35]-[45].

As a final remark of this first set of lectures we recall a statement of Wightman which, to a large extent, still is true [64]: *“Whether, in fact, the position of such particle is observable in the sense of quantum theory is, of course, a much deeper problem that probably can only be decided within the context of a specific consequent dynamical theory of particles. All investigations of localizability for relativistic particles up to now, including the present one, must be regarded as preliminary from this point of view: They construct position observables consistent with a given trans-*

formation law. It remains to construct complete dynamical theories consistent with a given transformation law and then to investigate whether the position observables are indeed observable with the apparatus that the dynamical theories themselves predict". This is, indeed, an ambitious programme to which we have not added very much in these lectures.

5 Resonant Cavities and the Micromaser System

“The interaction of a single dipole with a monochromatic radiation field presents an important problem in electrodynamics. It is an unrealistic problem in the sense that experiments are not done with single atoms or single-mode fields.”

L. Allen and J.H. Eberly

The highly idealized physical system of a single two-level atom in a super-conducting cavity, interacting with a quantized single-mode electro-magnetic field, has been experimentally realized in the micromaser [110]–[113] and microlaser systems [114]. It is interesting to consider this remarkable experimental development in view of the quotation above. Details and a limited set of references to the literature can be found in e.g. the reviews [115]–[121]. In the absence of dissipation (and in the rotating wave approximation) the two-level atom and its interaction with the radiation field is well described by the Jaynes–Cummings (JC) Hamiltonian [122]. Since this model is exactly solvable it has played an important role in the development of modern quantum optics (for recent accounts see e.g. Refs. [120, 121]). The JC model predicts non-classical phenomena, such as revivals of the initial excited state of the atom [124]–[130], experimental signs of which have been reported for the micromaser system [131].

Correlation phenomena are important ingredients in the experimental and theoretical investigation of physical systems. Intensity correlations of light was e.g. used by Hanbury–Brown and Twiss [52] as a tool to determine the angular diameter of distant stars. The quantum theory of intensity correlations of light was later developed by Glauber [14]. These methods have a wide range of physical applications including investigation of the space-time evolution of high-energy particle and nuclei interactions [53, 2]. In the case of the micromaser it has recently been suggested [3, 4] that correlation measurements on atoms leaving the micromaser system can be used to infer properties of the quantum state of the radiation field in the cavity.

We will now discuss in great detail the role of long-time correlations in the outgoing atomic beam and their relation to the various phases of the micromaser system. Fluctuations in the number of atoms in the lower maser level for a fixed transit time τ is known to be related to the photon-number statistics [132]–[135]. The experimental results of [136] are clearly consistent with the appearance of non-classical, sub-Poissonian statistics of the radiation field, and exhibit the intricate correlation between the atomic beam and the quantum state of the cavity. Related work on characteristic statistical properties of the beam of atoms emerging from the micromaser cavity may be found in Ref. [137, 138, 139].

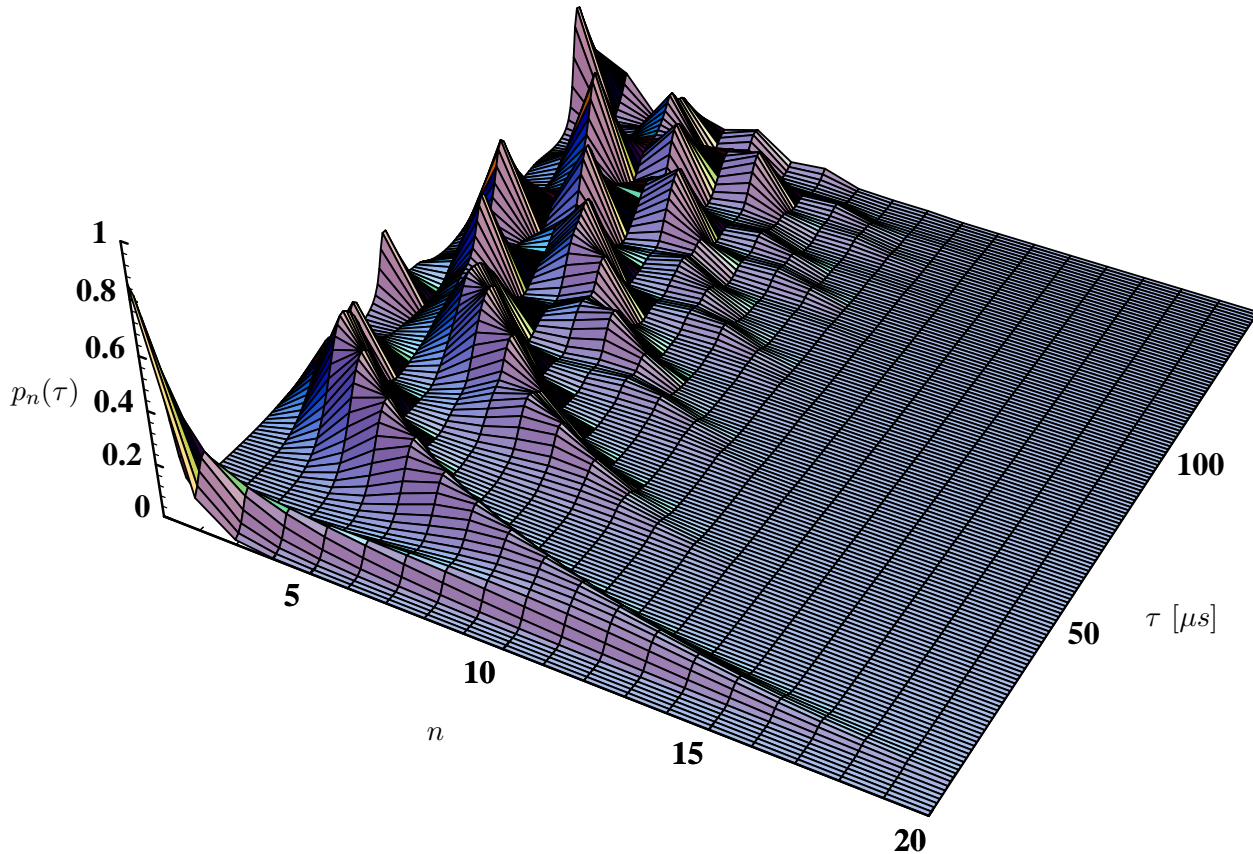


Figure 3: The rugged landscape of the photon distribution $p_n(\tau)$ in Eq. (6.32) at equilibrium for the micromaser as a function of the number of photons in the cavity, n , and the atomic time-of-flight τ . The parameters correspond to a super-conducting niobium maser, cooled down to a temperature of $T = 0.5$ K, with an average thermal photon occupation number of $n_b = 0.15$, at the maser frequency of 21.5 GHz. The single-photon Rabi frequency Ω is 44 kHz, the photon lifetime in the cavity is $T_{\text{cav}} = 0.2$ s, and the atomic beam intensity is $R = 50/\text{s}$.

6 Basic Micromaser Theory

“It is the enormous progress in constructing super-conducting cavities with high quality factors together with the laser preparation of highly excited atoms - Rydberg atoms - that have made the realization of such a one-atom maser possible.”

H. Walther

In the micromaser a beam of excited atoms is sent through a cavity and each atom interacts with the cavity during a well-defined transit time τ . The theory of the micromaser has been developed in [132, 133], and in this section we briefly review the standard theory, generally following the notation of that paper. We assume that excited atoms are injected into the cavity at an average rate R and that the typical decay rate for photons in the cavity is γ . The number of atoms passing the cavity in a single decay time $N = R/\gamma$ is an important dimensionless parameter, effectively controlling the average number of photons stored in a high-quality cavity. We shall

assume that the time τ during which the atom interacts with the cavity is so small that effectively only one atom is found in the cavity at any time, i.e. $R\tau \ll 1$. A further simplification is introduced by assuming that the cavity decay time $1/\gamma$ is much longer than the interaction time, i.e. $\gamma\tau \ll 1$, so that damping effects may be ignored while the atom passes through the cavity. This point is further elucidated in Appendix A. In the typical experiment of Ref. [136] these quantities are given the values $N = 10$, $R\tau = 0.0025$ and $\gamma\tau = 0.00025$.

6.1 The Jaynes–Cummings Model

The electro-magnetic interaction between a two-level atom with level separation ω_0 and a single mode with frequency ω of the radiation field in a cavity is described, in the rotating wave approximation, by the Jaynes–Cummings (JC) Hamiltonian [122]

$$H = \omega a^* a + \frac{1}{2} \omega_0 \sigma_z + g(a\sigma_+ + a^* \sigma_-) \quad , \quad (6.1)$$

where the coupling constant g is proportional to the dipole matrix element of the atomic transition². We use the Pauli matrices to describe the two-level atom and the notation $\sigma_{\pm} = (\sigma_x \pm i\sigma_y)/2$. The second quantized single mode electro-magnetic field is described in a conventional manner (see e.g. Ref.[140]) by means of an annihilation (creation) operator a (a^*), where we have suppressed the mode quantum numbers. For $g = 0$ the atom-plus-field states $|n, s\rangle$ are characterized by the quantum number $n = 0, 1, \dots$ of the oscillator and $s = \pm$ for the atomic levels (with $-$ denoting the ground state) with energies $E_{n,-} = \omega n - \omega_0/2$ and $E_{n,+} = \omega n + \omega_0/2$. At resonance $\omega = \omega_0$ the levels $|n-1, +\rangle$ and $|n, -\rangle$ are degenerate for $n \geq 1$ (excepting the ground state $n = 0$), but this degeneracy is lifted by the interaction. For arbitrary coupling g and detuning parameter $\Delta\omega = \omega_0 - \omega$ the system reduces to a 2×2 eigenvalue problem, which may be trivially solved. The result is that two new levels, $|n, 1\rangle$ and $|n, 2\rangle$, are formed as superpositions of the previously degenerate ones at zero detuning according to

$$\begin{aligned} |n, 1\rangle &= \cos(\theta_n) |n+1, -\rangle + \sin(\theta_n) |n, +\rangle \quad , \\ |n, 2\rangle &= -\sin(\theta_n) |n+1, -\rangle + \cos(\theta_n) |n, +\rangle \quad , \end{aligned} \quad (6.2)$$

with energies

$$\begin{aligned} E_{n1} &= \omega(n+1/2) + \sqrt{\Delta\omega^2/4 + g^2(n+1)} \quad , \\ E_{n2} &= \omega(n+1/2) - \sqrt{\Delta\omega^2/4 + g^2(n+1)} \quad , \end{aligned} \quad (6.3)$$

²This coupling constant turns out to be identical to the single photon Rabi frequency for the case of vanishing detuning, i.e. $g = \Omega$. There is actually some confusion in the literature about what is called the Rabi frequency [141]. With our definition, the energy separation between the shifted states at resonance is 2Ω .

respectively. The ground-state of the coupled system is given by $|0, -\rangle$ with energy $E_0 = -\omega_0/2$. Here the mixing angle θ_n is given by

$$\tan(\theta_n) = \frac{2g\sqrt{n+1}}{\Delta\omega + \sqrt{\Delta\omega^2 + 4g^2(n+1)}} . \quad (6.4)$$

The interaction therefore leads to a separation in energy $\Delta E_n = \sqrt{\Delta\omega^2 + 4g^2(n+1)}$ for quantum number n . The system performs Rabi oscillations with the corresponding frequency between the original, unperturbed states with transition probabilities [122, 123]

$$\begin{aligned} |\langle n, - | e^{-iH\tau} | n, - \rangle|^2 &= 1 - q_n(\tau) , \\ |\langle n-1, + | e^{-iH\tau} | n, - \rangle|^2 &= q_n(\tau) , \\ |\langle n, + | e^{-iH\tau} | n, + \rangle|^2 &= 1 - q_{n+1}(\tau) , \\ |\langle n+1, - | e^{-iH\tau} | n, + \rangle|^2 &= q_{n+1}(\tau) . \end{aligned} \quad (6.5)$$

These are all expressed in terms of

$$q_n(\tau) = \frac{g^2 n}{g^2 n + \frac{1}{4}\Delta\omega^2} \sin^2 \left(\tau \sqrt{g^2 n + \frac{1}{4}\Delta\omega^2} \right) . \quad (6.6)$$

Notice that for $\Delta\omega = 0$ we have $q_n = \sin^2(g\tau\sqrt{n})$. Even though most of the following discussion will be limited to this case, the equations given below will often be valid in general.

Denoting the probability of finding n photons in the cavity by p_n we find a general expression for the conditional probability that an excited atom decays to the ground state in the cavity to be

$$\mathcal{P}(-) = \langle q_{n+1} \rangle = \sum_{n=0}^{\infty} q_{n+1} p_n . \quad (6.7)$$

From this equation we find $\mathcal{P}(+) = 1 - \mathcal{P}(-)$, i.e. the conditional probability that the atom remains excited. In a similar manner we may consider a situation when two atoms, A and B , have passed through the cavity with transit times τ_A and τ_B . Let $\mathcal{P}(s_1, s_2)$ be the probability that the second atom B is in the state $s_2 = \pm$ if the first atom has been found in the state $s_1 = \pm$. Such expressions then contain information further information about the entanglement between the atoms and the state of the radiation field in the cavity. If damping of the resonant cavity is not taken into account than $\mathcal{P}(+, -)$ and $\mathcal{P}(-, +)$ are in general different. It is such sums like in Eq.(6.7) over the incommensurable frequencies $g\sqrt{n}$ that is the cause of some of the most important properties of the micromaser, such as quantum collapse and

revivals, to be discussed again in Section 10.1 (see e.g. Refs.[124]-[130], [142]-[145]). If we are at resonance, i.e. $\Delta\omega = 0$, we in particular obtain the expressions

$$\mathcal{P}(+) = \sum_{n=0}^{\infty} p_n \cos^2(g\tau\sqrt{n+1}) \quad , \quad (6.8)$$

for $\tau = \tau_A$ or τ_B , and

$$\begin{aligned} \mathcal{P}(+, +) &= \sum_{n=0}^{\infty} p_n \cos^2(g\tau_A\sqrt{n+1}) \cdot \cos^2(g\tau_B\sqrt{n+1}) \quad , \\ \mathcal{P}(+, -) &= \sum_{n=0}^{\infty} p_n \cos^2(g\tau_A\sqrt{n+1}) \cdot \sin^2(g\tau_B\sqrt{n+1}) \quad , \\ \mathcal{P}(-, +) &= \sum_{n=0}^{\infty} p_n \sin^2(g\tau_A\sqrt{n+1}) \cdot \cos^2(g\tau_B\sqrt{n+2}) \quad , \\ \mathcal{P}(-, -) &= \sum_{n=0}^{\infty} p_n \sin^2(g\tau_A\sqrt{n+1}) \cdot \sin^2(g\tau_B\sqrt{n+2}) \quad . \end{aligned} \quad (6.9)$$

It is clear that these expressions obey the general conditions $\mathcal{P}(+, +) + \mathcal{P}(+, -) = \mathcal{P}(+)$ and $\mathcal{P}(-, +) + \mathcal{P}(-, -) = \mathcal{P}(-)$. As a measure of the coherence due to the entanglement of the state of an atom and the state of the cavities radiation field one may consider the difference of conditional probabilities [146, 147], i.e.

$$\begin{aligned} \eta &= \frac{\mathcal{P}(+, +)}{\mathcal{P}(+, +) + \mathcal{P}(+, -)} - \frac{\mathcal{P}(-, +)}{\mathcal{P}(-, +) + \mathcal{P}(-, -)} \\ &= \frac{\mathcal{P}(+, +)}{\mathcal{P}(+)} - \frac{\mathcal{P}(-, +)}{1 - \mathcal{P}(+)} \quad . \end{aligned} \quad (6.10)$$

These effects of quantum-mechanical revivals are most easily displayed in the case that the cavity field is coherent with Poisson distribution

$$p_n = \frac{\langle n \rangle^n}{n!} e^{-\langle n \rangle} \quad . \quad (6.11)$$

In Figure 4 we exhibit the well-known revivals in the probability $\mathcal{P}(+)$ for a coherent state. In the same figure we also notice the existence of *prerevivals* [3, 4] expressed in terms $\mathcal{P}(+, +)$. In Figure 4 we also consider the same probabilities for the semi-coherent state considered in Figure 1. The presence of one additional photon clearly manifests itself in the revival and prerevival structures. For the purpose of illustrating the revival phenomena we also consider a special form of Schrödinger cat states (for an excellent review see e.g. Ref.[148]) which is a superposition of the coherent states $|z\rangle$ and $|-z\rangle$ for a real parameter z , i.e.

$$|z\rangle_{sc} = \frac{1}{(2 + 2\exp(-2|z|^2))^{1/2}} (|z\rangle + |-z\rangle) \quad . \quad (6.12)$$

In Figure 5 we exhibit revivals and prerevivals for such Schrödinger cat state with $z = 7$ ($\tau = \tau_A = \tau_B$). When compared to the revivals and prerevivals of a coherent state with the same value of z as in Figure 4 one observes that Schrödinger cat state revivals occur much earlier. It is possible to view these earlier revivals as due to a quantum-mechanical interference effect. It is known [149] that the Jaynes-Cummings model has the property that with a coherent state of the radiation field one reaches a *pure* atomic state at time corresponding to approximately one half of the first revival time *independent* of the initial atomic state. The states $|z\rangle$ and $| -z\rangle$ in the construction of the Schrödinger cat state are approximately orthogonal. These two states will then approximately behave as independent system. Since they lead to the same intermediate pure atomic state mentioned above, quantum-mechanical interferences will occur. It can be verified [150] that that this interference effect will survive moderate damping corresponding to present experimental cavity conditions. In Figure 5 we also exhibit the η for a coherent state with $z = 7$ (solid curve) and the same Schrödinger cat as above. The Schrödinger cat state interferences are clearly revealed. It can again be shown that moderate damping effects do not change the qualitative features of this picture [150] .

In passing we notice that revival phenomena and the appearance of Schrödinger like cat states have been studied and observed in many other physical systems like in atomic systems [154]-[158], in ion-traps [159, 160] and recently also in the case of Bose-Einstein condensates [161] (for a recent pedagogical account on revival phenomena see e.g. Ref.[162]).

In the more realistic case, where the changes of the cavity field due to the passing atoms is taken into account, a complicated statistical state of the cavity arises [132], [151]-[153, 182] (see Figure 3). It is the details of this state that are investigated in these lectures.

6.2 Mixed States

The above formalism is directly applicable when the atom and the radiation field are both in pure states initially. In general the statistical state of the system is described by an initial density matrix ρ , which evolves according to the usual rule $\rho \rightarrow \rho(t) = \exp(-iHt)\rho\exp(iHt)$. If we disregard, for the moment, the decay of the cavity field due to interactions with the environment, the evolution is governed by the JC Hamiltonian in Eq. (6.1). It is natural to assume that the atom and the radiation field of the cavity initially are completely uncorrelated so that the initial density matrix factors in a cavity part and a product of k atoms as

$$\rho = \rho_C \otimes \rho_{A_1} \otimes \rho_{A_2} \otimes \cdots \otimes \rho_{A_k} \quad . \quad (6.13)$$

When the first atom A_1 has passed through the cavity, part of this factorizability is destroyed by the interaction and the state has become

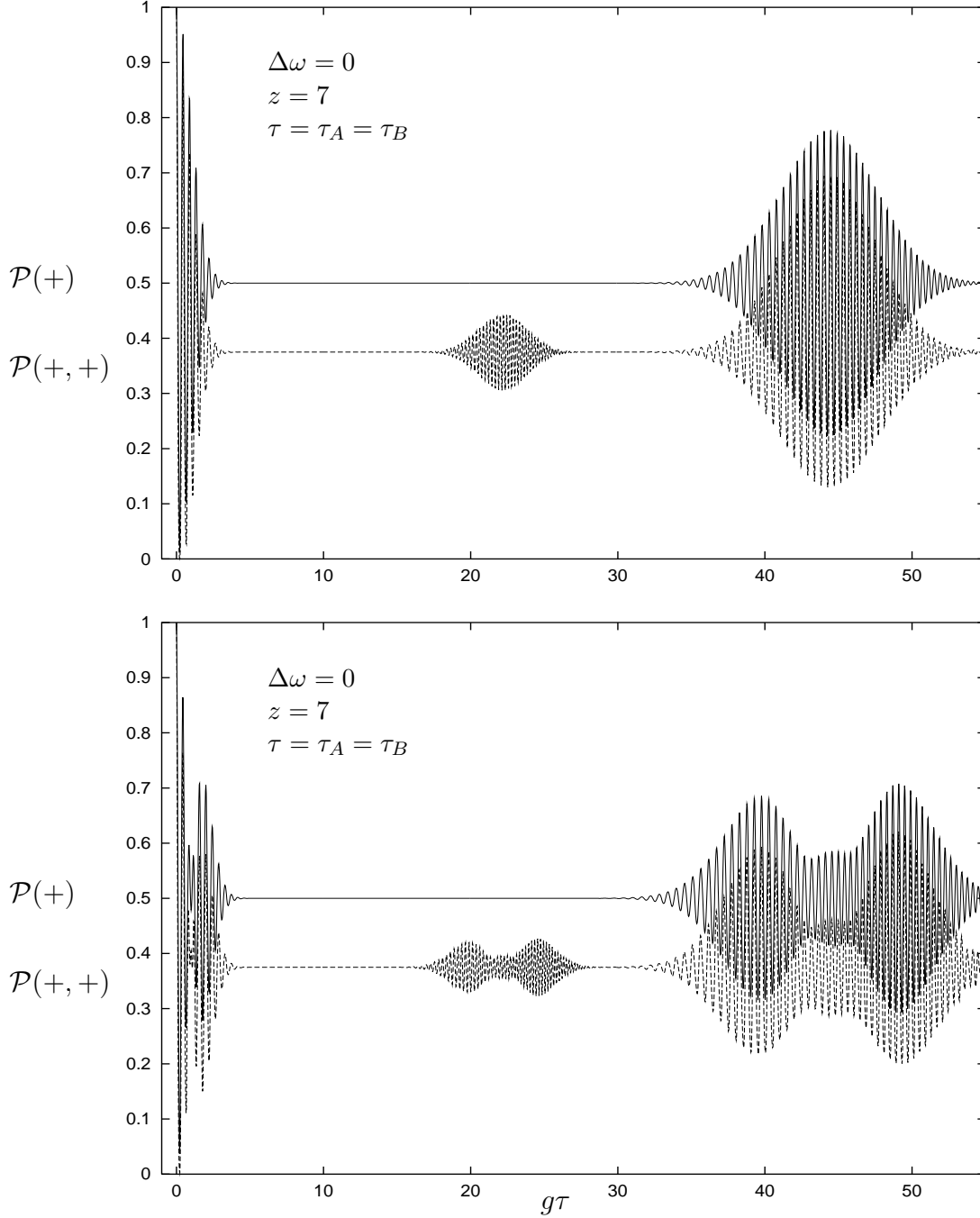


Figure 4: The upper figure shows the revival probabilities $\mathcal{P}(+)$ and $\mathcal{P}(+, +)$ for a coherent state $|z\rangle$ with a mean number $|z|^2 = 49$ of photons as a function of the atomic passage time $g\tau$. The lower figure shows the same revival probabilities for a displaced coherent state $|z, 1\rangle$ with a mean value of $|z|^2 + 1 = 50$ photons.

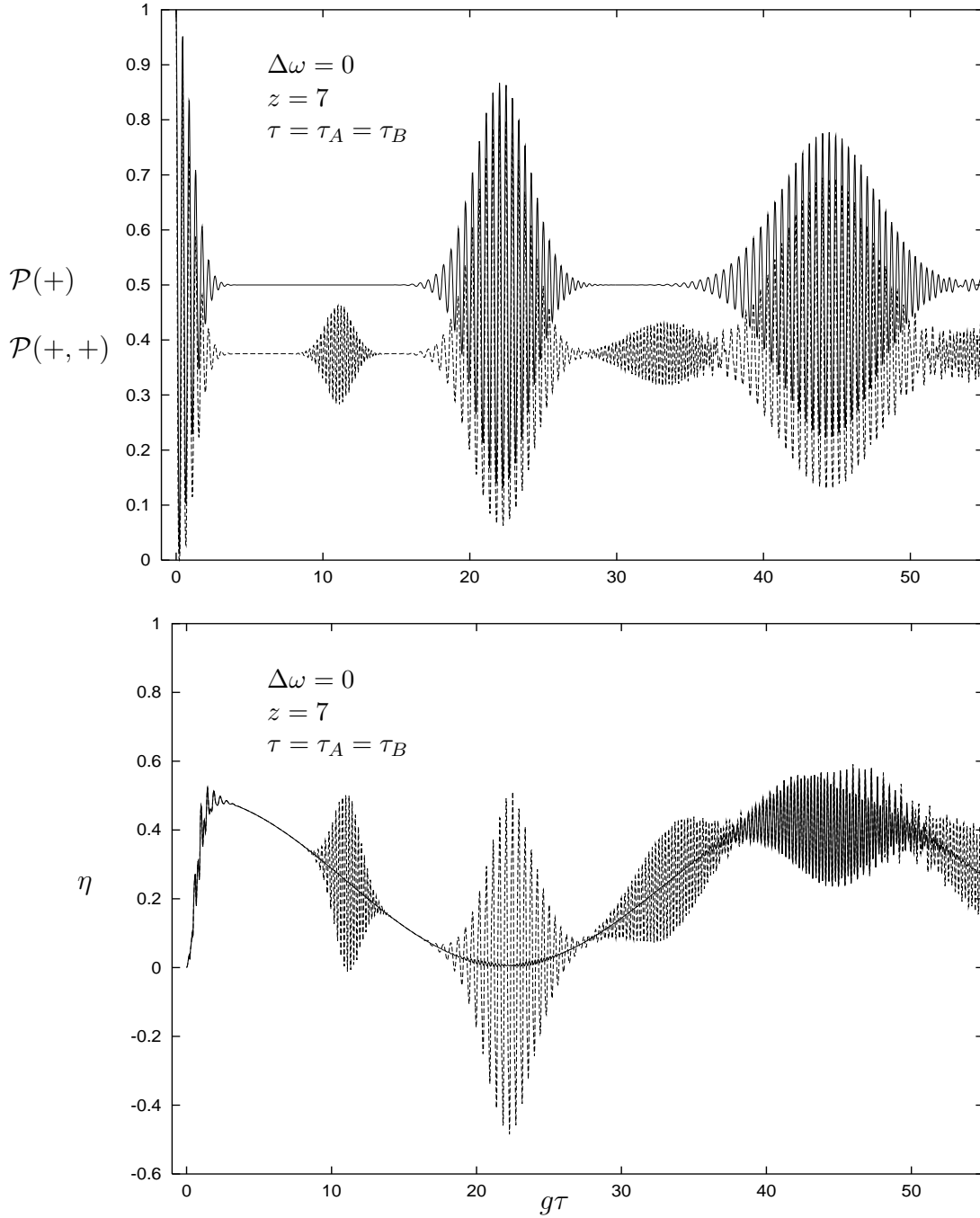


Figure 5: The upper figure shows the revival probabilities $\mathcal{P}(+)$ and $\mathcal{P}(+,+)$ for a normalized Schrödinger cat state as given by Eq.(6.12) with $z = 7$ as a function of the atomic passage time $g\tau$. The lower figure shows the correlation coefficient η for a coherent state with $z = 7$ (solid curve) and for the the same Schrödinger cat state (dashed curve) as in the upper figure.

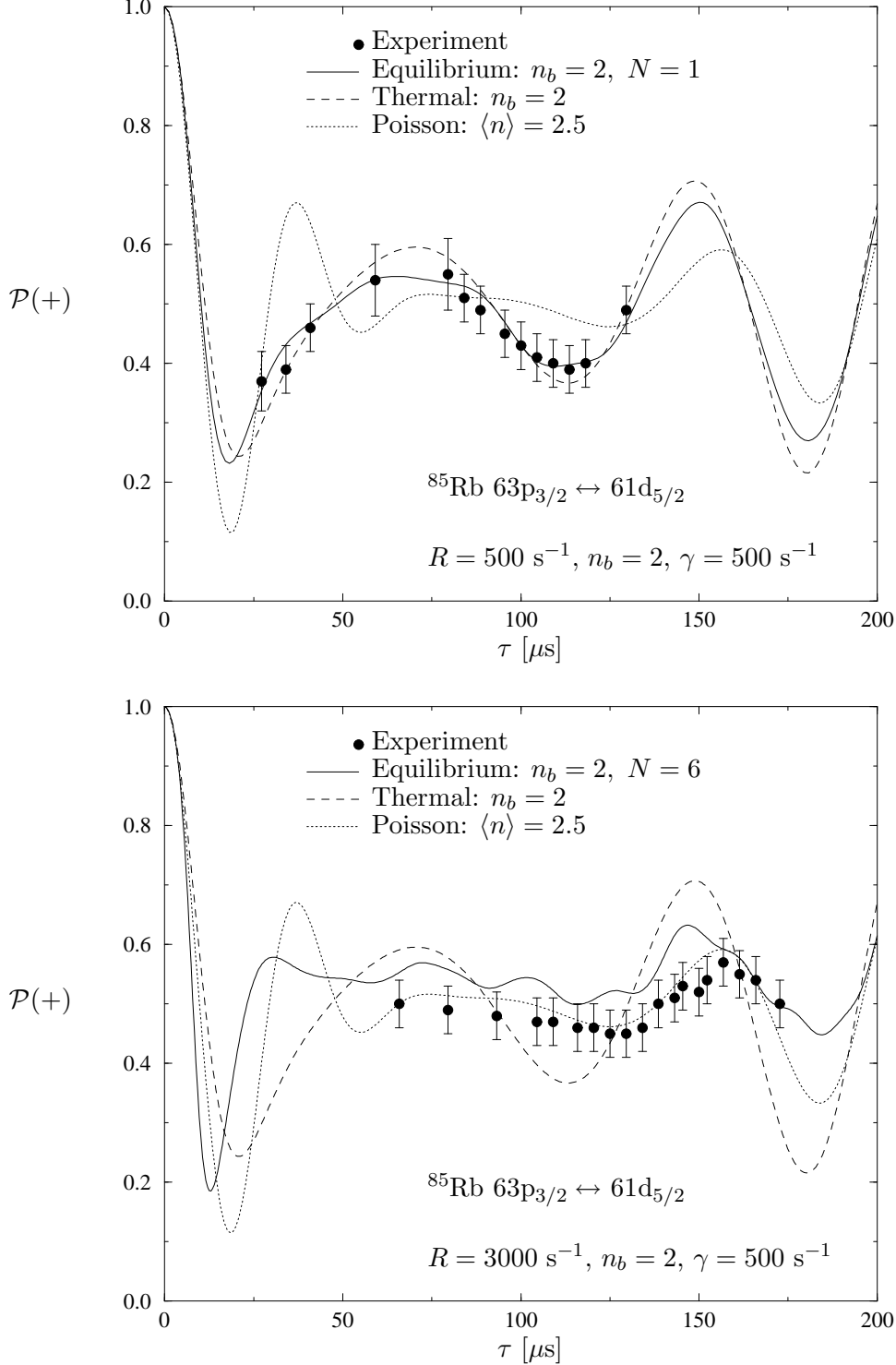


Figure 6: Comparison of $\mathcal{P}(+) = 1 - \mathcal{P}(-) = 1 - \langle q_{n+1} \rangle$ with experimental data of Ref. [131] for various probability distributions. The Poisson distribution is defined in Eq. (6.11), the thermal in Eq. (6.23), and the micromaser equilibrium distribution in Eq. (6.32). In the upper figure ($N = R/\gamma = 1$) the thermal distribution agrees well with the data and in the lower ($N = 6$) the Poisson distribution fits the data best. It is curious that the data systematically seem to deviate from the micromaser equilibrium distribution.

$$\rho(\tau) = \rho_{C,A_1}(\tau) \otimes \rho_{A_2} \otimes \cdots \otimes \rho_{A_k} . \quad (6.14)$$

The explicit form of the cavity-plus-atom entangled state $\rho_{C,A_1}(\tau)$ is analyzed in Appendix A. After the interaction, the cavity decays, more atoms pass through and the state becomes more and more entangled. If we decide never to measure the state of atoms $A_1 \dots A_i$ with $i < k$, we should calculate the trace over the corresponding states and only the ρ_{A_k} -component remains. Since the time evolution is linear, each of the components in Eq. (6.14) evolves independently, and it does not matter when we calculate the trace. We can do it after each atom has passed the cavity, or at the end of the experiment. For this we do not even have to assume that the atoms are non-interacting after they leave the cavity, even though this simplifies the time evolution. If we do perform a measurement of the state of an intermediate atom A_i , a correlation can be observed between that result and a measurement of atom A_k , but the statistics of the unconditional measurement of A_k is not affected by a measurement of A_i . In a real experiment also the efficiency of the measuring apparatus should be taken into account when using the measured results from atoms A_1, \dots, A_i to predict the probability of the outcome of a measurement of A_k (see Ref. [137] for a detailed investigation of this case).

As a generic case let us assume that the initial state of the atom is a diagonal mixture of excited and unexcited states

$$\rho_A = \begin{pmatrix} a & 0 \\ 0 & b \end{pmatrix} , \quad (6.15)$$

where, of course, $a, b \geq 0$ and $a+b = 1$. Using that both preparation and observation are diagonal in the atomic states, it may now be seen from the transition elements in Eq. (6.5) that the time evolution of the cavity density matrix does not mix different diagonals of this matrix. Each diagonal so to speak “lives its own life” with respect to dynamics. This implies that if the initial cavity density matrix is diagonal, i.e. of the form

$$\rho_C = \sum_{n=0}^{\infty} p_n |n\rangle \langle n| , \quad (6.16)$$

with $p_n \geq 0$ and $\sum_{n=0}^{\infty} p_n = 1$, then it stays diagonal during the interaction between atom and cavity and may always be described by a probability distribution $p_n(t)$. In fact, we easily find that after the interaction we have

$$p_n(\tau) = a q_n(\tau) p_{n-1} + b q_{n+1}(\tau) p_{n+1} + (1 - a q_{n+1}(\tau) - b q_n(\tau)) p_n , \quad (6.17)$$

where the first term is the probability of decay for the excited atomic state, the second the probability of excitation for the atomic ground state, and the third is the probability that the atom is left unchanged by the interaction. It is convenient to write this in matrix form [139]

$$p(\tau) = M(\tau)p \quad , \quad (6.18)$$

with a transition matrix $M = M(+)+M(-)$ composed of two parts, representing that the outgoing atom is either in the excited state (+) or in the ground state (-). Explicitly we have

$$\begin{aligned} M(+)_nm &= bq_{n+1}\delta_{n+1,m} + a(1 - q_{n+1})\delta_{n,m} \quad , \\ M(-)_nm &= aq_n\delta_{n,m+1} + b(1 - q_n)\delta_{n,m} \quad . \end{aligned} \quad (6.19)$$

Notice that these formulas are completely classical and may be simulated with a standard Markov process. The statistical properties are not quantum mechanical as long as the incoming atoms have a diagonal density matrix and we only measure elements in the diagonal. The only quantum-mechanical feature at this stage is the discreteness of the photon states, which has important consequences for the correlation length (see Section 6.3). The quantum-mechanical discreteness of photon states in the cavity can actually be tested experimentally [163].

If the atomic density matrix has off-diagonal elements, the above formalism breaks down. The reduced cavity density matrix will then also develop off-diagonal elements, even if initially it is diagonal. We shall not go further into this question here (see for example Refs. [164]–[166]).

6.3 The Lossless Cavity

The above discrete master equation (6.17) describes the pumping of a lossless cavity with a beam of atoms. After k atoms have passed through the cavity, its state has become $M^k p$. In order to see whether this process may reach statistical equilibrium for $k \rightarrow \infty$ we write Eq. (6.17) in the form

$$p_n(\tau) = p_n + J_{n+1} - J_n \quad , \quad (6.20)$$

where $J_n = -aq_n p_{n-1} + bq_n p_n$. In statistical equilibrium we must have $J_{n+1} = J_n$, and the common value $J = J_n$ for all n can only be zero since p_n , and therefore J , has to vanish for $n \rightarrow \infty$. It follows that this can only be the case for $a < b$ i.e. $a < 0.5$. There must thus be fewer than 50% excited atoms in the beam, otherwise the lossless cavity blows up. If $a < 0.5$, the cavity will reach an equilibrium distribution of the form of a thermal distribution for an oscillator $p_n = (1 - a/b)(a/b)^n$. The statistical

equilibrium may be shown to be stable, i.e. that all non-trivial eigenvalues of the matrix M are real and smaller than 1.

6.4 The Dissipative Cavity

A single oscillator interacting with an environment having a huge number of degrees of freedom, for example a heat bath, dissipates energy according to the well-known damping formula (see for example [174, 175]):

$$\begin{aligned} \frac{d\rho_C}{dt} = & i[\rho_C, \omega a^* a] \\ & - \frac{1}{2}\gamma(n_b + 1)(a^* a \rho_C + \rho_C a^* a - 2a \rho_C a^*) \\ & - \frac{1}{2}\gamma n_b (a a^* \rho_C + \rho_C a a^* - 2a^* \rho_C a) \ , \end{aligned} \quad (6.21)$$

where n_b is the average environment occupation number at the oscillator frequency and γ is the decay constant. This evolution also conserves diagonality, so we have for any diagonal cavity state:

$$\frac{1}{\gamma} \frac{dp_n}{dt} = -(n_b + 1)(np_n - (n + 1)p_{n+1}) - n_b((n + 1)p_n - np_{n-1}) \ , \quad (6.22)$$

which of course conserves probability. The right-hand side may as for Eq. (6.20) be written as $J_{n+1} - J_n$ with $J_n = (n_b + 1)np_n - n_b np_{n-1}$ and the same arguments as above lead to a thermal equilibrium distribution with

$$p_n = \frac{1}{1 + n_b} \left(\frac{n_b}{1 + n_b} \right)^n \ . \quad (6.23)$$

6.5 The Discrete Master Equation

We now take into account both pumping and damping. Let the next atom arrive in the cavity after a time $T \gg \tau$. During this interval the cavity damping is described by Eq. (6.22), which we shall write in the form

$$\frac{dp}{dt} = -\gamma L_C p \ , \quad (6.24)$$

where L_C is the cavity decay matrix from above

$$(L_C)_{nm} = (n_b + 1)(n\delta_{n,m} - (n + 1)\delta_{n+1,m}) + n_b((n + 1)\delta_{n,m} - n\delta_{n-1,m}) \ . \quad (6.25)$$

This decay matrix conserves probability, i.e. it is trace-preserving:

$$\sum_{n=0}^{\infty} (L_C)_{nm} = 0 \quad . \quad (6.26)$$

The statistical state of the cavity when the next atom arrives is thus given by

$$p(T) = e^{-\gamma L_C T} M(\tau) p \quad . \quad (6.27)$$

In using the full interval T and not $T - \tau$ we allow for the decay of the cavity in the interaction time, although this decay is not properly included with the atomic interaction (for a more correct treatment see Appendix A).

This would be the master equation describing the evolution of the cavity if the atoms in the beam arrived with definite and known intervals. More commonly, the time intervals T between atoms are Poisson-distributed according to $d\mathcal{P}(T) = \exp(-RT)RdT$ with an average time interval $1/R$ between them. Averaging the exponential in Eq. (6.27) we get

$$\langle p(T) \rangle_T = S p \quad , \quad (6.28)$$

where

$$S = \frac{1}{1 + L_C/N} M \quad , \quad (6.29)$$

and $N = R/\gamma$ is the dimensionless pumping rate already introduced.

Implicit in the above consideration is the lack of knowledge of the actual value of the atomic state after the interaction. If we know that the state of the atom is $s = \pm$ after the interaction, then the average operator that transforms the cavity state is instead

$$S(s) = (1 + L_C/N)^{-1} M(s) \quad , \quad (6.30)$$

with $M(s)$ given by Eq. (6.19). This average operator $S(s)$ is now by construction probability preserving, i.e.

$$\sum_{n,m=0}^{\infty} S_{nm}(s) p_m = 1 \quad . \quad (6.31)$$

Repeating the process for a sequence of k unobserved atoms we find that the initial probability distribution p becomes $S^k p$. In the general case this Markov process converges towards a statistical equilibrium state satisfying $S p = p$, which has the solution [132, 165] for $n \geq 1$

$$p_n = p_0 \prod_{m=1}^n \frac{n_b m + N a q_m}{(1 + n_b)m + N b q_m} . \quad (6.32)$$

The overall constant p_0 is determined by $\sum_{n=0}^{\infty} p_n = 1$. In passing we observe that if $a/b = n_b/(1+n_b)$ then this statistical equilibrium distribution is equal to the thermal statistical distribution Eq.(6.23) as it should. The photon landscape formed by this expression as a function of n and τ is shown in Figure 3 for $a = 1$ and $b = 0$. For greater values of τ it becomes very rugged.

7 Statistical Correlations

*“Und was in schwankender Erscheinung schwebt,
Befestiget mit dauernden Gedanken.”*

J. W. von Goethe

After studying stationary single-time properties of the micromaser, such as the average photon number in the cavity and the average excitation of the outgoing atoms, we now proceed to dynamical properties. Correlations between outgoing atoms are not only determined by the equilibrium distribution in the cavity but also by its approach to this equilibrium. Short-time correlations, such as the correlation between two consecutive atoms [135, 139], are difficult to determine experimentally, because they require efficient observation of the states of atoms emerging from the cavity in rapid succession. We propose instead to study and measure long-time correlations, which do not impose the same strict experimental conditions. These correlations turn out to have a surprisingly rich structure (see Figure 9) and reflect global properties of the photon distribution. In this section we introduce the concept of long-time correlations and present two ways of calculating them numerically. In the following sections we study the analytic properties of these correlations and elucidate their relation to the dynamical phase structure, especially those aspects that are poorly seen in the single-time observables or short-time correlations.

7.1 Atomic Beam Observables

Let us imagine that we know the state of all the atoms as they enter the cavity, for example that they are all excited, and that we are able to determine the state of each atom as it exits from the cavity. We shall assume that the initial beam is statistically stationary, described by the density matrix (6.15), and that we have obtained an experimental record of the exit states of all the atoms after the cavity has reached statistical equilibrium with the beam. The effect of non-perfect measuring efficiency has been considered in several papers [137, 138, 139] but we ignore that complication since it is a purely experimental problem. From this record we may estimate a number of quantities, for example the probability of finding the atom in

a state $s = \pm$ after the interaction, where we choose $+$ to represent the excited state and $-$ the ground state. The probability may be expressed in the matrix form

$$\mathcal{P}(s) = u^{0\top} M(s) p^0 \quad , \quad (7.1)$$

where $M(s)$ is given by Eq. (6.19) and p^0 is the equilibrium distribution (6.32). The quantity u^0 is a vector with all entries equal to 1, $u_n^0 = 1$, and represents the sum over all possible final states of the cavity. In Figure 6 we have compared the behavior of $\mathcal{P}(+)$ with some characteristic experiments.

Since $\mathcal{P}(+) + \mathcal{P}(-) = 1$ it is sufficient to measure the average spin value (see Figure 7):

$$\langle s \rangle = \mathcal{P}(+) - \mathcal{P}(-) \quad . \quad (7.2)$$

Since $s^2 = 1$ this quantity also determines the variance to be $\langle s^2 \rangle - \langle s \rangle^2 = 1 - \langle s \rangle^2$.

Correspondingly, we may define the joint probability for observing the states of two atoms, s_1 followed s_2 , with k unobserved atoms between them,

$$\mathcal{P}_k(s_1, s_2) = u^{0\top} S(s_2) S^k S(s_1) p^0 \quad , \quad (7.3)$$

where S and $S(s)$ are defined in Eqs. (6.29) and (6.30). The joint probability of finding two consecutive excited outgoing atoms, $\mathcal{P}_0(+, +)$, was calculated in [135]. It is worth noticing that since $S = S(+) + S(-)$ and $S p^0 = p^0$ we have $\sum_{s_1} \mathcal{P}_k(s_1, s_2) = \mathcal{P}(s_2)$. Since we also have $u^{0\top} L = u^{0\top} (M - 1) = 0$ we find likewise that $u^{0\top} S = u^{0\top}$ so that $\sum_{s_2} \mathcal{P}_k(s_1, s_2) = \mathcal{P}(s_1)$. Combining these relations we derive that $\mathcal{P}_k(+, -) = \mathcal{P}_k(-, +)$, as expected. Due to these relations there is essentially only one two-point function, namely the ‘‘spin–spin’’ covariance function

$$\begin{aligned} \langle ss \rangle_k &= \sum_{s_1, s_2} s_1 s_2 \mathcal{P}_k(s_1, s_2) \\ &= \mathcal{P}_k(+, +) + \mathcal{P}_k(-, -) - \mathcal{P}_k(+, -) - \mathcal{P}_k(-, +) \\ &= 1 - 4\mathcal{P}_k(+, -) \quad . \end{aligned} \quad (7.4)$$

From this we derive the properly normalized correlation function

$$\gamma_k^A = \frac{\langle ss \rangle_k - \langle s \rangle^2}{1 - \langle s \rangle^2} \quad , \quad (7.5)$$

which satisfies $-1 \leq \gamma_k^A \leq 1$.

At large times, when $k \rightarrow \infty$, the correlation function is in general expected to decay exponentially, and we define the atomic beam correlation length ξ_A by the asymptotic behavior for large $k \simeq Rt$

$$\gamma_k^A \sim \exp\left(-\frac{k}{R\xi_A}\right) . \quad (7.6)$$

Here we have scaled with R , the average number of atoms passing the cavity per unit of time, so that ξ_A is the typical length of time that the cavity remembers previous pumping events.

7.2 Cavity Observables

In the context of the micromaser cavity, one relevant observable is the instantaneous number of photons n , from which we may form the average $\langle n \rangle$ and correlations in time. The quantum state of light in the cavity is often characterized by the Fano–Mandel quality factor [177], which is related to the fluctuations of n through

$$Q_f = \frac{\langle n^2 \rangle - \langle n \rangle^2}{\langle n \rangle} - 1 . \quad (7.7)$$

This quantity vanishes for coherent (Poisson) light and is positive for classical light. (see Figure 7)

In equilibrium there is a relation between the average photon occupation number and the spin average in the atomic beam, which is trivial to derive from the equilibrium distribution (a=1)

$$\langle n \rangle = u^{0\top} \hat{n} p^0 = n_b + N\mathcal{P}(-) = n_b + N\frac{1 - \langle s \rangle}{2} , \quad (7.8)$$

where \hat{n} is a diagonal matrix representing the quantum number n . A similar but more uncertain relation between the Mandel quality factor and fluctuations in the atomic beam may also be derived [134].

The covariance between the values of the photon occupation number k atoms apart in equilibrium is easily seen to be given by

$$\langle nn \rangle_k = u^{0\top} \hat{n} S^k \hat{n} p^0 , \quad (7.9)$$

and again a normalized correlation function may be defined

$$\gamma_k^C = \frac{\langle nn \rangle_k - \langle n \rangle^2}{\langle n^2 \rangle - \langle n \rangle^2} . \quad (7.10)$$

The cavity correlation length ξ_C is defined by

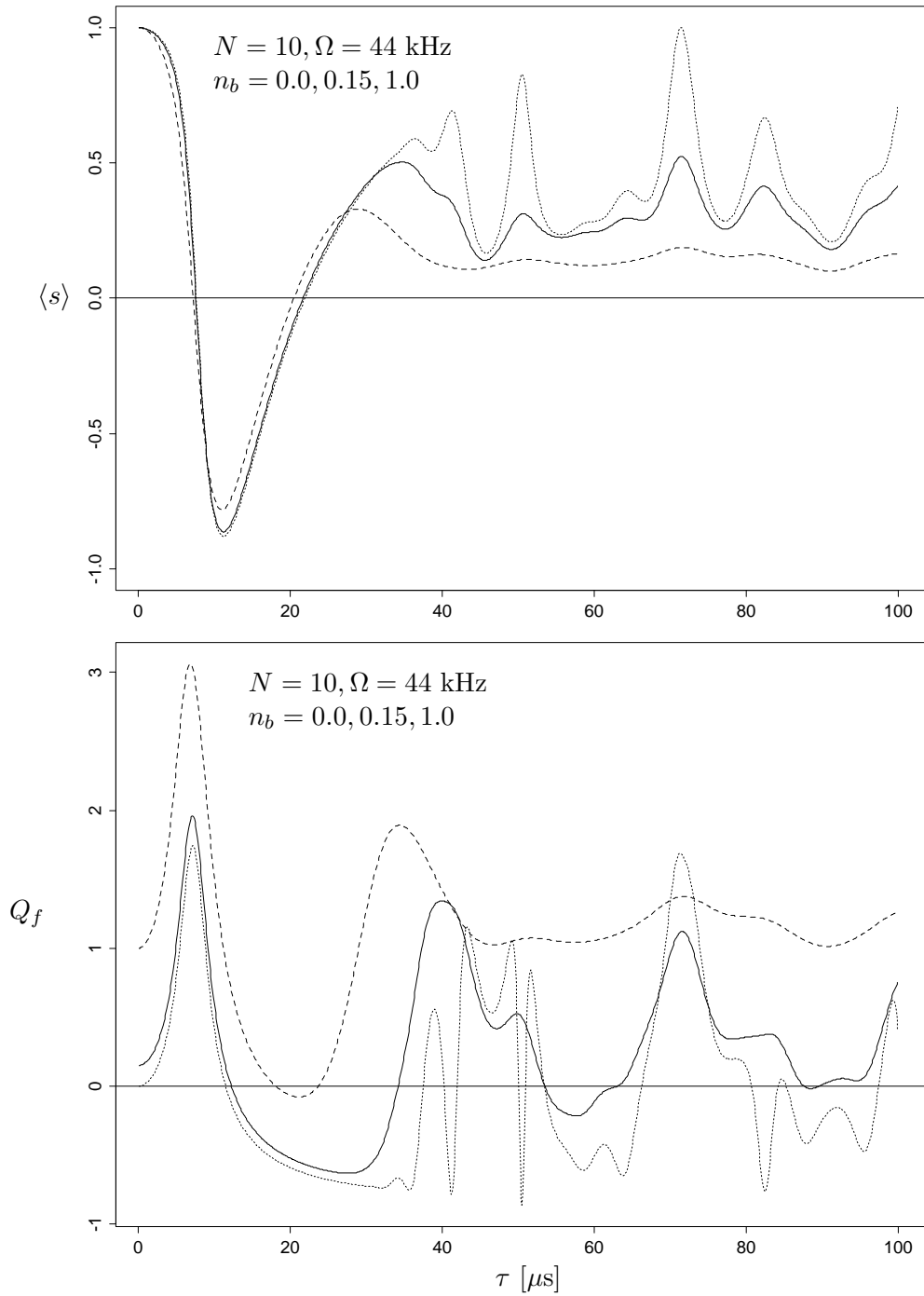


Figure 7: The upper figure shows the mean value of the spin variable as a function of the atomic passage time for three different values of n_b . The dotted line $n_b = 0$, the solid line $n_b = 0.15$, and the dashed line $n_b = 1.0$. The lower figure shows the Mandel quality factor in the same region for the same values of n_b . The pronounced structures in the case of $n_b = 0$ are caused by trapping states (see Section 11.1).

$$\gamma_k^C \sim \exp\left(-\frac{k}{R\xi_C}\right) . \quad (7.11)$$

Since the same power of the matrix S is involved, both correlation lengths are determined by the same eigenvalue, and the two correlation lengths are therefore identical $\xi_A = \xi_C = \xi$ and we shall no longer distinguish between them.

7.3 Monte Carlo Determination of Correlation Lengths

Since the statistical behaviour of the micromaser is a classical Markov process it is possible to simulate it by means of Monte Carlo methods using the cavity occupation number n as stochastic variable.

A sequence of excited atoms is generated at Poisson-distributed times and are allowed to act on n according to the probabilities given by Eq. (6.5). In these simulations we have for simplicity chosen $a = 1$ and $b = 0$. After the interaction the cavity is allowed to decay during the waiting time until the next atom arrives. The action of this process on the cavity variable n is simulated by means of the transition probabilities read off from the dissipative master equation (6.22) using a suitably small time step dt . The states of the atoms in the beam are determined by the pumping transitions and the atomic correlation function may be determined from this sequence of spin values $\{s_i\}$ by making suitable averages after the system has reached equilibrium. Observables are then measured in a standard manner. For the average spin Eq.(7.2) we e.g. write

$$\langle s \rangle = \lim_{L \rightarrow \infty} \frac{1}{L} \sum_{i=1}^L s_i , \quad (7.12)$$

and for the joint probability Eq.(7.3) we write

$$\mathcal{P}_k(s_1, s_2) = \lim_{L \rightarrow \infty} \frac{1}{L} \sum_{i=1}^L s_i s_{i+k} , \quad (7.13)$$

Finally we can then extract the correlation lengths numerically from the Monte Carlo data.

This extraction is, however, limited by noise due to the finite sample size which in our simulation is 10^6 atoms. In regions where the correlation length is large, it is fairly easy to extract it by fitting to the exponential decay, whereas it is more difficult in the regions where it is small (see Figure 8). This accounts for the differences between the exact numerical calculations and the Monte Carlo data in Figure 9. It is expected that real experiments will face the same type of problems in extracting the correlation lengths from real data.

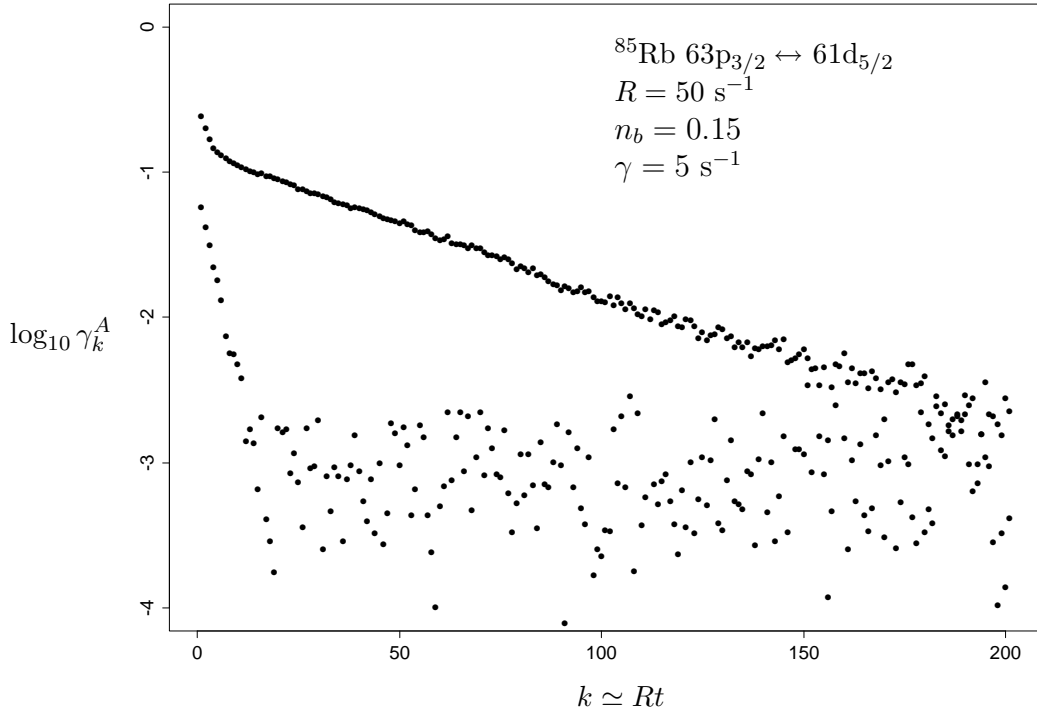


Figure 8: Monte Carlo data (with 10^6 simulated atoms) for the correlation as a function of the separation $k \simeq Rt$ between the atoms in the beam for $\tau = 25 \mu\text{s}$ (lower data points) and $\tau = 50 \mu\text{s}$ (upper data points). In the latter case the exponential decay at large times is clearly visible, whereas it is hidden in the noise in the former. The parameters are those of the experiment described in Ref. [136].

7.4 Numerical Calculation of Correlation Lengths

The micromaser equilibrium distribution is the solution of $Sp = p$, where S is the one-atom propagation matrix (6.29), so that p^0 is an eigenvector of S from the right with eigenvalue $\kappa_0 = 1$. The corresponding eigenvector from the left is u^0 and normalization of probabilities is expressed as $u^{0\top} p^0 = 1$. The general eigenvalue problem concerns solutions to $Sp = \kappa p$ from the right and $u^\top S = \kappa u^\top$ from the left. It is shown below that the eigenvalues are non-degenerate, which implies that there exists a spectral resolution of the form

$$S = \sum_{\ell=0}^{\infty} \kappa_\ell p^\ell u^{\ell\top} \quad , \quad (7.14)$$

with eigenvalues κ_ℓ and eigenvectors p^ℓ and u^ℓ from right and left respectively. The long-time behavior of the correlation function is governed by the next-to-leading eigenvalue $\kappa_1 < 1$, and we see that

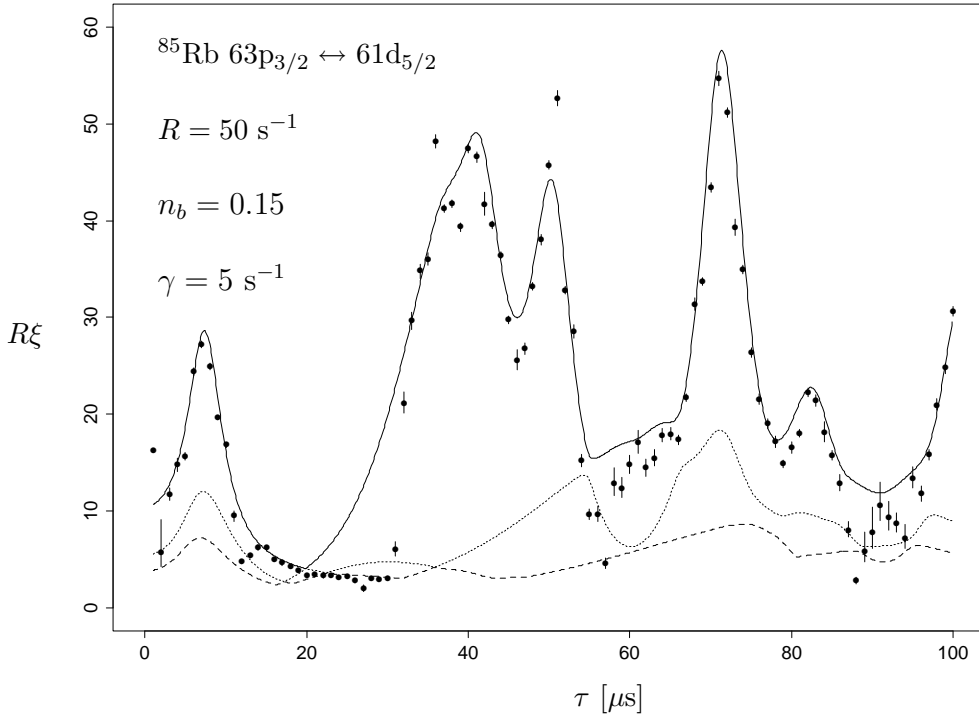


Figure 9: Comparison of theory (solid curve) and MC data (dots) for the correlation length $R\xi$ (sample size 10^6 atoms). The dotted and dashed curves correspond to sub-leading eigenvalues ($\kappa_{2,3}$) of the matrix S . The parameters are those of the experiment in Ref. [136].

$$R\xi = -\frac{1}{\log \kappa_1} . \quad (7.15)$$

The eigenvalues are determined by the characteristic equation $\det\{S - \kappa\} = 0$, which may be solved numerically. This procedure is, however, not well-defined for the infinite-dimensional matrix S , and in order to evaluate the determinant we have truncated the matrix to a large and finite-size $K \times K$ with typical $K \simeq 100$. The explicit form of S in Eq. (6.29) is used, which reduces the problem to the calculation of the determinant for a Jacobi matrix. Such a matrix vanishes outside the main diagonal and the two sub-leading diagonals on each side. It is shown in Section 8.3 that the eigenvalues found from this equation are indeed non-degenerate, real, positive and less than unity.

The next-to-leading eigenvalue is shown in Figure 9 and agrees very well with the Monte Carlo calculations. This figure shows a surprising amount of structure and part of the effort in the following will be to understand this structure in detail.

It is possible to derive an exact sum rule for the reciprocal eigenvalues (see Appendix B), which yields the approximate expression:

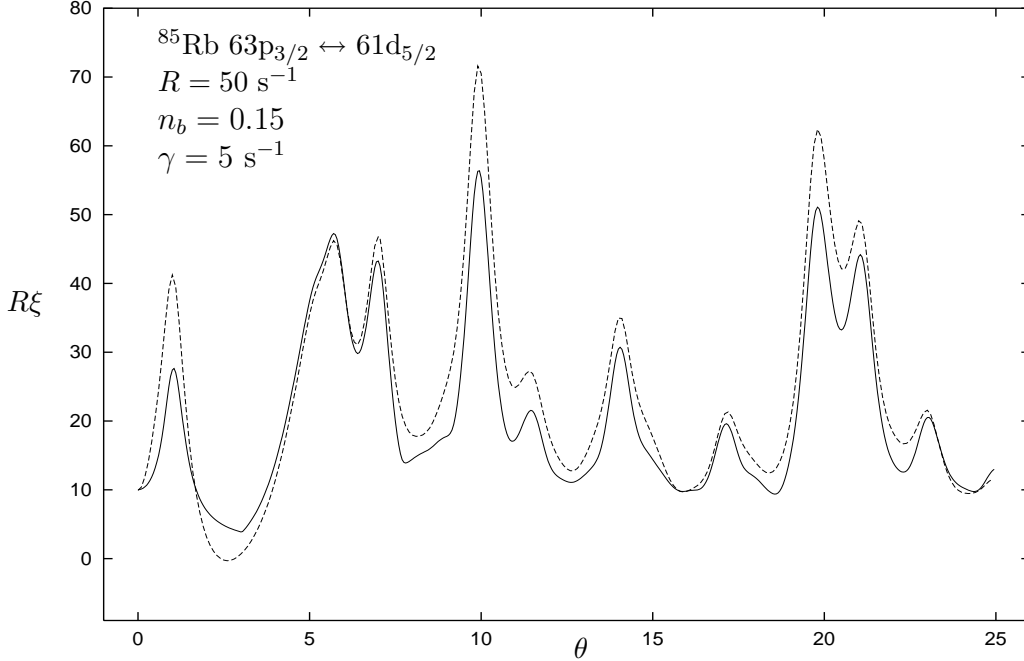


Figure 10: Comparison of the sum in Eq. (7.16) over reciprocal eigenvalues (dotted curve) with numerically determined correlation length (solid curve) for the same parameters as in Figure 9 as a function of $\theta = g\tau\sqrt{N}$, where $N = R/\gamma$. The difference between the curves is entirely due to the sub-dominant eigenvalues that have not been taken into account in Eq. (7.16).

$$\gamma\xi \simeq 1 + \sum_{n=1}^{\infty} \left(\frac{P_n(1 - P_n)}{((1 + n_b)n + Nbq_n)p_n} - \frac{1 - [n_b/(1 + n_b)]^n}{n} \right), \quad (7.16)$$

when the sub-dominant eigenvalues may be ignored. This formula for the correlation length is numerically rapidly converging. Here p_n is the equilibrium distribution Eq. (6.32) and $P_n = \sum_{m=0}^{n-1} p_m$ is the cumulative probability. In Figure 10 we compare the exact numerical calculation and the result of the sum rule in the case when $a = 1$, which is much less time-consuming to compute³.

It is also of importance to notice that the correlation length is very sensitive to the inversion to the atomic beam parameter a (see Figure 11) the detuning parameter $\delta = \Delta\omega/g$ (Figure 12).

Comparison of theory (solid curve) and MC data (dots) for the correlation length $R\xi$ (sample size 10^6 atoms). The dotted and dashed curves correspond to sub-leading eigenvalues ($\kappa_{2,3}$) of the matrix S . The parameters are those of the experiment in Ref. [136].

³Notice that we have corrected for a numerical error in Figure 4 of Ref.[4].

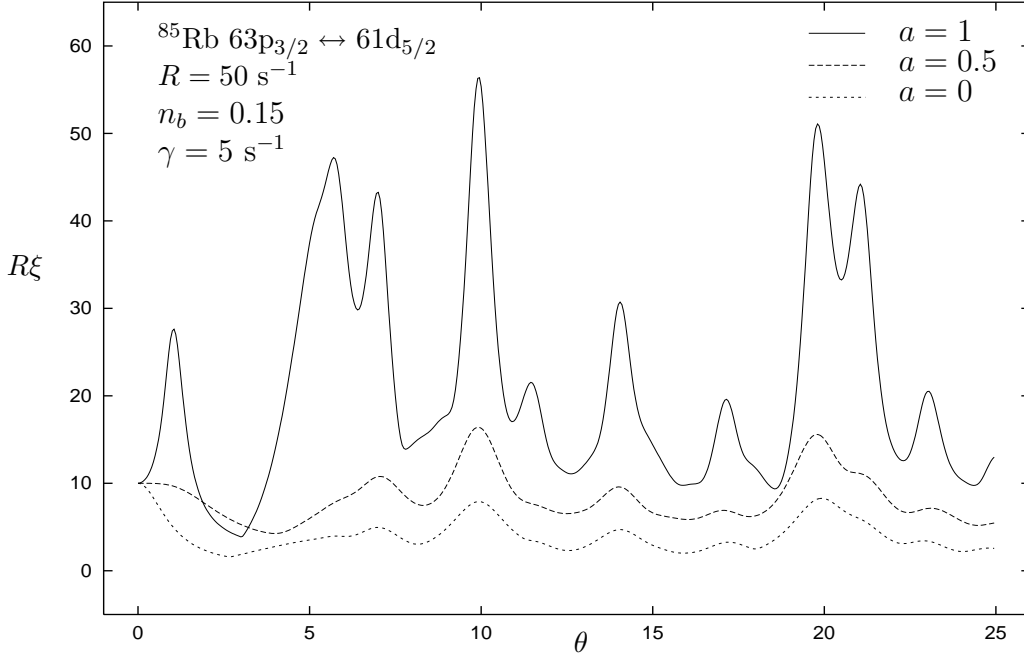


Figure 11: The correlation length $R\xi$ for the same parameters as in Figure 9 but for $a = 0, 0.5,$ and 1 as a function of $\theta = g\tau\sqrt{N}$, where $N = R/\gamma$.

8 Analytic Preliminaries

*“It is futile to employ many principles
when it is possible to employ fewer.”*

W. Ockham

In order to tackle the task of determining the phase structure in the micromaser we need to develop some mathematical tools. The dynamics can be formulated in two different ways which are equivalent in the large flux limit. Both are related to Jacobi matrices describing the stochastic process. Many characteristic features of the correlation length are related to scaling properties for $N \rightarrow \infty$, and require a detailed analysis of the continuum limit. Here we introduce some of the concepts that are used in the main analysis in Section 9.

8.1 Continuous Master Equation

When the atoms have Poisson distributed arrival times it is possible to formulate the problem as a differential equation [165]. Each atom has the same probability Rdt of arriving in an infinitesimal time interval dt . Provided the interaction with the cavity takes less time than this interval, i.e. $\tau \ll dt$, we may consider the transition to be instantaneous and write the transition matrix as $Rdt(M - 1)$ so that we get

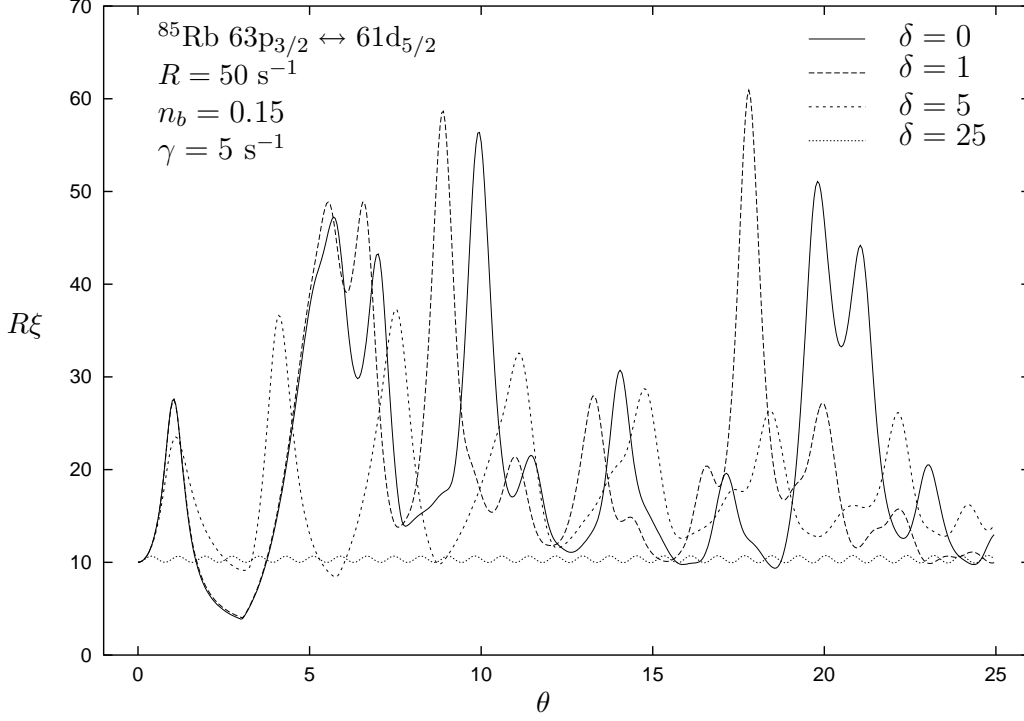


Figure 12: The correlation length $R\xi$ for the same parameters as in Figure 9 but for $\delta = \Delta\omega/g = 0, 1, 5$ and 25 as a function of $\theta = g\tau\sqrt{N}$, where $N = R/\gamma$.

$$\frac{dp}{dt} = -\gamma L_C p + R(M-1)p \equiv -\gamma L p \quad , \quad (8.1)$$

where $L = L_C - N(M-1)$. This equation obviously has the solution

$$p(t) = e^{-\gamma L t} p \quad . \quad (8.2)$$

Explicitly we have

$$\begin{aligned} L_{nm} = & (n_b + 1)(n\delta_{n,m} - (n+1)\delta_{n+1,m}) + n_b((n+1)\delta_{n,m} - n\delta_{n,m+1}) \\ & + N((aq_{n+1} + bq_n)\delta_{n,m} - aq_n\delta_{n,m+1} - bq_{n+1}\delta_{n+1,m}) \quad , \end{aligned} \quad (8.3)$$

and

$$\begin{aligned} \frac{1}{\gamma} \frac{dp_n}{dt} = & -(n_b + 1)(np_n - (n+1)p_{n+1}) - n_b((n+1)p_n - np_{n-1}) \\ & - N((aq_{n+1} + bq_n)p_n - aq_n p_{n-1} - bq_{n+1} p_{n+1}) \quad . \end{aligned} \quad (8.4)$$

The equilibrium distribution may be found by the same technique as before, writing the right-hand side of Eq. (8.4) as $J_{n+1} - J_n$ with

$$J_n = ((n_b + 1)n + Nbq_n)p_n - (n_b n + Naq_n)p_{n-1} \quad , \quad (8.5)$$

and setting $J_n = 0$ for all n . The equilibrium distribution is clearly given by the same expression (6.32) as in the discrete case.

8.2 Relation to the Discrete Case

Even if the discrete and continuous formulation has the same equilibrium distribution, there is a difference in the dynamical behavior of the two cases. In the discrete case the basic propagation matrix is S^k , where $S = (1 + L_C/N)^{-1}M$, whereas it is $\exp(-\gamma Lt)$ in the continuous case. For high pumping rate N we expect the two formalisms to coincide, when we identify $k \simeq Rt$. For the long-time behavior of the correlation functions this implies that the next-to-leading eigenvalues κ_1 of S and λ_1 of L must be related by $1/\xi = \gamma\lambda_1 \simeq -R \log \kappa_1$.

To prove this, let us compare the two eigenvalue problems. For the continuous case we have

$$(L_C - N(M - 1))p = \lambda p \quad , \quad (8.6)$$

whereas in the discrete case we may rewrite $Sp = \kappa p$ to become

$$\left(L_C - \frac{N}{\kappa}(M - 1)\right)p = N\left(\frac{1}{\kappa} - 1\right)p \quad . \quad (8.7)$$

Let a solution to the continuous case be $p(N)$ with eigenvalue $\lambda(N)$, making explicit the dependence on N . It is then obvious that $p(N/\kappa)$ is a solution to the discrete case with eigenvalue κ determined by

$$\lambda\left(\frac{N}{\kappa}\right) = N\left(\frac{1}{\kappa} - 1\right) \quad . \quad (8.8)$$

As we shall see below, for $N \gg 1$ the next-to-leading eigenvalue λ_1 stays finite or goes to zero, and hence $\kappa_1 \rightarrow 1$ at least as fast as $1/N$. Using this result it follows that the correlation length is the same to $\mathcal{O}(1/N)$ in the two formalisms.

8.3 The Eigenvalue Problem

The transition matrix L truncated to size $(K + 1) \times (K + 1)$ is a special kind of asymmetric Jacobi matrix

$$L_K = \left\{ \begin{array}{cccccc} A_0 + B_0 & -B_1 & 0 & 0 & \cdots & \\ -A_0 & A_1 + B_1 & -B_2 & 0 & \cdots & \\ 0 & -A_1 & A_2 + B_2 & -B_3 & & \\ \vdots & \vdots & \vdots & \vdots & \vdots & \\ & & & & -A_{K-2} & A_{K-1} + B_{K-1} & -B_K \\ & & & \cdots & 0 & -A_{K-1} & A_K + B_K \end{array} \right\}, \quad (8.9)$$

where

$$\begin{aligned} A_n &= n_b(n+1) + Naq_{n+1} \quad , \\ B_n &= (n_b+1)n + Nbq_n \quad . \end{aligned} \quad (8.10)$$

Notice that the sum over the elements in every column vanishes, except for the first and the last, for which the sums respectively take the values B_0 and A_K . In our case we have $B_0 = 0$, but A_K is non-zero. For $B_0 = 0$ it is easy to see (using row manipulation) that the determinant becomes $A_0 A_1 \cdots A_K$ and obviously diverges in the limit of $K \rightarrow \infty$. Hence the truncation is absolutely necessary. All the coefficients in the characteristic equation diverge, if we do not truncate. In order to secure that there is an eigenvalue $\lambda = 0$, we shall force $A_K = 0$ instead of the value given above. This means that the matrix is not just truncated but actually changed in the last diagonal element. Physically this secures that there is no external input to the process from cavity occupation numbers above K , a not unreasonable requirement.

An eigenvector to the right satisfies the equation $L_K p = \lambda p$, which takes the explicit form

$$-A_{n-1}p_{n-1} + (A_n + B_n)p_n - B_{n+1}p_{n+1} = \lambda p_n \quad . \quad (8.11)$$

Since we may solve this equation successively for p_1, p_2, \dots, p_K given p_0 , it follows that all eigenvectors are non-degenerate. The characteristic polynomial obeys the recursive equation

$$\det(L_K - \lambda) = (A_K + B_K - \lambda) \det(L_{K-1} - \lambda) - A_{K-1} B_K \det(L_{K-2} - \lambda) \quad , \quad (8.12)$$

and this is also the characteristic equation for a symmetric Jacobi matrix with off-diagonal elements $C_n = -\sqrt{A_{n-1}B_n}$. Hence the eigenvalues are the same and therefore all real and, as we shall see below, non-negative. They may therefore be

ordered $0 = \lambda_0 < \lambda_1 < \dots < \lambda_K$. The equilibrium distribution (6.32) corresponds to $\lambda = 0$ and is given by

$$p_n^0 = p_0^0 \prod_{m=1}^n \frac{A_{m-1}}{B_m} = p_0^0 \frac{A_0 A_1 \dots A_{n-1}}{B_1 B_2 \dots B_n} \quad \text{for } n = 1, 2, \dots, K \quad . \quad (8.13)$$

Notice that this expression does not involve the vanishing values $B_0 = A_K = 0$.

Corresponding to each eigenvector p to the right there is an eigenvector u to the left, satisfying $u^\top L_K = \lambda u^\top$, which in components reads

$$A_n(u_n - u_{n-1}) + B_n(u_n - u_{n+1}) = \lambda u_n \quad . \quad (8.14)$$

For $\lambda = 0$ we obviously have $u_n^0 = 1$ for all n and the scalar product $u^0 \cdot p^0 = 1$. The eigenvector to the left is trivially related to the eigenvector to the right via the equilibrium distribution

$$p_n = p_n^0 u_n \quad . \quad (8.15)$$

The full set of eigenvectors to the left and to the right $\{u^\ell, p^\ell \mid \ell = 0, 1, 2, \dots, K\}$ may now be chosen to be orthonormal $u^\ell \cdot p^{\ell'} = \delta_{\ell, \ell'}$, and is, of course, complete since the dimension K is finite.

It is useful to express this formalism in terms of averages over the equilibrium distribution $\langle f_n \rangle_0 = \sum_{n=0}^K f_n p_n^0$. Then using Eq. (8.15) we have, for an eigenvector with $\lambda > 0$, the relations

$$\begin{aligned} \langle u_n \rangle_0 &= 0 \quad , \\ \langle u_n^2 \rangle_0 &= 1 \quad , \\ \langle u_n u'_n \rangle_0 &= 0 \quad \text{for } \lambda \neq \lambda' \quad . \end{aligned} \quad (8.16)$$

Thus the eigenvectors with $\lambda > 0$ may be viewed as uncorrelated stochastic functions of n with zero mean and unit variance.

Finally, we rewrite the eigenvalue equation to the right in the form of $\lambda p_n = J_n - J_{n+1}$ with

$$J_n = B_n p_n - A_{n-1} p_{n-1} = p_n^0 B_n (u_n - u_{n-1}) \quad . \quad (8.17)$$

Using the orthogonality we then find

$$\lambda = \sum_{n=0}^K u_n (J_n - J_{n+1}) = \langle B_n (u_n - u_{n-1})^2 \rangle_0 \quad , \quad (8.18)$$

which incidentally proves that all eigenvalues are non-negative. It is also evident that an eigenvalue is built up from the non-constant parts, i.e. the jumps of u_n .

8.4 Effective Potential

It is convenient to introduce an effective potential V_n , first discussed by Filipowicz *et al.* [132] in the continuum limit, by writing the equilibrium distribution (6.32) in the form

$$p_n = \frac{1}{Z} e^{-NV_n} \quad , \quad (8.19)$$

with

$$V_n = -\frac{1}{N} \sum_{m=1}^n \log \frac{n_b m + Naq_m}{(1+n_b)m + Nbq_m} \quad , \quad (8.20)$$

for $n \geq 1$. The value of the potential for $n = 0$ may be chosen arbitrarily, for example $V_0 = 0$, because of the normalization constant

$$Z = \sum_{n=0}^{\infty} e^{-NV_n} \quad . \quad (8.21)$$

It is, of course, completely equivalent to discuss the shape of the equilibrium distribution and the shape of the effective potential. Our definition of V_n differs from the one introduced in Refs. [132, 152] in the sense that our V_n is *exact* while the one in [132, 152] was derived from a Fokker-Planck equation in the continuum limit.

8.5 Semicontinuous Formulation

Another way of making analytical methods, such as the Fokker-Planck equation, easier to use is to rewrite the formalism (exactly) in terms of the scaled photon number variable x and the scaled time parameter θ , defined by [132]

$$\begin{aligned} x &= \frac{n}{N} \quad , \\ \theta &= g\tau\sqrt{N} \quad . \end{aligned} \quad (8.22)$$

Notice that the variable x and not n is the natural variable when observing the field in the cavity by means of the atomic beam (see Eq.(7.9)). Defining $\Delta x = 1/N$ and introducing the scaled probability distribution $p(x) = Np_n$ the conservation of probability takes the form

$$\sum_{x=0}^{\infty} \Delta x p(x) = 1 \quad , \quad (8.23)$$

where the sum extends over all discrete values of x in the interval. Similarly the equilibrium distribution takes the form

$$p^0(x) = \frac{1}{Z_x} e^{-NV(x)} \quad , \quad (8.24)$$

with the effective potential given as an “integral”

$$V(x) = \sum_{x'>0}^x \Delta x' D(x') \quad , \quad (8.25)$$

with “integrand”

$$D(x) = -\log \frac{n_b x + a q(x)}{(1 + n_b)x + b q(x)} \quad . \quad (8.26)$$

The transition probability function is $q(x) = \sin^2 \theta \sqrt{x}$ and the normalization constant is given by

$$Z_x = \frac{Z}{N} = \sum_{x=0}^{\infty} \Delta x e^{-NV(x)} \quad . \quad (8.27)$$

In order to reformulate the master equation (8.4) it is convenient to introduce the discrete derivatives $\Delta_+ f(x) = f(x + \Delta x) - f(x)$ and $\Delta_- f(x) = f(x) - f(x - \Delta x)$. Then we find

$$\frac{1}{\gamma} \frac{dp(x)}{dt} = \frac{\Delta_+}{\Delta x} J(x) \quad , \quad (8.28)$$

with

$$J(x) = (x - (a - b)q(x))p(x) + \frac{1}{N}(n_b x + a q(x)) \frac{\Delta_-}{\Delta x} p(x) \quad . \quad (8.29)$$

For the general eigenvector we define $p(x) = N p_n$ and write it as $p(x) = p^0(x) u(x)$ with $u(x) = u_n$ and find the equations

$$\lambda p(x) = -\frac{\Delta_+}{\Delta x} J(x) \quad , \quad (8.30)$$

and

$$J(x) = \frac{1}{N} p^0(x) ((1 + n_b)x + bq(x)) \frac{\Delta_-}{\Delta x} u(x) . \quad (8.31)$$

Equivalently the eigenvalue equation for $u(x)$ becomes

$$\lambda u(x) = (x - (a - b)q(x)) \frac{\Delta_-}{\Delta x} u(x) - \frac{1}{N} \frac{\Delta_+}{\Delta x} \left[(n_b x + aq(x)) \frac{\Delta_-}{\Delta x} u(x) \right] . \quad (8.32)$$

As before we also have

$$\begin{aligned} \langle u(x) \rangle_0 &= 0 , \\ \langle u(x)^2 \rangle_0 &= 1 , \end{aligned} \quad (8.33)$$

where now the average over $p^0(x)$ is defined as $\langle f(x) \rangle_0 = \sum_x \Delta x f(x) p^0(x)$. As before we may also express the eigenvalue as an average

$$\lambda = \frac{1}{N} \left\langle ((1 + n_b)x + bq(x)) \left(\frac{\Delta_- u(x)}{\Delta x} \right)^2 \right\rangle_0 . \quad (8.34)$$

Again it should be emphasized that all these formulas are exact rewritings of the previous ones, but this formulation permits easy transition to the continuum case, wherever applicable.

8.6 Extrema of the Continuous Potential

The quantity $D(x)$ in Eq. (8.26) has a natural continuation to all real values of x as a smooth differentiable function. The condition for smoothness is that the change in the argument $\theta\sqrt{x}$ between two neighbouring values, x and $x + \Delta x$ is much smaller than 1, or $\theta \ll 2N\sqrt{x}$. Hence for $N \rightarrow \infty$ the function is smooth everywhere and the sum in Eq. (8.25) may be replaced by an integral

$$V(x) = \int_0^x dx' D(x') , \quad (8.35)$$

so that $D(x) = V'(x)$. In Figure 13 we illustrate the typical behaviour of the potential and the corresponding photon number distribution in the first critical region (see Section 9.6). Notice that the photon-number distribution exhibits Schleich–Wheeler oscillations typical of a squeezed state (see e.g. Refs. [48], [167]–[172]).

The extrema of this potential are located at the solutions to $q(x) = x$; they may be parametrized in the form

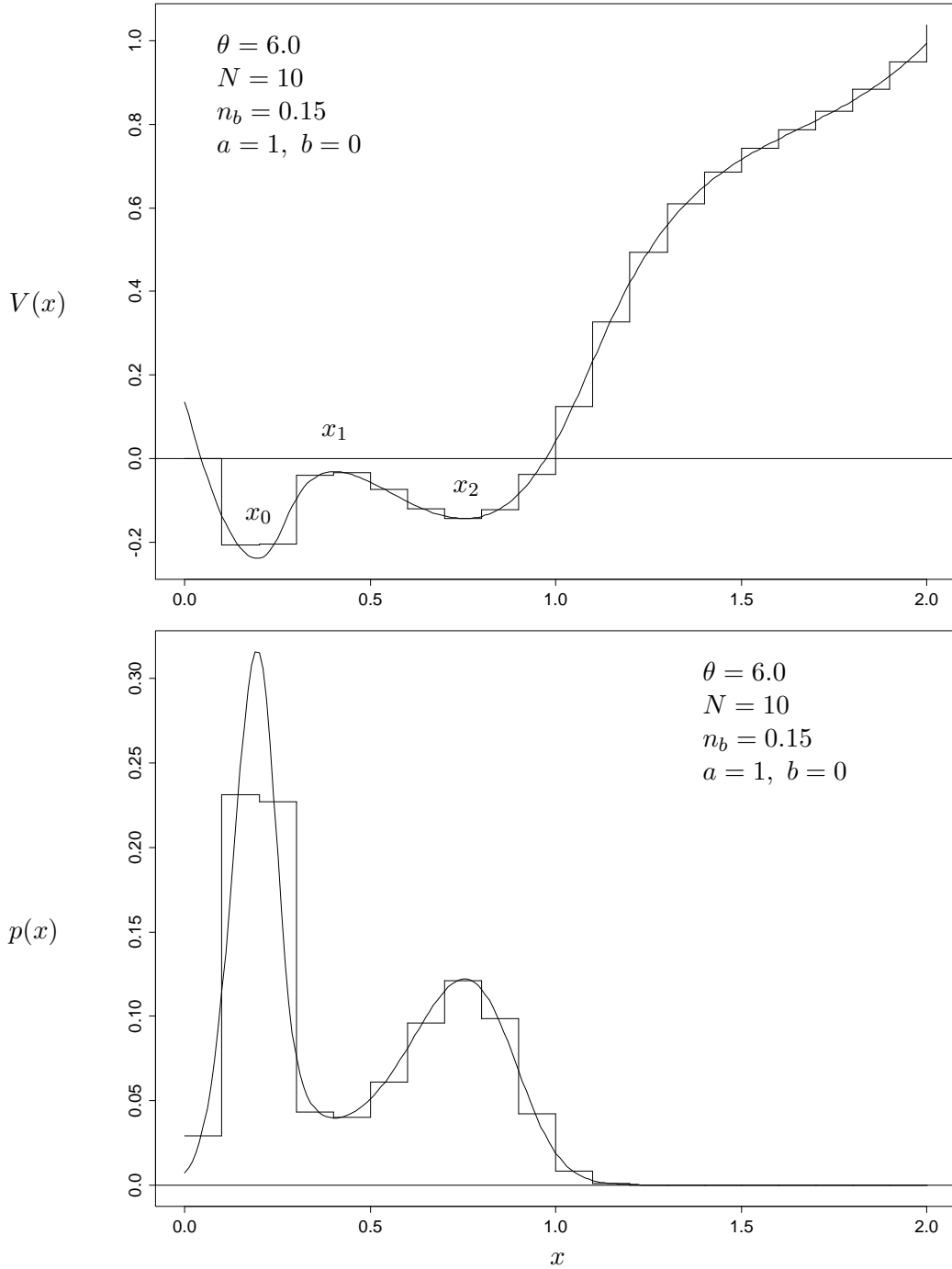


Figure 13: Example of a potential with two minima x_0, x_2 and one maximum x_1 (upper graph). The rectangular curve represents the exact potential (8.20), whereas the continuous curve is given by Eq. (8.25) with the summation replaced by an integral. The value of the continuous potential at $x = 0$ has been chosen such as to make the distance minimal between the two curves. In the lower graph the corresponding probability distribution is shown.

$$\begin{aligned}
x &= (a - b) \sin^2 \phi \ , \\
\theta &= \frac{1}{\sqrt{a - b}} \frac{\phi}{|\sin \phi|} \ ,
\end{aligned}
\tag{8.36}$$

with $0 \leq \phi < \infty$. These formulas map out a multibranched function $x(\theta)$ with critical points where the derivative

$$D'(x) = V''(x) = \frac{(a + n_b(a - b))(q(x) - xq'(x))}{((1 + n_b)x + bq(x))(n_b x + aq(x))}
\tag{8.37}$$

vanishes, which happens at the values of ϕ satisfying $\phi = \tan \phi$. This equation has an infinity of solutions, $\phi = \phi_k$, $k = 0, 1, \dots$, with $\phi_0 = 0$ and to a good approximation

$$\phi_k = (2k + 1) \frac{\pi}{2} - \frac{1}{(2k + 1) \frac{\pi}{2}} + \mathcal{O} \left(\left((2k + 1) \frac{\pi}{2} \right)^{-3} \right)
\tag{8.38}$$

for $k = 1, 2, \dots$, and each of these branches is double-valued, with a sub-branch corresponding to a minimum ($D' > 0$) and another corresponding to a maximum ($D' < 0$). Since there are always $k + 1$ minima and k maxima, we denote the minima $x_{2k}(\theta)$ and the maxima $x_{2k+1}(\theta)$. Thus the minima have even indices and the maxima have odd indices. They are given as a function of θ through Eq. (8.36) when ϕ runs through certain intervals. Thus, for the minima of $V(x)$, we have

$$\phi_k < \phi < (k + 1)\pi, \quad \theta_k < \theta < \infty, \quad a - b > x_{2k}(\theta) > 0, \quad k = 0, 1, \dots \ ,
\tag{8.39}$$

and for the maxima

$$k\pi < \phi < \phi_k, \quad \infty > \theta > \theta_k, \quad 0 < x_{2k+1}(\theta) < a - b, \quad k = 1, \dots
\tag{8.40}$$

Here $\theta_k = \phi_k / |\sin \phi_k| \sqrt{a - b}$ is the value of θ for which the k 'th branch comes into existence. Hence in the interval $\theta_k < \theta < \theta_{K+1}$ there are exactly $2K + 1$ branches, $x_0, x_1, x_2, \dots, x_{2K-1}, x_{2K}$, forming the $K + 1$ minima and K maxima of $V(x)$. For $0 < \theta < \theta_0 = 1/\sqrt{a - b}$ there are no extrema.

This classification allows us to discuss the different parameter regimes that arise in the limit of $N \rightarrow \infty$. Each regime is separated from the others by singularities and are thus equivalent to the phases that arise in the thermodynamic limit of statistical mechanics.

9 The Phase Structure of the Micromaser System

*“Generalization naturally starts from the simplest,
the most transparent particular case.”*

G. Polya

We shall from now on limit the discussion to the case of initially completely excited atoms, $a = 1$, $b = 0$, which simplifies the following discussion considerably. The case of $a \neq 1$ is considered in Ref.[173].

The central issue in these lectures is the phase structure of the correlation length as a function of the parameter θ . In the limit of infinite atomic pumping rate, $N \rightarrow \infty$, the statistical system described by the master equation (6.17) has a number of different dynamical phases, separated from each other by singular boundaries in the space of parameters. We shall in this section investigate the character of the different phases, with special emphasis on the limiting behavior of the correlation length. There turns out to be several qualitatively different phases within a range of θ close to experimental values. First, the thermal phase and the transition to the maser phase at $\theta = 1$ has previously been discussed in terms of $\langle n \rangle$ [132, 165, 152]. The new transition to the critical phase at $\theta_1 \simeq 4.603$ is not revealed by $\langle n \rangle$ and the introduction of the correlation length as an observable is necessary to describe it. In the large flux limit $\langle n \rangle$ and $\langle (\Delta n)^2 \rangle$ are only sensitive to the probability distribution close to its global maximum. The correlation length depends crucially also on local maxima and the phase transition at θ_1 occurs when a new local maximum emerges. At $\theta \simeq 6.3$ there is a phase transition in $\langle n \rangle$ taking a discrete jump to a higher value. It happens when there are two competing global minima in the effective potential for different values of n . At the same point the correlation length reaches its maximum. In Figure 14 we show the correlation length in the thermal and maser phases, and in Figure 16 the critical phases, for various values of the pumping rate N .

9.1 Empty Cavity

When there is no interaction, i.e. $M = 1$, or equivalently $q_n = 0$ for all n , the behavior of the cavity is purely thermal, and then it is possible to find the eigenvalues explicitly. Let us in this case write

$$L_C = (2n_b + 1)L_3 - (1 + n_b)L_- - n_b L_+ - \frac{1}{2} \quad , \quad (9.1)$$

where

$$\begin{aligned}
(L_3)_{nm} &= \left(n + \frac{1}{2}\right) \delta_{nm} \ , \\
(L_+)_{nm} &= n \delta_{n,m+1} \ , \\
(L_-)_{nm} &= (n + 1) \delta_{n+1,m} \ .
\end{aligned}
\tag{9.2}$$

These operators form a representation of the Lie algebra of SU(1,1)

$$[L_-, L_+] = 2L_3 \ , \quad [L_3, L_\pm] = \pm L_\pm \ . \tag{9.3}$$

It then follows that

$$L_C = e^{rL_+} e^{-(1+n_b)L_-} (L_3 - \frac{1}{2}) e^{(1+n_b)L_-} e^{-rL_+} \ , \tag{9.4}$$

where $r = n_b/(1 + n_b)$. This proves that L_C has the same eigenvalue spectrum as the simple number operator $L_3 - \frac{1}{2}$, i.e. $\lambda_n = n$ for $n = 0, 1, \dots$ independent of the n_b . Since $M = 1$ for $\tau = 0$ this is a limiting case for the correlation lengths $\gamma\xi_n = 1/\lambda_n = 1/n$ for $\theta = 0$. From Eq. (8.8) we obtain $\kappa_n = 1/(1 + n/N)$ in the non-interacting case. Hence in the discrete case $R\xi_n = -1/\log \kappa_n \simeq N/n$ for $N \gg n$ and this agrees with the values in Figure 9 for $n = 1, 2, 3$ near $\tau = 0$.

9.2 Thermal Phase: $0 \leq \theta < 1$

In this phase the natural variable is n , not $x = n/N$. The effective potential has no extremum for $0 < n < \infty$, but is smallest for $n = 0$. Hence for $N \rightarrow \infty$ it may be approximated by its leading linear term everywhere in this region

$$NV_n = n \log \frac{n_b + 1}{n_b + \theta^2} \ . \tag{9.5}$$

Notice that the slope vanishes for $\theta = 1$. The higher-order terms play no role as long as $1 - \theta^2 \gg 1/\sqrt{N}$, and we obtain a Planck distribution

$$p_n^0 = \frac{1 - \theta^2}{1 + n_b} \left(\frac{n_b + \theta^2}{1 + n_b} \right)^n \ , \tag{9.6}$$

with photon number average

$$\langle n \rangle = \frac{n_b + \theta^2}{1 - \theta^2} \ , \tag{9.7}$$

which (for $\theta > 0$) corresponds to an increased temperature. Thus the result of pumping the cavity with the atomic beam is simply to raise its effective temperature in

this region. The mean occupation number $\langle n \rangle$ does not depend on the dimensionless pumping rate N (for sufficiently large N).

The variance is

$$\sigma_n^2 = \langle n^2 \rangle - \langle n \rangle^2 = \langle n \rangle(1 + \langle n \rangle) = \frac{(1 + n_b)(n_b + \theta^2)}{(1 - \theta^2)^2} , \quad (9.8)$$

and the first non-leading eigenvector is easily shown to be

$$u_n = \frac{n - \langle n \rangle}{\sigma_n} , \quad (9.9)$$

which indeed has the form of a univariate variable. The corresponding eigenvalue is found from Eq. (8.34) $\lambda_1 = 1 - \theta^2$, or

$$\gamma\xi = \frac{1}{1 - \theta^2} . \quad (9.10)$$

Thus the correlation length diverges at $\theta = 1$ (for $N \rightarrow \infty$).

9.3 First Critical Point: $\theta = 1$

Around the critical point at $\theta = 1$ there is competition between the linear and quadratic terms in the expansion of the potential for small x

$$V(x) = x \log \frac{n_b + 1}{n_b + \theta^2} + \frac{1}{6} x^2 \frac{\theta^4}{\theta^2 + n_b} + \mathcal{O}(x^3) . \quad (9.11)$$

Expanding in $\theta^2 - 1$ we get

$$V(x) = \frac{1 - \theta^2}{1 + n_b} x + \frac{1}{6(1 + n_b)} x^2 + \mathcal{O}(x^3, (\theta^2 - 1)^2) . \quad (9.12)$$

Near the critical point, i.e. for $(1 - \theta^2)\sqrt{N} \ll 1$, the quadratic term dominates, so the average value $\langle x \rangle$ as well as the width σ_x becomes of $\mathcal{O}(1/\sqrt{N})$ instead of $\mathcal{O}(1/N)$.

Let us therefore introduce two scaling variables r and α through

$$x = r \sqrt{\frac{3(1 + n_b)}{N}} , \quad \theta^2 - 1 = \alpha \sqrt{\frac{1 + n_b}{3N}} , \quad (9.13)$$

so that the probability distribution in terms of these variables becomes a Gaussian on the half-line, i.e.

$$p^0(r) = \frac{1}{Z_r} e^{-\frac{1}{2}(r-\alpha)^2} \quad (9.14)$$

with

$$Z_r = \int_0^\infty dr e^{-\frac{1}{2}(r-\alpha)^2} = \sqrt{\frac{\pi}{2}} \left(1 + \operatorname{erf} \left(\frac{\alpha}{\sqrt{2}} \right) \right) . \quad (9.15)$$

From this we obtain

$$\langle r \rangle = \alpha + \frac{d \log Z_r}{d\alpha} , \quad \sigma_r^2 = \frac{d \langle r \rangle}{d\alpha} . \quad (9.16)$$

For $\alpha = 0$ we have explicitly

$$\langle x \rangle = \sqrt{\frac{12(1+n_b)}{\pi N}} , \quad \sigma_x^2 = \frac{6(n_b+1)}{N} \left(\frac{1}{2} - \frac{1}{\pi} \right) . \quad (9.17)$$

This leads to the following equation for $u(r)$

$$\rho u = r(r-\alpha) \frac{du}{dr} - \frac{d}{dr} \left[r \frac{du}{dr} \right] , \quad (9.18)$$

where

$$\rho = \lambda \sqrt{\frac{3N}{1+n_b}} = \left\langle r \left(\frac{du}{dr} \right)^2 \right\rangle_0 . \quad (9.19)$$

This eigenvalue problem has no simple solution.

We know, however, that $u(r)$ must change sign once, say at $r = r_0$. In the neighborhood of the sign change we have $u \simeq r - r_0$ and, inserting this into (9.18) we get $r_0 = (\alpha + \sqrt{4 + \alpha^2})/2$ and $\rho = \sqrt{4 + \alpha^2}$ such that

$$\gamma \xi = \sqrt{\frac{3N}{(1+n_b)(4+\alpha^2)}} . \quad (9.20)$$

9.4 Maser Phase: $1 < \theta < \theta_1 \simeq 4.603$

In the region above the transition at $\theta = 1$ the mean occupation number $\langle n \rangle$ grows proportionally with the pumping rate N , so in this region the cavity acts as a maser. There is a single minimum of the effective potential described by the branch $x_0(\theta)$, defined by the region $0 < \phi < \pi$ in Eq. (8.36). We find for $N \gg 1$ to a good approximation in the vicinity of the minimum a Gaussian behavior

$$p^0(x) = \sqrt{\frac{NV''(x_0)}{2\pi}} e^{-\frac{N}{2}V''(x_0)(x-x_0)^2} , \quad (9.21)$$

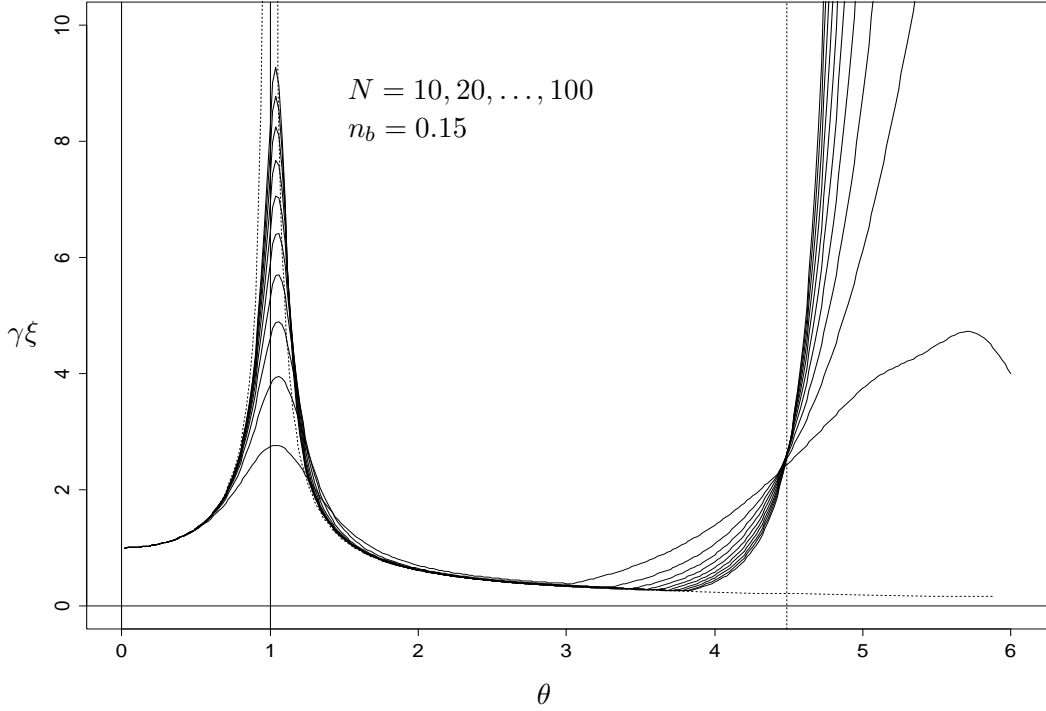


Figure 14: The correlation length in the thermal and maser phases as a function of θ for various values of N . The dotted curves are the limiting value for $N = \infty$. The correlation length grows as \sqrt{N} near $\theta = 1$ and exponentially for $\theta > \theta_1 \simeq 4.603$.

where

$$V''(x_0) = \frac{1 - q'(x_0)}{x_0(1 + n_b)} . \quad (9.22)$$

Hence for $(\theta^2 - 1)\sqrt{N} \gg 1$ we have a mean value $\langle x \rangle_0 = x_0$ and variance $\sigma_x^2 = 1/NV''(x_0)$. To find the next-to-leading eigenvalue in this case we introduce the scaling variable $r = \sqrt{NV''(x_0)}(x - x_0)$, which has zero mean and unit variance for large N . Then Eq. (8.32) takes the form (in the continuum limit $N \rightarrow \infty$)

$$\lambda u = (1 - q'(x_0)) \left(r \frac{du}{dr} - \frac{d^2u}{dr^2} \right) . \quad (9.23)$$

This is the differential equation for Hermite polynomials. The eigenvalues are $\lambda_n = n(1 - q'(x_0))$, $n = 0, 1, \dots$, and grow linearly with n . This may be observed in Figure 9. The correlation length becomes

$$\xi = \frac{1}{1 - q'(x_0)} = \frac{1}{1 - \phi \cot \phi} \quad \text{for } 0 < \phi < \pi . \quad (9.24)$$

As in the thermal phase, the correlation length is independent of N (for large N).

9.5 Mean Field Calculation

We shall now use a mean field method to get an expression for the correlation length in both the thermal and maser phases and in the critical region. We find from the time-dependent probability distribution (8.4) the following *exact* equation for the average photon occupation number:

$$\frac{1}{\gamma} \frac{d\langle n \rangle}{dt} = N\langle q_{n+1} \rangle + n_b - \langle n \rangle \quad , \quad (9.25)$$

or with $\Delta x = 1/N$

$$\frac{1}{\gamma} \frac{d\langle x \rangle}{dt} = \langle q(x + \Delta x) \rangle + n_b \Delta x - \langle x \rangle \quad . \quad (9.26)$$

We shall ignore the fluctuations of x around its mean value and simply replace this by

$$\frac{1}{\gamma} \frac{d\langle x \rangle}{dt} = q(\langle x \rangle + \Delta x) + n_b \Delta x - \langle x \rangle \quad . \quad (9.27)$$

This is certainly a good approximation in the limit of $N \rightarrow \infty$ for the maser phase because the relative fluctuation $\sigma_x/\langle x \rangle$ vanishes as $\mathcal{O}(1/\sqrt{N})$ here, but it is of dubious validity in the thermal phase, where the relative fluctuations are independent of N . Nevertheless, we find numerically that the mean field description is rather precise in the whole interval $0 < \theta < \theta_1$.

The fixed point x_0 of the above equation satisfies the mean field equation

$$x_0 = q(x_0 + \Delta x) + n_b \Delta x \quad , \quad (9.28)$$

which may be solved in parametric form as

$$\begin{aligned} x_0 &= \sin^2 \phi + n_b \Delta x \quad , \\ \theta &= \frac{\phi}{\sqrt{\sin^2 \phi + (1 + n_b) \Delta x}} \quad . \end{aligned} \quad (9.29)$$

We notice here that there is a maximum region of existence for any branch of the solution. The maximum is roughly given by $\theta_k^{\max} = (k + 1)\pi\sqrt{N/(1 + n_b)}$.

For small perturbations $\langle x \rangle = x_0 + \epsilon$ we find the equation of motion

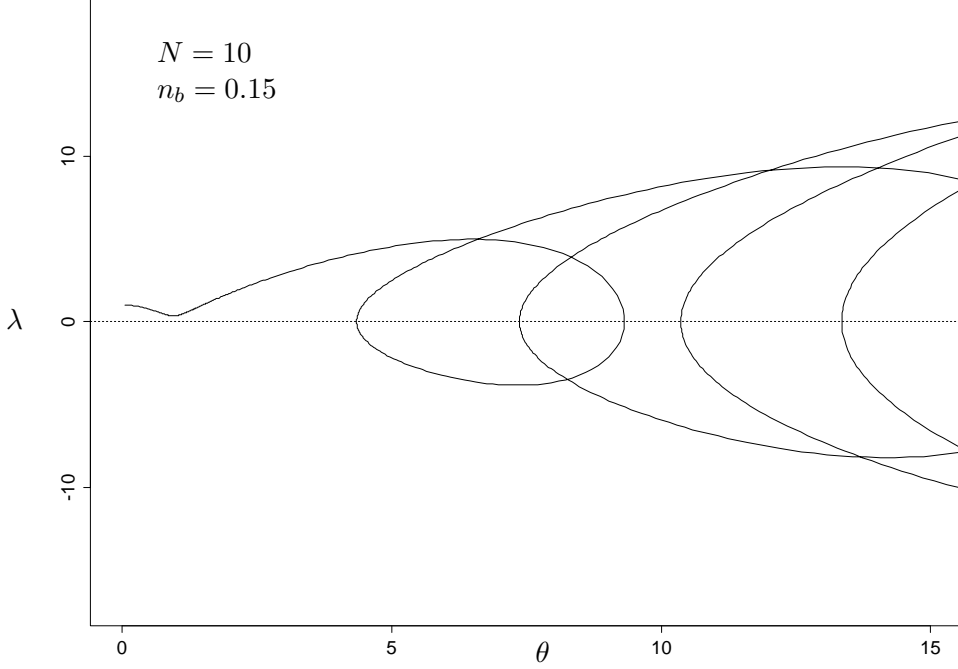


Figure 15: Mean field solution for the sub-leading eigenvalue.

$$\frac{1}{\gamma} \frac{d\epsilon}{dt} = -(1 - q'(x_0 + \Delta x))\epsilon \quad , \quad (9.30)$$

from which we estimate the leading eigenvalue

$$\lambda = 1 - q'(x_0 + \Delta x) = 1 - \frac{\phi \sin \phi \cos \phi}{\sin^2 \phi + (1 + n_b)\Delta x} \quad . \quad (9.31)$$

In Figure 15 this solution is plotted as a function of θ . Notice that it takes negative values in the unstable regions of ϕ . This eigenvalue does not vanish at the critical point $\theta = 1$ which corresponds to

$$\phi \simeq \phi_0 = \left(\frac{3(1 + n_b)}{N} \right)^{\frac{1}{4}} \quad , \quad (9.32)$$

but only reaches a small value

$$\lambda \simeq 2\sqrt{\frac{1 + n_b}{3N}} \quad , \quad (9.33)$$

which agrees exactly with the previously obtained result (9.20). Introducing the scaling variable α from (9.13) and defining $\psi = (\phi/\phi_0)^2$ we easily get

$$\begin{aligned}
\alpha &= (\psi^2 - 1)/\psi \quad , \\
r &= \psi \quad , \\
\rho &= (\psi^2 + 1)/\psi \quad ,
\end{aligned}
\tag{9.34}$$

and after eliminating ψ

$$\begin{aligned}
r &= \frac{1}{2}(\alpha + \sqrt{\alpha^2 + 4}) \quad , \\
\rho &= \sqrt{4 + \alpha^2} \quad ,
\end{aligned}
\tag{9.35}$$

which agrees with the previously obtained results.

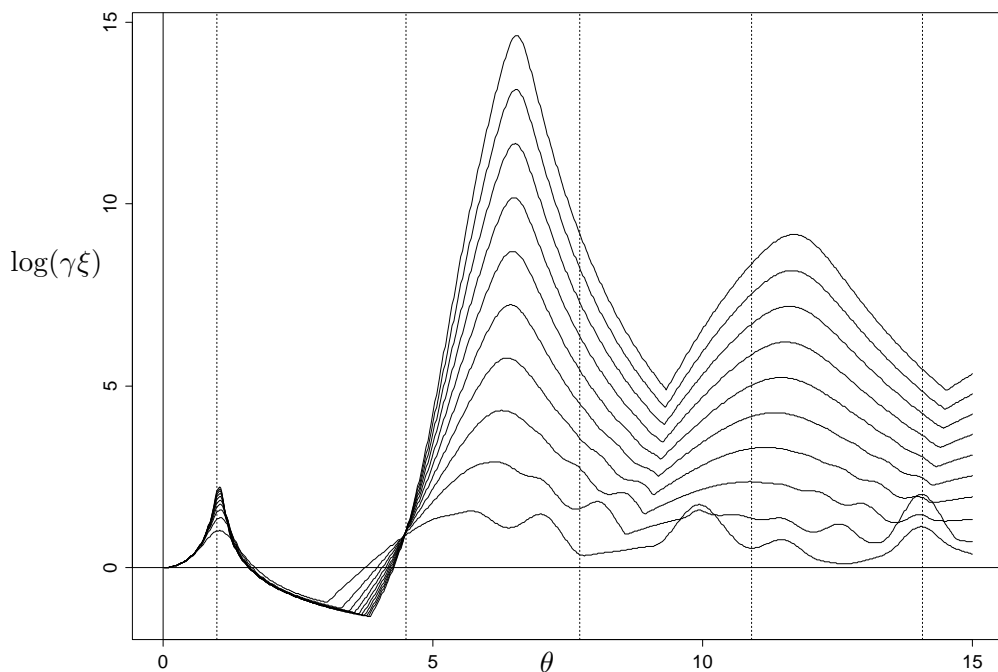


Figure 16: *The logarithm of the correlation length as a function of θ for various values of N (10, 20, ..., 100). We have $n_b = 0.15$ here. Notice that for $\theta > \theta_1$ the logarithm of the correlation length grows linearly with N for large N . The vertical lines indicate $\theta_0 = 1$, $\theta_1 = 4.603$, $\theta_2 = 7.790$, $\theta_3 = 10.95$ and $\theta_4 = 14.10$.*

9.6 The First Critical Phase: $4.603 \simeq \theta_1 < \theta < \theta_2 \simeq 7.790$

We now turn to the first phase in which the effective potential has two minima (x_0, x_2) and a maximum (x_1) in between (see Figure 13 in Section 8.6). In this case there is competition between the two minima separated by the barrier and for

$N \rightarrow \infty$ this barrier makes the relaxation time to equilibrium exponentially long. Hence we expect λ_1 to be exponentially small for large N (see Figure 16)

$$\lambda_1 = C e^{-\eta N} \quad , \quad (9.36)$$

where C and η are independent of N . It is the extreme smallness of the sub-leading eigenvalue that allows us to calculate it with high precision.

For large N the probability distribution consists of two well-separated narrow maxima, each of which is approximately a Gaussian. We define the *a priori* probabilities for each of the peaks

$$P_0 = \sum_{0 \leq x < x_1} \Delta x p^0(x) = \frac{Z_0}{Z} \quad , \quad (9.37)$$

and

$$P_2 = \sum_{x_1 \leq x < \infty} \Delta x p^0(x) = \frac{Z_2}{Z} \quad . \quad (9.38)$$

The Z -factors are

$$Z_0 = \sum_{x=0}^{x_1} \Delta x e^{-NV(x)} \simeq e^{-NV_0} \sqrt{\frac{2\pi}{NV_0''}} \quad , \quad (9.39)$$

and

$$Z_2 = \sum_{x=x_1}^{\infty} \Delta x e^{-NV(x)} \simeq e^{-NV_2} \sqrt{\frac{2\pi}{NV_2''}} \quad , \quad (9.40)$$

with $Z = Z_0 + Z_2$. The probabilities satisfy of course $P_0 + P_2 = 1$ and we have

$$p^0(x) = P_0 p_0^0(x) + P_2 p_2^0(x) \quad , \quad (9.41)$$

where $p_{0,2}^0$ are individual probability distributions with maximum at $x_{0,2}$. The overlap error in these expressions vanishes rapidly for $N \rightarrow \infty$, because the ratio P_0/P_2 either converges towards 0 or ∞ for $V_0 \neq V_2$. The transition from one peak being the highest to the other peak being the highest occurs when the two maxima coincide, i.e. at $\theta \simeq 7.22$ at $N = 10$, whereas for $N = \infty$ it happens at $\theta \simeq 6.66$. At this point the correlation length is also maximal.

Using this formalism, many quantities may be evaluated in the limit of large N . Thus for example

$$\langle x \rangle_0 = P_0 x_0 + P_2 x_2 \quad , \quad (9.42)$$

and

$$\sigma_x^2 = \langle (x - \langle x \rangle_0)^2 \rangle_0 = \sigma_0^2 P_0 + \sigma_2^2 P_2 + (x_0 - x_2)^2 P_0 P_2 \quad . \quad (9.43)$$

Now there is no direct relation between the variance and the correlation length.

Consider now the expression (8.30), which shows that since λ_1 is exponentially small we have an essentially constant J_n , except near the maxima of the probability distribution, i.e. near the minima of the potential. Furthermore since the right eigenvector of λ_1 satisfies $\sum_x p(x) = 0$, we have $0 = J(0) = J(\infty)$ so that

$$J(x) \simeq \begin{cases} 0 & 0 < x < x_0 \quad , \\ J_1 & x_0 < x < x_2 \quad , \\ 0 & x_2 < x < \infty \quad . \end{cases} \quad (9.44)$$

This expression is more accurate away from the minima of the potential, x_0 and x_2 .

Now it follows from Eq. (8.31) that the left eigenvector $u(x)$ of λ_1 must be constant, except near the minimum x_1 of the probability distribution, where the derivative could be sizeable. So we conclude that $u(x)$ is constant away from the maximum of the potential. Hence we must approximately have

$$u(x) \simeq \begin{cases} u_0 & 0 < x < x_1 \quad , \\ u_2 & x_1 < x < \infty \quad . \end{cases} \quad (9.45)$$

This expression is more accurate away from the maximum of the potential.

We may now relate the values of J and u by summing Eq. (8.30) from x_1 to infinity

$$J_1 = J(x_1) = \lambda_1 \sum_{x=x_1}^{\infty} \Delta x p^0(x) u(x) \simeq \lambda_1 P_2 u_2 \quad . \quad (9.46)$$

From Eq. (8.31) we get by summing over the interval between the minima

$$u_2 - u_0 = \frac{N J_1}{1 + n_b} \sum_{x=x_0}^{x_2} \Delta x \frac{1}{x p^0(x)} \quad . \quad (9.47)$$

The inverse probability distribution has for $N \rightarrow \infty$ a sharp maximum at the maximum of the potential. Let us define

$$Z_1 = \sum_{x=x_0}^{x_2} \Delta x \frac{1}{x} e^{NV(x)} \simeq \frac{1}{x_1} e^{NV_1} \sqrt{\frac{2\pi}{N(-V_1'')}} \quad . \quad (9.48)$$

Then we find

$$u_2 - u_0 = \frac{NZZ_1J_1}{1+n_b} = \frac{N\lambda_1Z_1Z_2u_2}{1+n_b} . \quad (9.49)$$

But $u(x)$ must be univariate, i.e.

$$\begin{aligned} u_0P_0 + u_2P_2 &= 0 , \\ u_0^2P_0 + u_2^2P_2 &= 1 , \end{aligned} \quad (9.50)$$

from which we get

$$\begin{aligned} u_0 &= -\sqrt{\frac{P_2}{P_0}} = -\sqrt{\frac{Z_2}{Z_0}} , \\ u_2 &= \sqrt{\frac{P_0}{P_2}} = \sqrt{\frac{Z_0}{Z_2}} . \end{aligned} \quad (9.51)$$

Inserting the above solution we may solve for λ_1

$$\lambda_1 = \frac{1+n_b}{N} \frac{Z_0+Z_2}{Z_0Z_1Z_2} , \quad (9.52)$$

or more explicitly

$$\lambda_1 = \frac{x_1(1+n_b)}{2\pi} \sqrt{-V_1''} \left(\sqrt{V_0''} e^{-N(V_1-V_0)} + \sqrt{V_2''} e^{-N(V_1-V_2)} \right) . \quad (9.53)$$

Finally we may read off the coefficients η and C from Eq. (9.36). We get

$$\eta = \begin{cases} V_1 - V_0 & \text{for } V_0 > V_2 , \\ V_1 - V_2 & \text{for } V_2 > V_0 , \end{cases} \quad (9.54)$$

and

$$C = \frac{x_1(1+n_b)}{2\pi} \sqrt{-V_1''} \begin{cases} \sqrt{V_0''} & \text{for } V_0 > V_2 , \\ \sqrt{V_2''} & \text{for } V_2 > V_0 . \end{cases} \quad (9.55)$$

This expression is nothing but the result of a barrier penetration of a classical statistical process [181]. We have derived it in detail in order to get all the coefficients right.

It is interesting to check numerically how well Eq. (9.53) actually describes the correlation length. The coefficient η is given by Eq. (9.54), and we have numerically computed the highest barrier from the potential $V(x)$ and compared it with an exact

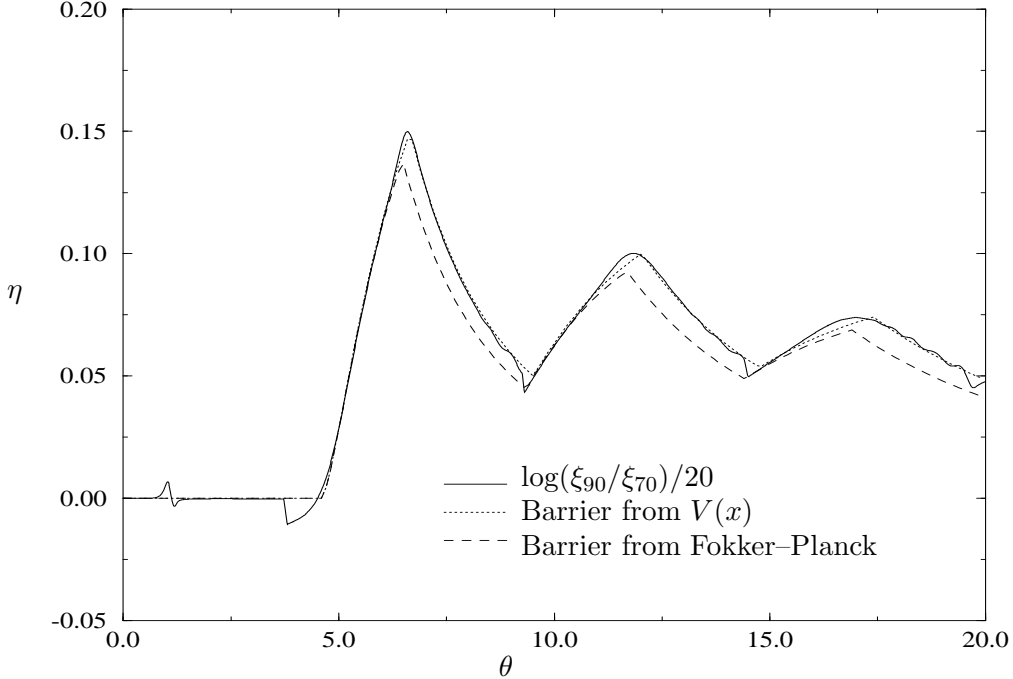


Figure 17: Comparing the barrier height from the potential $V(x)$ with the exact correlation length and the barrier from an approximate Fokker–Planck formula.

calculation in Figure 17. The exponent η is extracted by comparing two values of the correlation length, ξ_{70} and ξ_{90} , for large values of N (70 and 90), where the difference in the prefactor C should be unimportant. The agreement between the two calculations is excellent when we use the exact potential. As a comparison we also calculate the barrier height from the approximative potential in the Fokker–Planck equation derived in [132, 133]. We find a substantial deviation from the exact value in that case. It is carefully explained in [132, 133] why the Fokker–Planck potential cannot be expected to give a quantitatively correct result for small n_b . The exact result (solid line) has some extra features at $\theta = 1$ and just below $\theta = \theta_1 \simeq 4.603$, due to finite-size effects.

When the first sub-leading eigenvalue goes exponentially to zero, or equivalently the correlation length grows exponentially, it becomes important to know the density of eigenvalues. If there is an accumulation of eigenvalues around 0, the long-time correlation cannot be determined by only the first sub-leading eigenvalue. It is quite easy to determine the density of eigenvalues simply by computing them numerically.

In Figure 18 we show the first seven sub-leading eigenvalues for $N = 50$ and $n_b = 0.15$. It is clear that at the first critical point after the maser phase ($\theta = \theta_1$) there is only one eigenvalue going to zero. At the next critical phase ($\theta = \theta_2$) there is one more eigenvalue coming down, and so on. We find that there is only one exponentially small eigenvalue for each new minimum in the potential, and thus there is no accumulation of eigenvalues around 0.

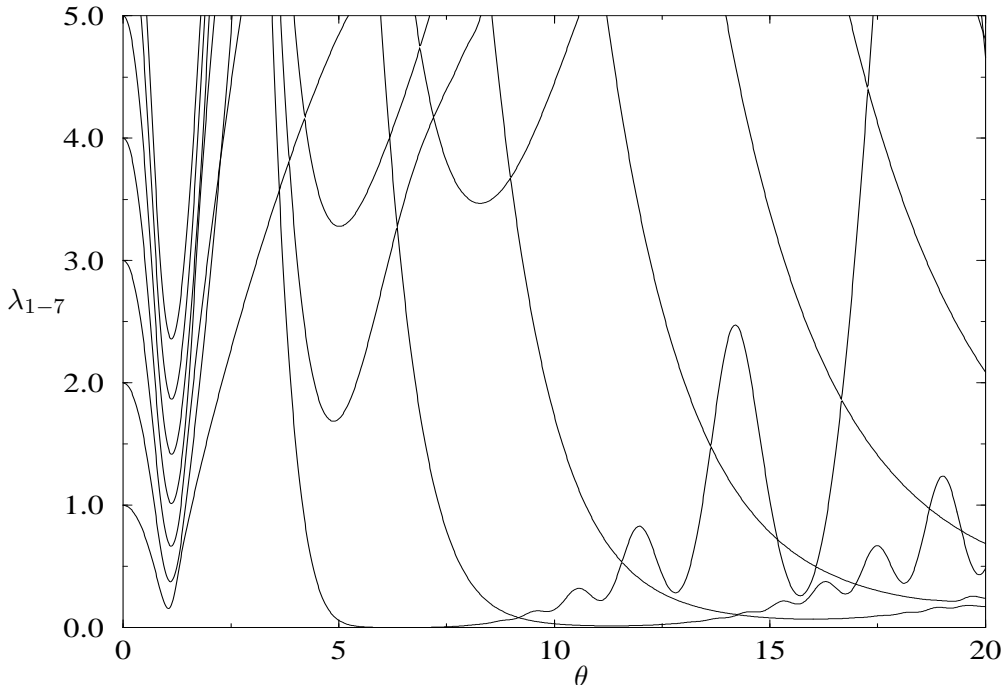


Figure 18: *The first seven sub-leading eigenvalues for $N = 50$ and $n_b = 0.15$.*

10 Effects of Velocity Fluctuations

“Why, these balls bound; there’s noise in it.”

W. Shakespeare

The time it takes an atom to pass through the cavity is determined by a velocity filter in front of the cavity. This filter is not perfect and it is relevant to investigate what a spread in flight time implies for the statistics of the interaction between cavity and beam. Noisy pump effects has been discussed before in the literature [183]. To be specific, we will here consider the flight time as an independent stochastic variable. Again, it is more convenient to work with the rescaled variable θ , and we denote the corresponding stochastic variable by ϑ . In order to get explicit analytic results we choose the following gamma probability distribution for positive ϑ

$$f(\vartheta, \alpha, \beta) = \frac{\beta^{\alpha+1}}{\Gamma(\alpha + 1)} \vartheta^\alpha e^{-\beta\vartheta} \quad , \quad (10.1)$$

with $\beta = \theta/\sigma_\theta^2$ and $\alpha = \theta^2/\sigma_\theta^2 - 1$, so that $\langle \vartheta \rangle = \theta$ and $\langle (\vartheta - \theta)^2 \rangle = \sigma_\theta^2$. Other choices are possible, but are not expected to change the overall qualitative picture. The discrete master equation (6.27) for the equilibrium distribution can be averaged to yield

$$\langle p(t+T) \rangle = e^{-\gamma L_C T} \langle M(\vartheta) \rangle \langle p(t) \rangle \quad , \quad (10.2)$$

The factorization is due to the fact that $p(t)$ only depends on ϑ for the preceding atoms, and that all atoms are statistically independent. The effect is simply to average $q(\vartheta) = \sin^2(\vartheta\sqrt{x})$ in $M(\vartheta)$, and we get

$$\langle q \rangle = \frac{1}{2} \left[1 - \left(1 + \frac{4x\sigma_\theta^4}{\theta^2} \right)^{-\frac{\theta^2}{2\sigma_\theta^2}} \cos \left(\frac{\theta^2}{\sigma_\theta^2} \arctan \left(\frac{2\sqrt{x}\sigma_\theta^2}{\theta} \right) \right) \right] \quad . \quad (10.3)$$

This averaged form of $q(\theta)$, which depends on the two independent variables θ/σ_θ and $\theta\sqrt{x}$, enters in the analysis of the phases in exactly the same way as before. In the limit $\sigma_\theta \rightarrow 0$ we regain the original $q(\theta)$, as we should. For very large σ_θ and fixed θ , and $\langle q \rangle$ approaches zero.

10.1 Revivals and Prerevivals

The phenomenon of quantum revival is an essential feature of the microlaser system (see e.g. Refs. [124]–[128], and [142]–[145]). The revivals are characterized by the reappearance of strongly oscillating structures in the excitation probability of an outgoing atom which is given by Eq. (7.1):

$$\mathcal{P}(+) = u^{0T} M(+) p^0 = \sum_n (1 - q_{n+1}(\theta)) p_n^0 \quad , \quad (10.4)$$

where p_n^0 is the photon distribution (6.32) in the cavity before the atom enters. Here the last equality sign in Eq.(10.4) is valid only for $a = 1$. Revivals occur when there is a resonance between the period in q_n and the discreteness in n [145]. If the photon distribution in the cavity has a sharp peak at $n = n_0$ with a position that does not change appreciably when θ changes, as for example for a fixed Poisson distribution, then it is easy to see that the first revival becomes pronounced in the region of $\theta_{\text{rev}} \simeq 2\pi\sqrt{n_0 N}$. For the equilibrium distribution without any spread in the velocities we do not expect any dramatic signature of revival, the reason being that the peaks in the equilibrium distribution $p_n^0(\theta)$ move rapidly with θ . In this context it is also natural to study the short-time correlation between two consecutive atoms, or the probability of finding two consecutive atoms in the excited level [135]. This quantity is given by

$$\begin{aligned} \mathcal{P}_0(+, +) &= u^{0T} M(+) (1 + L_C/N)^{-1} M(+) p^0 \\ &= \sum_{n,m} (1 - q_{n+1}(\theta)) (1 + L_C/N)^{-1}_{nm} (1 - q_{m+1}(\theta)) p_m^0 \quad , \end{aligned} \quad (10.5)$$

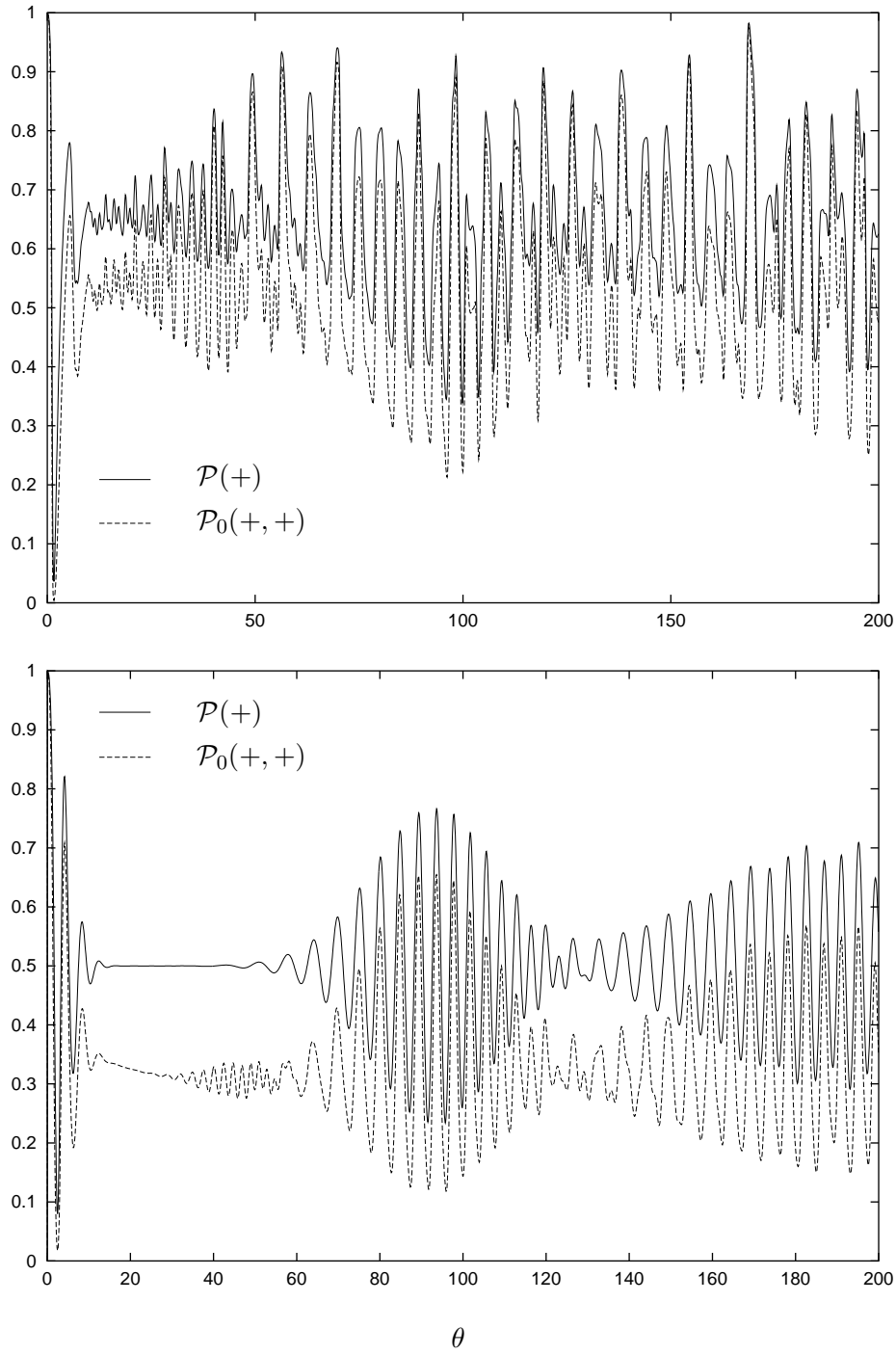


Figure 19: Upper graph: Probabilities of finding one atom, or two consecutive ones, in the excited state. The flux is given by $N = 20$ and the thermal occupation number is $n_b = 0.15$. The curves show no evidence for the resonant behavior of revivals. Lower graph: Presence of revival resonances in equilibrium after averaging the photon distribution over θ . The same parameters as in the upper graph are used but the variance in θ is now given by $\sigma_\theta^2 = 10$.

defined in Eq. (7.3). Here again the last equality sign is valid only for $a = 1$. In Appendix C we give an analytic expression for the matrix elements of $(1 + L_C/N)^{-1}$. In Figure 19 (upper graph) we present $\mathcal{P}(+)$ and $\mathcal{P}_0(+, +)$ for typical values of N and n_b ⁴.

If we on the other hand smear out the equilibrium distribution sufficiently as a function of θ , revivals will again appear. The experimental situation we envisage is that the atoms are produced with a certain spread in their velocities. The statistically averaged stationary photon distribution depends on the spread. After the passage through the cavity we measure both the excitation level and the speed of the atom. There is thus no averaging in the calculation of $\mathcal{P}(+)$ and $\mathcal{P}_0(+, +)$, but these quantities now also depend on the actual value ϑ for each atom. For definiteness we select only those atoms that fall in a narrow range around the average value θ , in effect putting in a sharp velocity filter *after* the interaction. The result for an averaged photon distribution is presented in Figure 19 (lower graph), where clear signs of revival are found. We also observe that in $\mathcal{P}_0(+, +)$ there are *prerevivals*, occurring for a value of θ half as large as for the usual revivals. Its origin is obvious since in $\mathcal{P}_0(+, +)$ there are terms containing q_n^2 that vary with the double of the frequency of q_n . It is clear from Figure 19 (lower graph) that the addition of noise to the system can enhance the signal. This observation suggest a connection to noise synchronization in non-linear systems [184]. The micromaser system can also be used to study the phenomena of stochastic resonance (see Ref.[185] and references therein) which, however, corresponds to a different mechanism for signal-noise amplification due to the presence of additional noise in a physical system.

10.2 Phase Diagram

The different phases discussed in Section 9 depend strongly on the structure of the effective potential. Averaging over θ can easily change this structure and the phases. For instance, averaging with large σ_θ would typically wash out some of the minima and lead to a different critical behavior. We shall determine a two-dimensional phase diagram in the parameters θ and σ_θ by finding the lines where new minima occur and disappear. They are determined by the equations

$$\begin{aligned} \langle q \rangle &= x \quad , \\ \frac{d\langle q \rangle}{dx} &= 1 \quad . \end{aligned} \tag{10.6}$$

The phase boundary between the thermal and the maser phase is determined by the effective potential for small x . The condition $\theta^2 = 1$ is now simply replaced by $\langle \vartheta^2 \rangle = \theta^2 + \sigma_\theta^2 = 1$, which also follows from the explicit form of $\langle q \rangle$ in Eq. (10.3). The transitions from the maser phase to the critical phases are determined numerically

⁴Notice that we have corrected for a numerical error in Figure 10 of Ref.[4].

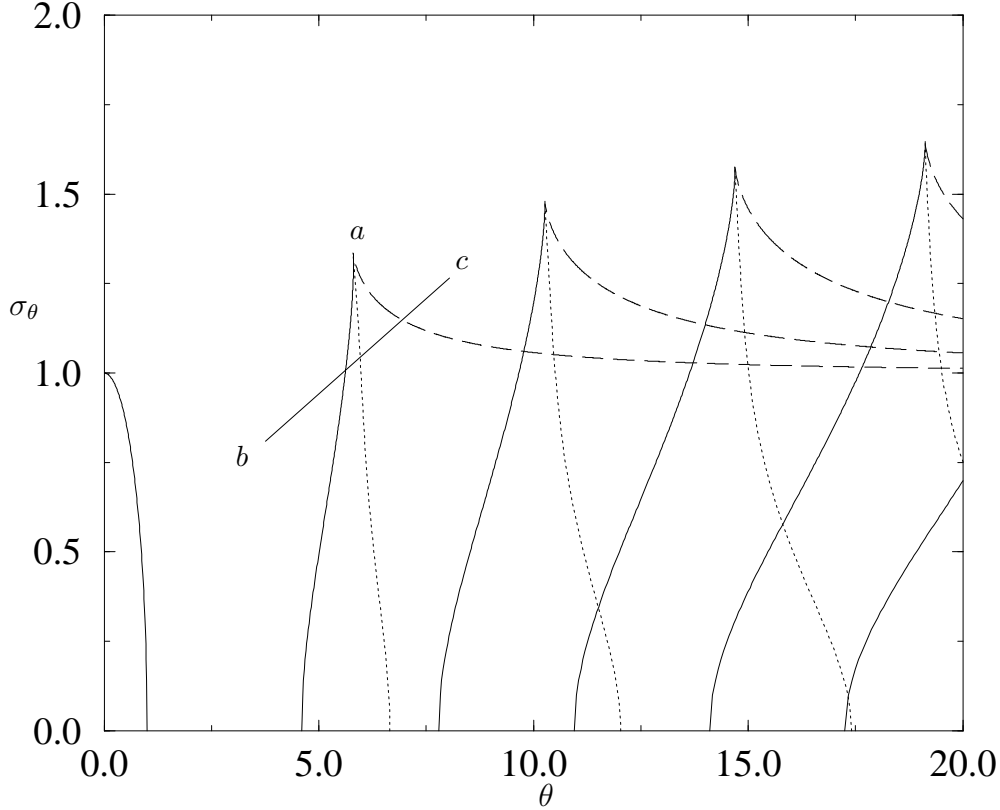


Figure 20: Phase diagram in the θ - σ_θ plane. The solid lines indicate where new minima in the effective potential emerge. In the lower left corner there is only one minimum at $n = 0$, this is the thermal phase. Outside that region there is always a minimum for non-zero n implying that the cavity acts as a maser. To the right of the solid line starting at $\theta \simeq 4.6$, and for not too large σ_θ , there are two or more minima and thus the correlation length grows exponentially with the flux. For increasing σ_θ minima disappear across the dashed lines, starting with those at small n . The dotted lines show where the two lowest minima are equally deep.

and presented in Figure 20. The first line starting from $\theta \simeq 4.6$ shows where the second minimum is about to form, but exactly on this line it is only an inflection point. At the point a about $\sigma_\theta \simeq 1.3$ it disappears, which occurs when the second minimum fuses with the first minimum. From the cusp at point a there is a new line (dashed) showing where the first minimum becomes an inflection point. Above the cusp at point a there is only one minimum. Going along the line from point b to c we thus first have one minimum, then a second minimum emerges, and finally the first minimum disappears before we reach point c . Similar things happens at the other cusps, which represent the fusing points for other minima. Thus, solid lines show where a new minimum emerges for large n ($\sim N$) as θ increases, while dashed lines show where a minimum disappears for small n as σ_θ increases. We have also indicated (by dotted lines) the first-order maser transitions where the two dominant

minima are equally deep. These are the lines where ξ and Q_f have peaks and $\langle n \rangle$ makes a discontinuous jump.

11 Finite-Flux Effects

*“In this age people are experiencing a delight, the tremendous
delight that you can guess how nature will work
in a new situation never seen before.”*

R. Feynman

So far, we have mainly discussed characteristics of the large flux limit. These are the defining properties for the different phases in Section 9. The parameter that controls finite flux effects is the ratio between the period of oscillations in the potential and the size of the discrete steps in x . If $q = \sin^2(\theta\sqrt{x})$ varies slowly over $\Delta x = 1/N$, the continuum limit is usually a good approximation, while it can be very poor in the opposite case. In the discrete case there exist, for certain values of θ , states that cannot be pumped above a certain occupation number since $q_n = 0$ for that level. This effect is not seen in the continuum approximation. These states are called *trapping states* [180] and we discuss them and their consequences in this section.

The continuum approximation starts breaking down for small photon numbers when $\theta \gtrsim 2\pi\sqrt{N}$, and is completely inappropriate when the discreteness is manifest for all photon numbers lower than N , i.e. for $\theta \gtrsim 2\pi N$. In that case our analysis in Section 9 breaks down and the system may occasionally, for certain values of θ , return to a non-critical phase.

11.1 Trapping States

The equilibrium distribution in Eq. (6.32) has peculiar properties whenever $q_m = 0$ for some value of m , in particular when n_b is small, and dramatically so when $n_b = 0$. This phenomenon occurs when $\theta = k\pi\sqrt{N/m}$ and is called a trapping state. When it happens, we have $p_n = 0$ for all $n \geq m$ (for $n_b = 0$). The physics behind this can be found in Eq. (6.19), where $M(-)$ determines the pumping of the cavity by the atoms. If $q_m = 0$ the cavity cannot be pumped above m photons by emission from the passing atoms. For any non-zero value of n_b there is still a possibility for thermal fluctuation above m photons and $p_n \neq 0$ even for $n \geq m$. The effect of trapping is lost in the continuum limit where the potential is approximated by Eq. (8.35). Some experimental consequences of trapping states were studied for very low temperature in [179] and it was stated that in the range $n_b = 0.1$ – 1.0 no experimentally measurable effects were present. Recently trapping states have actually been observed in the micromaser system [186]. Below we show that there are clear signals of trapping states in the correlation length even for $n_b = 1.0$.

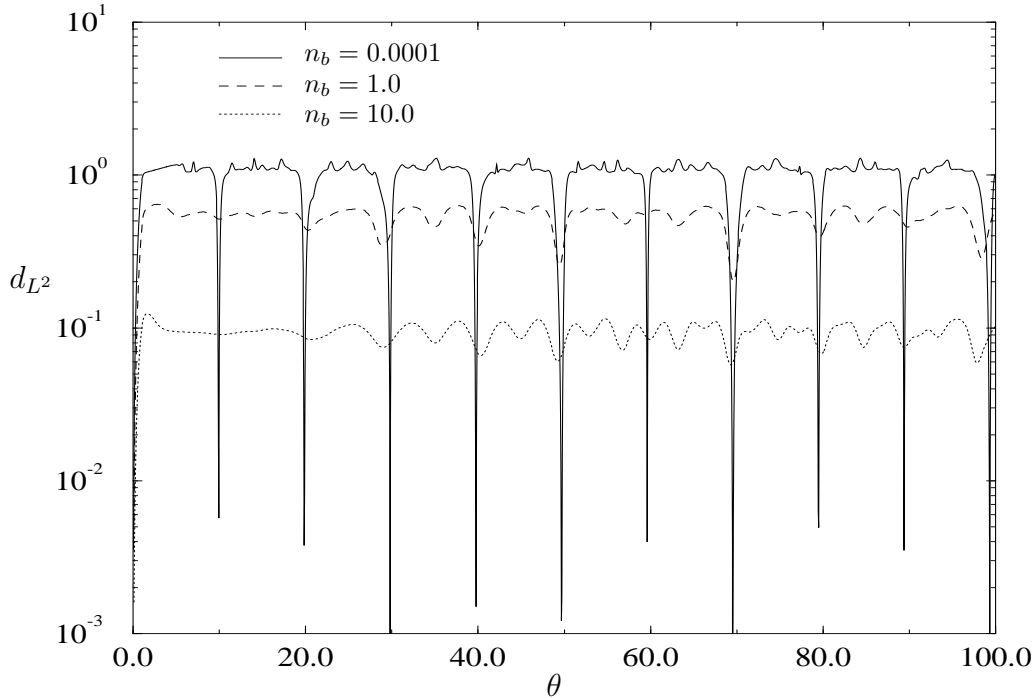


Figure 21: Distance between the initial probability distribution $p_n(0)$ and $p_n(\theta)$ measured by $d_{L^2}(\theta)$ in Eq. (11.1).

11.2 Thermal Cavity Revivals

Due to the trapping states, the cavity may revert to a statistical state, resembling the thermal state at $\theta = 0$, even if $\theta > 0$. By thermal revival we mean that the state of the cavity returns to the $\theta = 0$ thermal state for other values of θ . Even if the equilibrium state for non-zero θ can resemble a thermal state, it does not at all mean that the dynamics at that value of θ is similar to what it is at $\theta = 0$, since the deviations from equilibrium can have completely different properties. A straightforward measure of the deviation from the $\theta = 0$ state is the distance in the L^2 norm

$$d_{L^2}(\theta) = \left(\sum_{n=0}^{\infty} [p_n(0) - p_n(\theta)]^2 \right)^{1/2}. \quad (11.1)$$

In Figure 21 we exhibit $d_{L^2}(\theta)$ for $N = 10$ and several values of n_b .

For small values of n_b we find cavity revivals at all multiples of $\sqrt{10}\pi$, which can be explained by the fact that $\sin(\theta\sqrt{n/N})$ vanishes for $n = 1$ and $N = 10$ at those points, i.e. the cavity is in a trapping state. That implies that p_n vanishes for $n \geq 1$ (for $n_b = 0$) and thus there are no photons in the cavity. For larger values of n_b the trapping is less efficient and the thermal revivals go away.

Going to much larger values of θ we can start to look for periodicities in the fluctuations in $d_{L^2}(\theta)$. In Figure 22 (upper graph) we present the spectrum of periods occurring in $d_{L^2}(\theta)$ over the range $0 < \theta < 1024$.

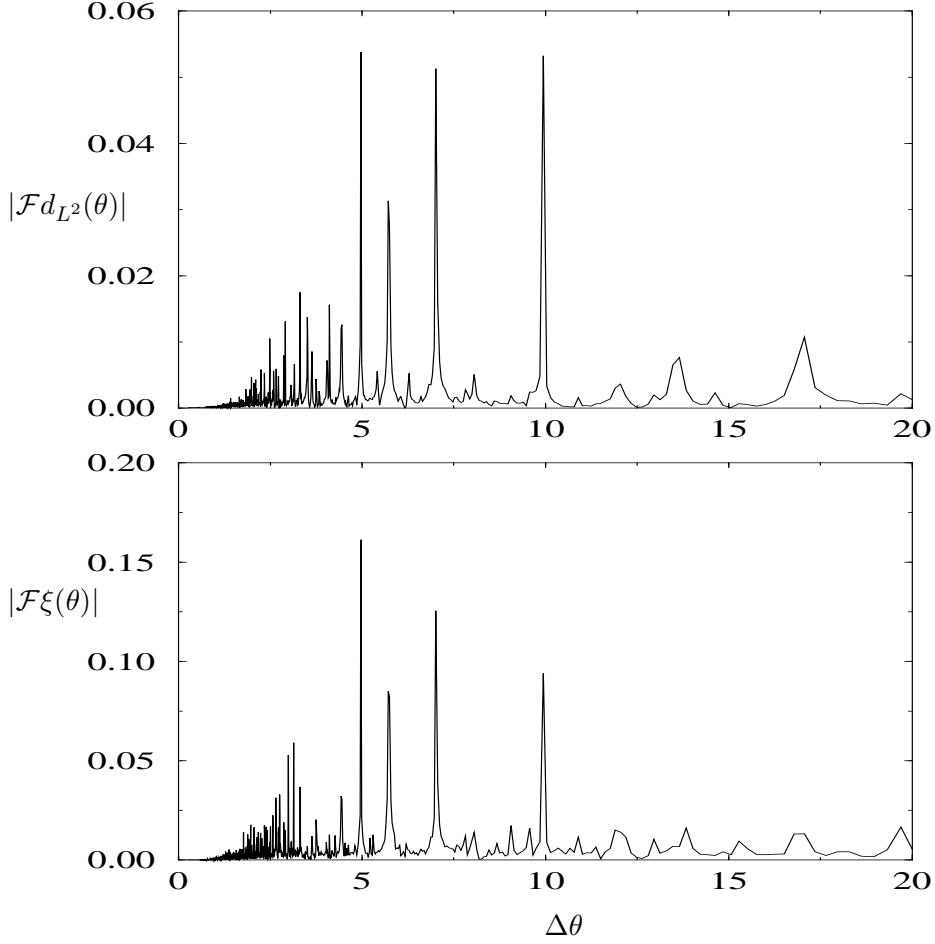


Figure 22: Amplitudes of Fourier modes of $d_{L^2}(\theta)$ (upper graph) and $\xi(\theta)$ (lower graph) as functions of periods using $N = 10$, $n_b = 1.0$ and scanning $0 < \theta < 1024$. There are pronounced peaks at the values of trapping states: $\Delta\theta = \pi\sqrt{N/n}$.

Standard revivals should occur with a periodicity of $\Delta\theta = 2\pi\sqrt{\langle n \rangle N}$, which is typically between 15 and 20, but there are hardly any peaks at these values. On the other hand, for periodicities corresponding to trapping states, i.e. $\Delta\theta = \pi\sqrt{10/n}$, there are very clear peaks, even though $n_b = 1.0$, which is a relatively large value.

In order to see whether trapping states influence the correlation length we present in Figure 22 a similar spectral decomposition of $\xi(\theta)$ (lower graph) and we find the same peaks. A more direct way of seeing the effect of trapping states is to study the correlation length for small n_b . In Figure 23 we see some very pronounced peaks for small n_b which rapidly go away when n_b increases. They are located at $\theta = \pi k\sqrt{N/n}$ for every integer k and n . The effect is most dramatic when k is small. In Figure 23 there are conspicuous peaks at $\theta = \pi\sqrt{10} \cdot \{1/\sqrt{3}, 1/\sqrt{2}, 1, 2/\sqrt{3}, 2/\sqrt{2}\}$, agreeing well with the formula for trapping states. Notice how sensitive the correlation length is to the temperature when n_b is small [179].

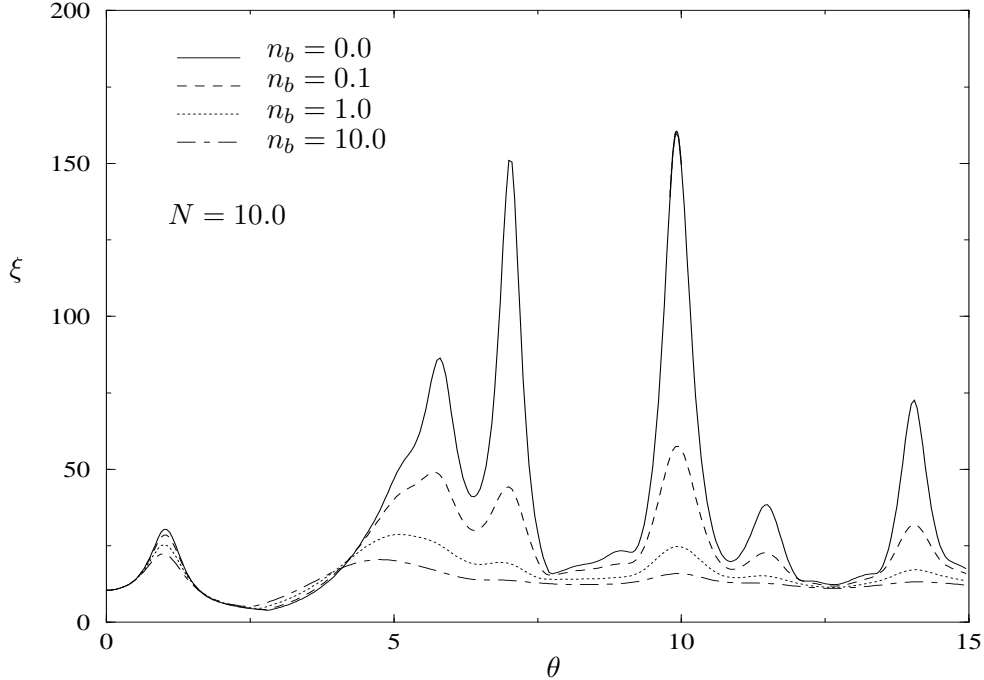


Figure 23: Correlation lengths for different values of n_b . The high peaks occur for trapping states and go away as n_b increases.

12 Conclusions

“The more the island of knowledge expands in the sea of ignorance, the larger its boundary to the unknown.”

V. F. Weisskopf

In the first set of lectures we have discussed the notion of a photon in quantum physics. We have observed that single photon states can be generated in the laboratory and that the physics of such quantum states can be studied under various experimental conditions. A relativistic quantum-mechanical description of single photon states has been outlined which constitutes an explicit realization of a representation (irreducible or reducible) of the Poincaré group. The Berry phase for a *single* photon has been derived within such a framework.

In the second set of lectures we have outlined the physics of the micromaser system. We have thoroughly discussed various aspects of long-time correlations in the micromaser. It is truly remarkable that this simple dynamical system can show such a rich structure of different phases. The two basic parameters, for $a = 1$, in the theory are the time the atom spends in the cavity, τ , and the ratio $N = R/\gamma$ between the rate at which atoms arrive and the decay constant of the cavity. We have also argued that the population probability of the excited state of in the atoms entering into the cavity is of importance. The natural observables are related to

the statistics of the outgoing atom beam, the average excitation being the simplest one. In Refs.[3, 4] it is proposed to use the long-time correlation length as a second observable describing different aspects of the photon statistics in the cavity. The phase structure we have investigated is defined in the limit of large flux, and can be summarized as follows:

- **Thermal phase**, $0 \lesssim \theta < 1$.
The mean number of photons $\langle n \rangle$ is low (finite in the limit $N \rightarrow \infty$), and so is the variance σ_n and the correlation length ξ .
- **Transition to maser phase**, $\theta \simeq 1$.
The maser is starting to get pumped up and ξ , $\langle n \rangle$, and σ_n grow like \sqrt{N} .
- **Maser phase**, $1 < \theta < \theta_1 \simeq 4.603$.
The maser is pumped up to $\langle n \rangle \sim N$, but fluctuations remain smaller, $\sigma_n \sim \sqrt{N}$, whereas ξ is finite.
- **First critical phase**, $\theta_1 < \theta < \theta_2 \simeq 7.790$.
The correlation length increases exponentially with N , but nothing particular happens with $\langle n \rangle$ and σ_n at θ_1 .
- **Second maser transition**, $\theta \simeq 6.6$
As the correlation length reaches its maximum, $\langle n \rangle$ makes a discontinuous jump to a higher value, though in both phases it is of the order of N . The fluctuations grow like N at this critical point.

At higher values of θ there are more maser transitions in $\langle n \rangle$, accompanied by critical growth of σ_n , each time the photon distribution has two competing maxima. The correlation length remains exponentially large as a function of N , as long as there are several maxima, though the exponential factor depends on the details of the photon distribution.

No quantum interference effects have been important in our analysis of the *phase structure* of the micromaser system, apart from field quantization in the cavity, and the statistical aspects are therefore purely classical. The reason is that we only study one atomic observable, the excitation level, which can take the values ± 1 . Making an analogy with a spin system, we can say that we only measure the spin along one direction. It would be very interesting to measure non-commuting variables, i.e. the spin in different directions or linear superpositions of an excited and decayed atom, and see how the phase transitions can be described in terms of such observables [164, 166]. Most effective descriptions of phase transitions in quantum field theory rely on classical concepts, such as the free energy and the expectation value of some field, and do not describe coherent effects. Since linear superpositions of excited and decayed atoms can be injected into the cavity, it is therefore possible to study coherent phenomena in phase transitions both theoretically and experimentally, using resonant micro cavities (see e.g. Refs.[146, 147]). The long-time correlation effects we have discussed in great detail in these lectures have actually recently been observed in the laboratory [187].

13 Acknowledgment

*“The faculty of being acquainted with things other than
itself is the main characteristic of a mind.”*

B. Russell

We are very grateful to Professor Choonkyu Lee and the organizers of this wonderful meeting and for providing this opportunity to present various ideas in the field of modern quantum optics. The generosity shown to us during the meeting is ever memorable. The work presented in these lectures is based on fruitful collaborations with many of our friends. The work done on resonant cavities and the micromaser system has been done in collaboration with Per Elmfors, Benny Lautrup and also, recently, with Per Kristian Rekdal. Most of the other work has been done in collaboration with A. P. Balachandran, G. Marmo and A. Stern. We are grateful to all of our collaborators for allowing us to present joint results in the form of these lectures at the Seoul 1998 meeting. I am grateful to John R. Klauder for his encouragement and enthusiastic support over the years and for all these interesting things I have learned from him on the notion of coherent states. We are also very grateful for many useful comments, discussions and communications with M. Berry, R. Y. Chiao, P. L. Knight, N. Gisin, R. Glauber, W. E. Lamb Jr., D. Leibfried, E. Lieb, Y. H. Shih, C. R. Stroud Jr., A. Zeilinger, and in particular H. Walther. The friendly and spiritual support of Johannes M. Hansteen, University of Bergen, is deeply acknowledged. Selected parts of the material presented in these lectures have also been presented in lectures/seminars at e.g.: the *1997 Nordic Meeting on Basic Problems in Quantum Mechanics*, Rosendal Barony; the 1997 ESF Research Conference on *Quantum Optics*, Castelvechio Pascoli; the *1998 Symposium on the Foundations of Quantum Theory*, Uppsala University; the *1998 NorFA Iceland Meeting on Laser-Atom Interactions*; the University of Alabama, Tuscaloosa; the University of Arizona, Tucson; the University of Bergen; Chalmers University of Technology, Ericssons Components, Kista; Linköping University; the Max-Planck Institute of Quantum Optics, Garching; the University of Oslo, the University of Uppsala, and at the Norwegian University of Science and Technology. We finally thank the participants at these lectures/seminars for their interest and all their intriguing, stimulating questions and remarks on the topics discussed.

A Jaynes–Cummings With Damping

In most experimental situations the time the atom spends in the cavity is small compared to the average time between the atoms and the decay time of the cavity. Then it is a good approximation to neglect the damping term when calculating the transition probabilities from the cavity–atom interaction. In order to establish the range of validity of the approximation we shall now study the full interaction governed by the JC Hamiltonian in Eq. (6.1) and the damping in Eq. (6.21). The density matrix for the cavity and one atom can be written as

$$\rho = \rho^0 \otimes \mathbb{1} + \rho^z \otimes \sigma_z + \rho^+ \otimes \sigma_- + \rho^- \otimes \sigma_+ , \quad (\text{A.1})$$

where $\rho^\pm = \rho^x \pm i\rho^y$ and $\sigma_\pm = (\sigma_x \pm i\sigma_y)/2$. We want to restrict the cavity part of the density matrix to be diagonal, at least the ρ_0 part, which is the only part of importance for the following atoms, provided that the first one is left unobserved (see discussion in Section 6.2). Introducing the notation

$$\begin{aligned} \rho_n^0 &= \langle n | \rho_0 | n \rangle , \\ \rho_n^z &= \langle n | \rho_z | n \rangle , \\ \rho_n^\pm &= \langle n | \rho_\pm | n-1 \rangle - \langle n-1 | \rho_\mp | n \rangle , \end{aligned} \quad (\text{A.2})$$

the equations of motion can be written as

$$\begin{aligned} \frac{d\rho_n^0}{dt} &= \frac{ig}{2}(\sqrt{n}\rho_n^\pm - \sqrt{n+1}\rho_{n+1}^\pm) - \gamma \sum_m L_{nm}^C \rho_m^0 , \\ \frac{d\rho_n^z}{dt} &= -\frac{ig}{2}(\sqrt{n}\rho_n^\pm + \sqrt{n+1}\rho_{n+1}^\pm) - \gamma \sum_m L_{nm}^C \rho_m^z , \\ \frac{d\rho_n^\pm}{dt} &= i2g\sqrt{n}(\rho_n^0 - \rho_{n-1}^0 - \rho_n^z - \rho_{n-1}^z) - \gamma \sum_m L_{nm}^\pm \rho_m^\pm , \end{aligned} \quad (\text{A.3})$$

where

$$\begin{aligned} L_{nm}^C &= [(n_b + 1)n + n_b(n + 1)] \delta_{n,m} - (n_b + 1)(n + 1) \delta_{n,m-1} - n_b n \delta_{n,m+1} , \\ L_{mn}^\pm &= [n_b(2n + 1) - \frac{1}{2}] \delta_{n,m} - (n_b + 1)\sqrt{n(n + 1)} \delta_{n,m-1} - n_b\sqrt{n(n - 1)} \delta_{n,m+1} . \end{aligned} \quad (\text{A.4})$$

It is thus consistent to study the particular form of the cavity density matrix, which has only one non-zero diagonal or sub-diagonal for each component, even when damping is included. Our strategy shall be to calculate the first-order correction in

γ in the interaction picture, using the JC Hamiltonian as the free part. The JC part of Eq. (A.3) can be drastically simplified using the variables

$$\begin{aligned}\rho_n^s &= \rho_0^n + \rho_0^{n-1} - \rho_z^n + \rho_z^{n-1} , \\ \rho_n^a &= \rho_0^n - \rho_0^{n-1} - \rho_z^n - \rho_z^{n-1} .\end{aligned}\tag{A.5}$$

The equations of motion then take the form

$$\begin{aligned}\frac{d\rho_n^s}{dt} &= -\frac{\gamma}{2} \sum_m \left[(L_{nm}^C + L_{n-1,m-1}^C) \rho_m^s + (L_{nm}^C - L_{n-1,m-1}^C) \rho_m^a \right] , \\ \frac{d\rho_n^a}{dt} &= 2ig\sqrt{n} \rho_n^\pm - \frac{\gamma}{2} \sum_m \left[(L_{nm}^C - L_{n-1,m-1}^C) \rho_m^s + (L_{nm}^C + L_{n-1,m-1}^C) \rho_m^a \right] , \\ \frac{d\rho_n^\pm}{dt} &= 2ig\sqrt{n} \rho_n^a - \gamma \sum_m L_{nm}^\pm \rho_m^\pm .\end{aligned}\tag{A.6}$$

The initial conditions $\rho_n^s(0) = p_{n-1}$, $\rho_n^a(0) = -p_{n-1}$ and $\rho_n^\pm(0) = 0$ are obtained from

$$\begin{aligned}\text{Tr}(\rho(0)|n\rangle\langle n| \otimes \mathbb{1}) &= 2\rho_0^n(0) = p_n , \\ \text{Tr}\left(\rho(0)|n\rangle\langle n| \otimes \frac{1}{2}(\mathbb{1} - \sigma_z)\right) &= \rho_0^n(0) - \rho_z^n(0) = 0 , \\ \text{Tr}(\rho(0)|n\rangle\langle n| \otimes \sigma_x) &= \text{Tr}(\rho(0)|n\rangle\langle n| \otimes \sigma_y) = 0 .\end{aligned}\tag{A.7}$$

In the limit $\gamma \rightarrow 0$ it is easy to solve Eq. (A.6) and we get back the standard solution of the JC equations, which is

$$\begin{aligned}\rho_s^n(t) &= p_{n-1} , \\ \rho_a^n(t) &= -p_{n-1} \cos(2gt\sqrt{n}) , \\ \rho_\pm^n(t) &= -ip_{n-1} \sin(2gt\sqrt{n}) .\end{aligned}\tag{A.8}$$

Equation (A.6) is a matrix equation of the form $\dot{\rho} = (C_0 - \gamma C_1)\rho$. When C_0 and C_1 commute the solution can be written as $\rho(t) = \exp(\gamma C_1 t) \exp(C_0 t) \rho(0)$, which is the expression used in Eq. (6.27). In our case C_0 and C_1 do not commute and we have to solve the equations perturbatively in γ . Let us write the solution as $\rho(t) = \exp(C_0 t) \rho_1(t)$ since $\exp(C_0 t)$ can be calculated explicitly. The equation for $\rho_1(t)$ becomes

$$\frac{d\rho_1}{dt} = -\gamma e^{-C_0 t} C_1 e^{C_0 t} \rho_1(t) ,\tag{A.9}$$

which to lowest order in γ can be integrated as

$$\rho_1(\tau) = -\gamma \int_0^\tau dt e^{-C_0 t} C_1 e^{C_0 t} \rho(0) + \rho(0) . \quad (\text{A.10})$$

The explicit expression for $\exp(C_0 t)$ is

$$e^{C_0 t} = \delta_{nm} \begin{pmatrix} 1 & 0 & 0 \\ 0 & \cos(2gt\sqrt{n}) & i \sin(2gt\sqrt{n}) \\ 0 & i \sin(2gt\sqrt{n}) & \cos(2gt\sqrt{n}) \end{pmatrix} , \quad (\text{A.11})$$

and, therefore, $\exp(-C_0 t) C_1 \exp(C_0 t)$ is a bounded function of t . The elements of C_1 are given by various combinations of L_{nm}^C and L_{nm}^\pm in Eq. (A.4) and they grow at most linearly with the photon number. Thus the integrand of Eq. (A.10) is of the order of $\langle n \rangle$ up to an n_b -dependent factor. We conclude that the damping is negligible as long as $\gamma\tau\langle n \rangle \ll 1$, unless n_b is very large. When the cavity is in a maser phase, $\langle n \rangle$ is of the same order of magnitude as $N = R/\gamma$, so the condition becomes $\tau R \ll 1$.

Even though this equation can be integrated explicitly it only results in a very complicated expression which does not really tell us directly anything about the approximation. It is more useful to estimate the size by recognizing that C_0 only has one real eigenvalue which is equal to zero, and two imaginary ones, so the norm of $\exp(-C_0 t)$ is 1. The condition for neglecting the damping while the atom is in the cavity is that $\gamma C_1 \tau \rho_1$ should be small. Since C_1 is essentially linear in n the condition reads $\gamma\tau\langle n \rangle \ll 1$. In the maser phase and above we have that $\langle n \rangle$ is of the same order of magnitude as $N = R/\gamma$, so the condition becomes $\tau R \ll 1$.

B Sum Rule for the Correlation Lengths

In this appendix we derive the sum rule quoted in Eq. (7.16) and use the notation of Section 8.3. No assumptions are made for the parameters in the problem.

For $A_K = 0$ the determinant $\det L_K$ becomes $B_0 B_1 \cdots B_K$ as may be easily derived by row manipulation. Since A_K only occurs linearly in the determinant it must obey the recursion relation $\det L_K = B_0 \cdots B_K + A_K \det L_{K-1}$. Repeated application of this relation leads to the expression

$$\det L_K = \sum_{k=0}^{K+1} B_0 \cdots B_{k-1} A_k \cdots A_K . \quad (\text{B.1})$$

This is valid for arbitrary values of B_0 and A_K . Notice that here we define $B_0 \cdots B_{k-1} = 1$ for $k = 0$ and similarly $A_k \cdots A_K = 1$ for $k = K + 1$.

In the actual case we have $B_0 = A_K = 0$, so that the determinant vanishes. The characteristic polynomial consequently takes the form

and

$$D_2 = \frac{B_1 \cdots B_K}{p_0^0} \sum_{k=0}^{K-1} \sum_{l=k+1}^K \sum_{m=k+1}^l \frac{p_k^0 p_l^0}{B_m p_m^0} . \quad (\text{B.9})$$

Introducing the cumulative probability

$$P_n^0 = \sum_{m=0}^{n-1} p_m^0 , \quad (\text{B.10})$$

and interchanging the sums, we get the correlation sum rule

$$\sum_{n=1}^K \frac{1}{\lambda_n} = \sum_{n=1}^K \frac{P_n^0 (1 - P_n^0 / P_{K+1}^0)}{B_n p_n^0} . \quad (\text{B.11})$$

This sum rule is valid for finite K but diverges for $K \rightarrow \infty$, because the equilibrium distribution p_n^0 approaches a thermal distribution for $n \gg N$. Hence the right-hand side diverges logarithmically in that limit. The left-hand side also diverges logarithmically with the truncation size because we have $\lambda_n^0 = n$ for the untruncated thermal distribution. We do not know the thermal eigenvalues for the truncated case, but expect that they will be of the form $\lambda_n^0 = n + \mathcal{O}(n^2/K)$ since they should vanish for $n = 0$ and become progressively worse as n approaches K . Such a correction leads to a finite correction to $\sum_n 1/\lambda_n$. In fact, evaluating the right-hand side of Eq. (B.11), we get for large K

$$\sum_{n=1}^K \frac{1}{\lambda_n^0} \simeq \sum_{n=1}^K \frac{1 - [n_b/(1 + n_b)]^n}{n} \simeq \sum_{n=1}^K \frac{1}{n} - \log(1 + n_b) . \quad (\text{B.12})$$

Subtracting the thermal case from Eq. (B.11) we get in the limit of $K \rightarrow \infty$

$$\sum_{n=1}^{\infty} \left(\frac{1}{\lambda_n} - \frac{1}{\lambda_n^0} \right) = \sum_{n=1}^{\infty} \left(\frac{P_n^0 (1 - P_n^0)}{B_n p_n^0} - \frac{1 - [n_b/(1 + n_b)]^n}{n} \right) . \quad (\text{B.13})$$

Here we have extended the summation to infinity under the assumption that for large n we have $\lambda_n \simeq \lambda_n^0$. The left-hand side can be approximated by $\xi - 1$ in regions where the leading correlation length is much greater than the others. A comparison of the exact eigenvalue and the sum-rule prediction is made in Figure 10.

C Damping Matrix

In this appendix we find an integral representation for the matrix elements of $(x + L_C)^{-1}$, where L_C is given by Eq. (6.25). Let

$$v_n = \sum_{m=0}^{\infty} (x\delta_{nm} + (L_C)_{nm})w_m \quad , \quad (\text{C.1})$$

and introduce generating functionals $v(z)$ and $w(z)$ for complex z defined by

$$v(z) = \sum_{n=0}^{\infty} z^n v_n \quad , \quad w(z) = \sum_{n=0}^{\infty} z^n w_n \quad . \quad (\text{C.2})$$

By making use of

$$v(z) = \sum_{n,m=0}^{\infty} (x + L_C)_{nm} z^n w_m \quad , \quad (\text{C.3})$$

one can derive a first-order differential equation for $w(z)$,

$$(x + n_b(1 - z))w(z) + (1 + n_b(1 - z))(z - 1)\frac{dw(z)}{dz} = v(z) \quad , \quad (\text{C.4})$$

which can be solved with the initial condition $v(1) = 1$, i.e. $w(1) = 1/x$. If we consider the monomial $v(z) = v_m z^m$ and the corresponding $w(z) = w_m(z)$, we find that

$$w_m(z) = \int_0^1 dt (1-t)^{x-1} \frac{[z(1-t(1+n_b)) + t(1+n_b)]^m}{[1+n_b t(1-z)]^{m+1}} \quad . \quad (\text{C.5})$$

Therefore $(x + L_C)_{nm}^{-1}$ is given by the coefficient of z^n in the series expansion of $w_m(z)$. In particular, we obtain for $n_b = 0$ the result

$$(x + L_C)_{nm}^{-1} = \binom{m}{n} \frac{\Gamma(x+n)\Gamma(m-n+1)}{\Gamma(x+m+1)} \quad , \quad (\text{C.6})$$

where $m \geq n$. We then find that

$$\mathcal{P}_0(+, +) = \sum_{n=0}^{\infty} \cos^2(g\tau\sqrt{n+1}) \sum_{m=n}^{\infty} \frac{m!}{n!} \frac{N\Gamma(N+n)}{\Gamma(N+m+1)} \cos^2(g\tau\sqrt{m+1}) p_m^0 \quad , \quad (\text{C.7})$$

where p_m^0 is the equilibrium distribution given by Eq. (6.32), and where $x = N = R/\gamma$. Equation (C.7) can also be derived from the known solution of the master equation in Eq. (6.21) for $n_b = 0$ [174]. For small n_b and/or large x , Eq. (C.5) can be used to find a series expansion in n_b .

For the convenience of the readers we have attached a capital **R** to those references which are reprinted in Ref.[7]. We apologize to the many authors whose work we may have overlooked or to those feel that their work should have been referred to.

References

- [1] B.-S. Skagerstam. “*Localization of Massless Spinning Particles and the Berry Phase*” in “*On Klauders Path: A Field Trip. Festschrift for John R. Klauder on Occasion of His 60th Birthday*”, pp. 209-222, Eds. G. G. Emch, G. C. Hegerfeldt and L. Streit (World Scientific, 1994).
- [2] B.-S. Skagerstam, “*Coherent States — Some Applications in Quantum Field Theory and Particle Physics*”, in “*Coherent states: Past, Present, and the Future*”, pp. 469-506, Eds. D. H. Feng, J. R. Klauder and M. R. Strayer (World Scientific, 1994).
- [3] P. Elmfors, B. Lautrup and B.-S. Skagerstam, “*Correlations as a Handle on the Quantum State of the Micromaser*”, CERN/TH 95-154 (cond-mat/9506058), CERN, 1995, and “*Atomic Beam Correlations and the Quantum State of the Micromaser*”, Physica Scripta **55** (1997) 724-727.
- [4] P. Elmfors, B. Lautrup and B.-S. Skagerstam, “*Dynamics and the Phases of the Micromaser*”, CERN/TH 95-333 (atom-phys/9601004), CERN, 1995, and in Phys. Rev. **A54** (1996) 5171-5192.
- [5] P. A. M. Dirac, “*Generalized Hamiltonian Dynamics*”, Can. J. Math. **2** (1950) 129-148; “*Generalized Hamiltonian Dynamics*”, Proc. Roy. Soc. **A246** (1958) 326-332; “*Lectures on Quantum Mechanics*”, Yeshiva University (Academic Press, New York, 1967). (Accademia Nazionale dei Lincei, Roma 1976).
- [6] A. J. Hansson, T. Regge and C. Teitelboim, “*Constrained Hamiltonian Systems*” (Accademia Nazionale dei Lincei, Roma 1976).
- [7] J. R. Klauder and B.-S. Skagerstam, “*Coherent States-Applications in Physics and Mathematical Physics*” (World Scientific, Singapore, 1985 and Beijing 1988).
- [8] R. J. Glauber, “*Optical Coherence and Photon Statistics*” in “*Quantum Optics and Electronics*”, Les Houches 1964, pp.63-185, Eds. C. DeWitt, A. Blandin and C. Cohen-Tannoudji (Gordon and Breach, New York, 1965).
- [9] J. R. Klauder and E. C. G. Sudarshan, “*Fundamentals of Quantum Optics*” (W. A. Benjamin, New York, 1968)
- [10] A. Perelomov, “*Generalized Coherent States and Their Applications*” (Springer Verlag, London, 1986).
- [11] Wei-Min Zhang, Da Husan Feng and R. Gilmore, “*Coherent States: Theory and Some Applications*”, Rev. Mod. Phys. **62** (1990) 867-927.

- [12] T. D. Lee, F. E. Low and D. Pines, “*The Motion of Slow Electrons in a Polar Crystal*”, Phys. Rev. **90** (1953) 297-302.
- [13] J. R. Klauder, “*The Action Option and a Feynman Quantization of Spinor Fields in Terms of Ordinary C-Numbers*”, Ann. Phys. (N.Y.) **11** (1960) 123-168 (**R**).
- [14] R. J. Glauber, “*Photon Correlations*”, Phys. Rev. Lett. **10** (1963) 84-86 (**R**); “*The Quantum Theory of Optical Coherence*”, Phys. Rev. **130** (1963) 2529-2539 (**R**) and “*Coherent and Incoherent States of the Radiation Field*”, *ibid.* **131** (1963) 2766-2788 (**R**).
- [15] E. C. G. Sudarshan, “*Equivalence of Semiclassical and Quantum Mechanical Descriptions of Statistical Light*”, Phys. Rev. Lett. **10** (1963) 277-279 (**R**).
- [16] K.-E. Eriksson, “*Summation Methods for Radiative Corrections*” in “*Cargèse Lectures in Physics, 1967*”, pp. 245-274, Ed. M. Lévy (Gordon and Breach, New York, 1968).
- [17] F. Aversa and M. Greco, “*Coherent States and Structure Functions in QED*”, Phys. Lett. **228B** (1989) 134-138.
- [18] D. R. Yennie, S. C. Frautschi and H. Suura, “*The Infrared Divergence Phenomena and High-Energy Processes*”, Ann. Phys. (N.Y.) **13** (1961) 379-452.
- [19] V. Chung, “*Infrared Divergences in Quantum Electrodynamics*”, Phys. Rev. **140** (1965) B1110-B1122 (**R**).
- [20] T. W. B. Kibble, “*Coherent Soft-Photon States and Infrared Divergences*”, J. Math. Phys. **9** (1968) 315-324; “*II. Mass-Shell Singularities of Greens Functions*”, Phys. Rev. **173** (1968) 1527-1535; “*III. Asymptotic States and Reduction Formulas*”, Phys. Rev. **174** (1968) 1882-1901; “*IV. The Scattering Operator*”, Phys. Rev. **175** (1968) 1624-1640;
- [21] M. Greco and G. Rossi, “*A Note on the Infra-Red Divergence*”, Nuovo Cimento **50** (1967) 167-175.
- [22] S. Weinberg, “*Infrared Photons and Gravitons*”, Phys. Rev. **140** (1965) B516-B524.
- [23] C. Alvegard, K.-E. Eriksson and C. Högfors, “*Soft Graviton Radiation*”, Physica Scripta **17** (1978) 95-102.
- [24] K.-E. Eriksson and B.-S. Skagerstam, “*A Classical Source Emitting Self-Interacting Bosons*”, Phys. Rev. **D18** (1978) 3958-3862 (**R**).
- [25] H. Letz, “*Evolution Operator and Stable Coherent States*”, Phys. Lett. **60A** (1977) 399-400.
- [26] W. H. Zurek, S. Habib and J. P. Paz, “*Coherent States Via Decoherence*”, Phys. Rev. Lett. **70** (1993) 1187-1190.
- [27] V. G. Bagrov, D. M. Gitman and V. A. Kuchin, “*External Field in Quantum Electrodynamics and Coherent States*” in “*Actual Problems of Theoretical Problems*”. Collection of papers to D. D. Ivanenko (MGU, Moscow 1976).

- [28] E. S. Fradkin, D. M. Gitman and S. M. Shvartsman “*Quantum Electrodynamics with Unstable Vacuum*” (Springer Verlag, 1991).
- [29] F. A. M. de Olivera, M. S. Kim and P. L. Knight, “*Properties of Displaced Number States*”, Phys. Rev. **A41** (1990) 2645-2652.
- [30] K. B. Møller, T. G. Jørgensen and J. P. Dahl, “*Displaced Squeezed Numbers States: Position Space Representations, Inner Product and Some Other Applications*”, Phys. Rev. **A54** (1996) 5378-5385.
- [31] M. M. Nieto, “*Displaced and Squeezed Number States*”, Phys. Lett. **A229** (1997) 135-143.
- [32] Y. T. Chough and H. J. Carmichael, “*Nonlinear Oscillator Behaviour in the Jaynes-Cummings Model*”, Phys. Rev. **A54** (1996) 1709-1714.
- [33] C. T. Bodendorf, G. Antesberger, M.S. Kim and H. Walther, “*Quantum-State Reconstruction in the One-Atom Maser*”, Phys. Rev. **A57** (1998) 1371-1378.
- [34] P. Carruthers and M. N. Nieto, “*Coherent States and the Harmonic Oscillator*”, Am. J. Phys. **33** (1965) 537-544 (**R**).
- [35] C. K. Hong and L. Mandel, “*Experimental Realization of a Localized One-Photon State*”, Phys. Rev. Lett. **56** (1986) 58-60;
C. K. Hong, Z. Y. and L. Mandel, “*Measurement of Subpicosecond Time Intervals Between Two Photons by Interference*”, Phys. Rev. Lett. **59** (1987) 2044-2046;
- [36] J. D. Franson and K. A. Potocki, “*Single-Photon Interference Over Large Distances*”, Phys. Rev. **A37** (1988) 2511-2515.
- [37] P. G. Kwiat, A. M. Steinberg, R. Y. Chiao, P. H. Eberhard and M. D. Petroff, “*High-Efficiency Single-Photon Detectors*”, Phys. Rev. **A48** (1993) R867-R870.
- [38] T. E. Kiess, Y. H. Shih, A. V. Sergienko and C. O. Alley, “*Einstein-Podolsky-Rosen-Bohm Experiment Using Pairs of Light Quanta Produced by Type-II Parametric Down-Conversion*”, Phys. Rev. Lett. **71** (1993) 3893-3897.
- [39] Y. H. Shih and A. V. Sergienko, “*Observation of Quantum Beating in a Simple Beam-Splitting Experiment: Two-Particle Entanglement in Spin and Space-Time*”, Phys. Rev. **A50** (1994) 2564-2568.
- [40] T. B. Pittman, Y. H. Shih, A. V. Sergienko and M. H. Rubin, “*Experimental Test of Bell’s Inequalities Based on Space-Time and Spin Variables*”, Phys. Rev. **A51** (1995) 3495-3498.
- [41] P. G. Kwiat, K. Mattle, H. Weinfurter and A. Zeilinger, “*New High-Intensity Source of Polarization-Entangled Photon Pairs*”, Phys. Rev. Lett. **75** (1995) 4337-4341.
- [42] T. B. Pittman, D. V. Strekalov, A. Migdall, M. H. Rubin, A. V. Sergienko and Y. H. Shih, “*Can Two-Photon Interference be Considered the Interference of Two Photons?*”, Phys. Rev. Lett. **77** (1996) 3495-3498.

- [43] G. Di Giuseppe, L. Haiberger, F. De Martini and A. V. Sergienko, “*Quantum Interference and Indistinguishability With Femtosecond Pulses*”, Phys. Rev. **A56** (1997) R21-R24.
- [44] D. V. Strekalov and Y. H. Shih, “*Two-Photon Geometrical Phase*”, Phys. Rev. **A56** (1997) 3129-3133.
- [45] D. V. Strekalov, T. B. Pittman and Y. H. Shih, “*What Can We Learn About Single Photons in a Two-Photon Interference Experiment*”, Phys. Rev. **A57** (1998) 567-570.
- [46] M. C. Teich and B. E. A. Saleh, “*Photon Bunching and Antibunching*”, in “*Progress in Optics XXVI*”, pp. 3-100, Ed. E. Wolf, (North-Holland, 1988).
- [47] D. F. Walls, “*Evidence for the Quantum Nature of Light*”, Nature **280** (1979) 451-545.
- [48] D. F. Smirnov and A. S. Troshin, “*New Phenomena in Quantum Optics: Photon Antibunching, Sub-Poisson Photon Statistics, and Squeezed States*”, Sov. Phys. Usp. **30** (1987) 851-874.
- [49] A. Aspect and P. Grangier, “*Wave-Particle Duality for Single Photons*”, *Hyperfine Interactions* **37** (1987) 3-18;
P. Grangier, G. Roger and A. Aspect, “*Experimental Evidence for a Photon Anticorrelation Effect on a Beam Splitter: A New Light on Single-Photon Interferences*”, *Europhys. Lett.* **1** (1986) 173-179.
- [50] F. Rieke and D. A. Baylor, “*Single-Photon Detection by Rod Cells in the Retina*”, Rev. Mod. Phys. **70** (1998) 1027-1036.
- [51] W. T. Buttler, R. J. Hughes, P. G. Kwiat, S. K. Lamoreaux, G. G. Luther, G. L. Morgan, J. E. Nordholt, C. G. Peterson and C. M. Simmons, “*Practical Free-Space Quantum Key Distribution Over 1 km*”, Phys. Rev. Lett. **81** (1998) 3283-3286.
- [52] R. Hanbury-Brown and R. Q. Twiss, “*Correlation Between Photons in Two Coherent Beams*”, Nature **177** (1956) 27-29 and “*The Question of Correlation Between Photons in Coherent Light Rays*”, *ibid.* **178** (1956) 1447-1450.
- [53] D. H. Boal, C.-H. Gelbke and D. K. Jennings, “*Intensity Interferometry in Subatomic Physics*”, Rev. Mod. Phys. **62** (1990) 553-603.
- [54] The OPAL Collaboration, “*A Study of Bose-Einstein Correlations in e^+e^- Anihilations at LEP*”, Phys. Lett. **B267** (1991) 143-153.
- [55] H. Bøggild et al., “*Identified Pion Interferometry in Heavy-Ion Collisions at CERN*”, Phys. Lett. **B302** (1993) 510-516.
- [56] J. P. Sullivan et al., “*Bose-Einstein Correlations of Pion Pairs and Kaon Pairs from Relativistic Quantum Molecular Dynamics*”, Phys. Rev. Lett. **70** (1993) 3000-3003.

- [57] D. K. Srivastava and J. I. Kapusta, “*History of Quark- Gluon Plasma Evolution from Photon Interferometry* ”, Phys. Rev. **C48** (1993) 1335-1345.
- [58] A. Pais, “*Subtle is the Lord. The Science and the Life of Albert Einstein* ”, p. 382 (Oxford University Press, 1982).
- [59] D. N. Klyshko, “*Quantum Optics: Quantum, Classical, and Metaphysical Aspects* ”, Sov. Phys. Usp. **37** (1994) 1097-1122.
- [60] W. E. Lamb, Jr., “*Anti-Photon* ”, Applied Physics **B60** (1995) 77-84.
- [61] D. T. Smithey, M. Beck, M. G. Raymer and A. Faridani, “*Measurement of the Wigner Distribution and the Density Matrix of a Light Mode Using Optical Homodyne Tomography: Application to Squeezed and the Vacuum* ”, Phys. Rev. Lett. **70** (1993) 1244-1247.
- [62] X. Maitre, E. Hagley, C. Nogues, C. Wunderlich, P. Goy, M. Brune, J. M. Raimond and S. Haroche, “*Quantum Memory With a Single Photon in a Cavity* ”, Phys. Rev. Lett. **79** (1997) 769-772.
- [63] T. Newton and E. P. Wigner, “*Localized States for Elementary Systems*”, Rev. Mod Phys. **21** (1949) 400-406.
- [64] A. S. Wightman, “*On the Localizability of Quantum Mechanical Systems*”, Rev. Mod. Phys. **34**(1962) 845-872.
- [65] J. M. Jauch and C. Piron, “*Generalized Localizability*”, Helv. Phys. Acta **40** (1967) 559-570;
W. O. Amrein, “*Localizability for Particles of Mass Zero*”, Helv. Phys. Acta **42** (1969) 149-190.
- [66] T. F. Jordan and N. Mukunda, “*Lorentz-Covariant Position Operators for Spinning Particles*”, Phys. Rev. **132** (1963) 1842-1848;
A. L. Licht, “*Local States*”, J. Math. Phys. **7** (1966) 1656-1669;
K. Krauss, “*Position Observables of the Photon*” in “*The Uncertainty Principle and Foundations of Quantum Mechanics*”, pp. 293-320, Eds. W.C. Price and S.S. Chissick (John Wiley & Sons, 1977);
M. I. Shirokov, “*Strictly Localized States and Particles*”, Theor. Math. Phys. **42** (1980) 134-140;
S. N. M. Ruijsenaars, “*On Newton-Wigner Localization and Superluminal Propagation Speeds*”, Ann. Phys. (N.Y.) **137** (1981) 33-43;
E. Prugovecki, “*Stochastic Quantum Mechanics and Quantum Spacetime*” (Kluwer Academic, Hingham, Mass., 1984).
- [67] L. Hardy, “*Nonlocality of a Single Photon Revisted* ”, Phys. Rev. Lett. **73** (1994) 2279-2283.
- [68] C. C. Gerry, “*Nonlocality of a Single Photon in Cavity QED* ”, Phys. Rev. **A53** (1996) 4583-4586.
- [69] C. Adlard, E. R. Pike and S. Sarkar, “*Localization of One-Photon States* ”, Phys. Rev. Lett. **79** (1997) 1585-1587.

- [70] J. Ehlers, A. E. Pirani and A. Schild, “*The Geometry of Free-Fall and Light Propagation*” in “*General Relativity. Papers in Honor of J. L. Synge*”, pp. 63-84, Ed. L. O’Raifeartaigh (Oxford University Press, London, 1972).
- [71] E. Wigner, “*Unitary Representations of the Inhomogeneous Lorentz Group*”, *Ann. Math.* **40** (1939) 149-204.
- [72] G. C. Hegerfeldt, “*Remark on the Causality and Particle Localization*”, *Phys. Rev.* **D10** (1974) 3320-3321;
 B.-S. Skagerstam, “*Some Remarks Concerning the Question of Localization of Elementary Particles*”, *Int. J. Theor. Phys.* **15** (1976) 213-230;
 J. F. Perez and I. F. Wilde, “*Localization and Causality in Relativistic Quantum Mechanics*”, *Phys. Rev.* **D16** (1977) 315-317;
 G. C. Hegerfeldt and S. N. M. Ruijsenaars, “*Remarks on Causality, Localization and Spreading of Wave Packets*”, *Phys. Rev.* **D22** (1980) 377-384.
- [73] G. C. Hegerfeldt, “*Violation of Causality in Relativistic Quantum Theory?*”, *Phys. Rev. Lett.* **54** (1985) 2395-2398. Also see “*Instantaneous Spreading and Einstein Causality in Quantum Theory*”, *Ann. Phys. (Leipzig)* **7** (1998) 716-725.
- [74] D. Buchholz and J. Yngvason, “*There Are No Causality Problems for Fermi’s Two-Atom System*”, *Phys. Rev. Lett.* **73** (1994) 613-616.
- [75] A. P. Balachandran, G. Marmo, B.-S. Skagerstam and A. Stern, “*Spinning Particles in General Relativity*”, *Phys. Lett.* **89B** (1980) 199-202 and “*Gauge Symmetries and Fibre Bundles: Applications to Particle Dynamics*”, *Lecture Notes in Physics Vol. 188*, Section 5.6 (Springer Verlag, 1983);
 B.-S. Skagerstam and A. Stern, “*Lagrangian Description of Classical Charged Particles with Spin*”, *Physica Scripta* **24** (1981) 493-497.
- [76] M. Atre, A. P. Balachandran and T. V. Govindarajan, “*Massless Spinning Particles in All Dimensions and Novel Magnetic Monopoles*”, *Int. J. Mod. Phys.* **A2** (1987) 453-493.
- [77] B.-S. Skagerstam and A. Stern, “*Light-Cone Gauge Versus Proper-Time Gauge for Massless Spinning Particles*”, *Nucl. Phys.* **B294** (1987) 636-670.
- [78] I. Bialynicki-Birula and Z. Bialynicka-Birula, “*Berry’s Phase in the Relativistic Theory of Spinning of Particles*”, *Phys. Rev.* **D33** (1987) 2383-2387.
- [79] E. P. Wigner, “*Relativistic Invariance and Quantum Phenomena*”, *Rev. Mod. Phys.* **29** (1957) 355-268.
- [80] B. Ek and B. Nagel, “*Differentiable Vectors and Sharp Momentum States of Helicity Representations of the Poincaré Group*”, *J. Math. Phys.* **25** (1984) 1662-1670.
- [81] G. W. Whitehead, “*Elements of Homotopy Theory*” (Springer Verlag, 1978).
- [82] P. A. M. Dirac “*Quantized Singularities in the Electromagnetic Field*”, *Proc. Roy. Soc.* **A133** (1931) 60-72; “*The Theory of Magnetic Monopoles*”, *Phys. Rev.* **74** (1948) 817-830.

- [83] T. T. Wu and C. N. Yang, in “*Properties of Matter Under Unusual Conditions*”, pp. 349-354, Ed. S. Fernbach (Interscience, New York 1969) and “*Some Remarks About Unquantized Non-Abelian Gauge Fields*”, Phys. Rev. **D12** (1975) 3843-3857.
- [84] P. Goddard, J. Nuyts and D. Olive, “*Gauge Theories and Magnetic Charge*”, Nucl. Phys. **B125** (1977) 1-28.
- [85] A. A. Kirillov, “*Elements of the Theory of Representations*”, A Series of Comprehensive Studies in Mathematics **220** (Springer Verlag, Berlin 1976). For some recent applications see e.g. E. Witten, “*Coadjoint Orbits of the Virasoro Group*”, Commun. Math. Phys. **114** (1988) 1-53;
 A. Aleksev, L. Fadeev and S. Shatashvili, “*Quantization of the Symplectic Orbits of the Compact Lie Groups by Means of the Functional Integral*”, J. Geom. Phys. **3** (1989) 391-406;
 A. Aleksev and S. Shatashvili, “*Path Integral Quantization of the Coadjoint Orbits of the Virasoro Group and 2D Gravity*”, Nucl. Phys. **B323** (1989) 719-733;
 O. Alvarez, I. M. Singer and P. Windey, “*Quantum Mechanics and the Geometry of the Weyl Character Formula*”, Nucl. Phys. **B337** (1990) 467-486;
 B. Rai and V. G. J. Rodgers, “*From Coadjoint Orbits to Scale Invariant WZNW Type Actions and 2-D Quantum Gravity Action*”, Nucl. Phys. **B341** (1990) 119-133;
 G. W. Delius, P. van Nieuwenhuizen and V. G. J. Rodgers, “*The Method of Coadjoint Orbits: An Algorithm for the Construction of Invariant Actions*”, Int. J. Mod. Phys. **A5** (1990) 3943-3983.
- [86] L. G. Yaffe, “*Large N Limits as Classical Mechanics*”, Rev. Mod. Phys. **54** (1982) 407-435 (**R**).
- [87] N. M. J. Woodhouse, “*Geometric Quantization*” (Clarendon Press, Oxford 1992).
- [88] J. Wess and B. Zumino, “*Consequences of Anomalous Ward Identities*”, Phys. Lett. **37B** (1971) 95-97.
- [89] A. P. Balachandran, G. Marmo, B.-S. Skagerstam and A. Stern, “*Classical Topology and Quantum States*” (World Scientific Publ. Co. Pte. Ltd., Singapore, 1991).
- [90] A. P. Balachandran, G. Marmo, B.-S. Skagerstam and A. Stern, “*Gauge Symmetries and Fibre Bundles - Applications to Particle Dynamics*”, Lecture Notes in Physics **188** (Springer Verlag, Berlin 1983).
- [91] J. R. Klauder, “*Quantization Is Geometry, After All*”, Ann. Phys. (N.Y.) **188** (1988) 120-141.
- [92] A. P. Balachandran, S. Borchardt and A. Stern, “*Lagrangian and Hamiltonian Descriptions of Yang-Mills Particles*”, Phys. Rev. **D11**(1978) 3247-3256.

- [93] J. R. Klauder, “*Continuous-Representation Theory.II. Generalized Relation Between Quantum and Classical Dynamics.*”, J. Math. Phys. **4**(1963) 1058-1077.
- [94] E. Witten, “*2 + 1 Dimensional Gravity As An Exactly Solvable System*”, Nucl. Phys. **B311** (1988) 46-78.
- [95] B.-S. Skagerstam and A. Stern, “*Topological Quantum Mechanics in 2+1 Dimensions*”, Int. J. Mod. Phys. **A5** (1990) 1575-1595.
- [96] V. Bargmann, L. Michel and V. L. Telegdi, “*Precession of the Polarization of Particles Moving in a Homogeneous Electromagnetic Field*”, Phys. Rev. Lett. **2** (1959) 435-436.
- [97] A. Papapetrou, “*Spinning Test-Particles in General Relativity.I.*”, Proc. R. Soc. London **A209** (1951) 248-258.
- [98] S. K. Wong, “*Field and Particle Equations for the Classical Yang-Mills Field and Particles with Isotopic Spin*”, Nuovo Cimento **65A** (1979) 689-694.
- [99] A. P. Balachandran, P. Salomonson, B.-S. Skagerstam and J.-O. Winnberg, “*Classical Description of a Particle Interacting With a Non-Abelian Gauge Field*”, Phys. Rev. **D15** (1977) 2308-2317.
- [100] M. V. Berry, “*Quantal Phase Factors Accompanying Adiabatic Changes*”, Proc. Roy. Soc. (London) **392** (1984) 45-47;
 B. Simon, “*Holonomy, the Quantum Adiabatic Theorem, and Berry’s Phase*”, Phys. Rev. Lett. **51** (1983) 2167-2170.
 For reviews see e.g. I. J. R. Aitchison, “*Berry Phases, Magnetic Monopoles, and Wess-Zumino Terms or How the Skyrmion Got Its Spin*”, Acta. Phys. Polon, **B18** (1987) 207-235; “*Berry’s Topological Phase in Quantum Mechanics and Quantum Field Theory*”, Physica Scripta **T23** (1988) 12-20;
 M. V. Berry, “*Quantum Adiabatic Anholonomy*” in “*Anomalies, Phases, Defects...*”, Eds. M. Bregola, G. Marmo and G. Morandi (Bibliopolis, Napoli, 1990);
 S. I. Vinitiskii, V. L. Derbov, V. N. Dubovik, B. L. Markovski and Yu P. Stepanovskii, “*Topological Phases in Quantum Mechanics and Polarization Optics*”, Sov. Phys. Usp. **33** (1990) 403-428.
- [101] R.Y. Chiao and Y.-S. Wu, “*Manifestations of Berry’s Topological Phase for the Photon*”, Phys. Rev. Lett. **57** (1986) 933-935 and *ibid.* **59**(1987) 1789.
- [102] R. Jackiw, “*Three-Cocycle in Mathematics and Physics*”, Phys. Rev. Lett. **54** (1985) 159-162; “*Magnetic Sources and 3-Cocycles (Comment)*”, Phys. Lett. **154B** (1985) 303-304;
 B. Grossman, “*A 3-Cocycle in Quantum Mechanics*”, Phys. Lett. **152B** (1985) 93-97; “*The Meaning of the Third Cocycle in the Group Cohomology of Non-Abelian Gauge Theories*”, Phys. Lett. **160B** (1985) 94-100; “*Three-Cocycle in Quantum Mechanics. II*”, Phys. Rev. **D33** (1986) 2922-2929;
 Y. S. Wu and A. Zee, “*Cocycles and Magnetic Monopole*”, Phys. Lett. **152B**

- (1985) 98-102;
 J. Mickelsson, “*Comment on “Three-Cocycle in Mathematics and Physics”*”, Phys. Rev. Lett. **54** (1985) 2379;
 D. Boulware, S. Deser and B. Zumino, “*Absence of 3-Cocycles in the Dirac Monopole Problem*”, Phys. Lett. **153B** (1985) 307-310;
 Bo-Yu Hou, Bo-Yuan Hou and Pei Wang, “*How to Eliminate the Dilemma in 3-Cocycle*”, Ann. Phys. (N.Y.) **171** (1986) 172-185.
- [103] A. Tomita and R. Y. Chiao, “*Observation of Berry’s Topological Phase by Use of an Optical Fiber*”, Phys. Rev. Lett. **57** (1986) 937-940.
- [104] P. F. Kwiat and R. Y. Chiao, “*Observation of Nonclassical Berry’s Phase for the Photon*”, Phys. Rev. Lett. **66** (1991) 588-591.
- [105] B.-S. Skagerstam, “*One the Localization of Single-Photon States*” (in progress).
- [106] R. W. Ziolkowski, “*Propagation of Directed Localized Energy in Maxwells Theory*”, Phys. Rev. **A39** (1989) 2005-2033.
- [107] J. K. Ranka, R. Schrimmer and A. L. Gaeta, “*Observation of Pulse Slitting in Nonlinear Dispersive Media*”, Phys. Rev. Lett. **77** (1996) 3783-3786.
- [108] “*Monopoles in Quantum Field Theory*”, Eds. N. S. Craigie, P. Goddard and W. Nahm (World Scientific, 1982).
- [109] L. Mandel, “*Configuration-Space Photon Number Operators in Quantum Optics*”, Phys. Rev. **144** (1966) 1071-1077 and “*Photon Interference and Correlation Effects Produced by Independent Quantum Sources*”, Phys. Rev. **A28** (1983) 929-943.
- [110] P. Goy, J. M. Raimond, M. Gross and S. Haroche, “*Observation of Cavity-Enhanced Single-Atom Spontaneous Emission*”, Phys. Rev. Lett. **50** (1983) 1903-1906.
- [111] H. J. Kimble, “*Strong Interactions of Single Atoms and Photons in Cavity QED*”, Physica Scripta **T76** (1998) 127-137.
- [112] D. Meschede, H. Walther and G. Müller, “*One-Atom Maser*”, Phys. Rev. Lett. **54** (1985) 551-554.
- [113] H. Walther, “*The Single Atom Maser and the Quantum Electrodynamics in a Cavity*”, Physica Scripta **T23** (1988) 165-169; “*Experiments on Cavity Quantum Electrodynamics*” Phys. Rep. **219** (1992) 263-282; “*Experiments With Single Atoms in Cavities and Traps*” in “*Fundamental Problems in Quantum Theory*”, Eds. D. M. Greenberger and A. Zeilinger, Ann. N.Y. Acad. Sci. **755** (1995) 133-161; “*Single Atom Experiments in Cavities and Traps*”, Proc. Roy. Soc. **A454** (1998) 431-445; “*Quantum Optics of a Single Atom*”, Laser Physics **8** (1998) 1-9 and in Physica Scripta **T76** (1998) 138-146.
- [114] K. An, J. J. Childs, R. R. Dasari, and M. S. Feld, “*Microlaser: A Laser With One Atom in an Optical Resonator*”, Phys. Rev. Lett. **73** (1994) 3375-3378.

- [115] S. Haroche, “*Cavity Quantum Electrodynamics*”, in *Fundamental Systems in Quantum Optics*, p. 767, Eds. J. Dalibard, J. M. Raimond and J. Zinn-Justin, (Elsevier, 1992).
- [116] D. Meschede, “*Radiating Atoms in Confined Space: From Spontaneous Emission to Micromasers*”, Phys. Rep. **211** (1992) 201-250.
- [117] P. Meystre, “*Cavity Quantum Optics and the Quantum Measurement Process*”, “*Progress in Optics XXX*”, pp. 261-355, Ed. E. Wolf, (Elsevier, 1992).
- [118] E. I. Aliskenderov, A. S. Shumovsii and H. Trung Dung, “*Quantum Effects in the Interaction of an Atom With Radiation*”, Phys. Part. Nucl. **24** (1993) 177-199.
- [119] A. N. Oraevskii, “*Spontaneous Emission in a Cavity*”, Physics Uspekhi **37** (1994) 393-405.
- [120] S. M. Barnett, F. Filipowicz, J. Javanainen, P. L. Knight and P. Meystre, “*The Jaynes-Cummings Model and Beyond*”, in “*Frontiers in Quantum Optics*”, pp. 485-520, Eds. E. R. Pike and S. Sarkar, (Adam Bilger, 1986).
- [121] P. W. Milonni and S. Singh, “*Some Recent Developments in the Fundamental Theory of Light*”, in *Advances in Atomic, Molecular, and Optical Physics* **28** (1991) 75-142, Eds. D. Bates and B. Bederson, (Academic Press, 1991).
- [122] E. T. Jaynes and F. W. Cummings, “*Comparison of Quantum and Semiclassical Radiation Theories With Application to the Beam Maser*”, Proc. IEEE **51** (1963) 89-102.
- [123] S. Stenholm, “*Quantum Theory of Electromagnetic Fields Interacting With Atoms and Molecules*”, Phys. Rep. **6C** (1973) 1-122.
- [124] P. Meystre, E. Geneux, A. Quattropani and A. Faist, “*Long-Time Behaviour of a Two-Level System in Interaction With an Electromagnetic Field*”, Nuovo Cimento **25B** (1975) 521-537.
- [125] J. H. Eberly, N. B. Narozhny and J. J. Sanchez-Mondragon, “*Periodic Spontaneous Collapse and Revivals in a Simple Quantum Model*”, Phys. Rev. Lett. **44** (1980) 1323-1326.
- [126] N. B. Narozhny, J. J. Sanchez-Mondragon and J. H. Eberly, “*Coherence Versus Incoherence: Collapse and Revival in a Simple Quantum Model*”, Phys. Rev. **A23** (1981) 236-247.
- [127] P. L. Knight and P. M. Radmore, “*Quantum Revivals of a Two-Level System Driven by Chaotic Radiation*”, Phys. Lett. **90A** (1982) 342-346.
- [128] P. Filipowicz, “*Quantum Revivals in the Jaynes-Cummings Model*”, J. Phys. A: Math. Gen. **19** (1986) 3785-3795.
- [129] N. Nayak, R. K. Bulloch, B. V. Thompson and G. S. Agarwal, “*Quantum Collapse and Revival of Rydberg Atoms in Cavities of Arbitrary Q at Finite Temperature*”, IEEE J. Quantum Electronics **24** (1988) 1331-1337.

- [130] G. Arroyo-Correa and J. J. Sanchez-Mondragon, “*The Jaynes-Cummings Model Thermal Revivals*”, *Quantum Opt.* **2** (1990) 409-421.
- [131] G. Rempe, H. Walther and N. Klein, “*Observation of Quantum Collapse and Revival in a One-Atom Maser*”, *Phys. Rev. Lett.* **58** (1987) 353-356.
- [132] D. Filipowicz, J. Javanainen and P. Meystre, “*The Microscopic Maser*”, *Opt. Commun.* **58** (1986) 327-330.
- [133] D. Filipowicz, J. Javanainen and P. Meystre, “*Theory of a Microscopic Maser*”, *Phys. Rev.* **A34** (1986) 3077-3087.
- [134] G. Rempe and H. Walther, “*Sub-Poissonian Atomic Statistics in a Micromaser*”, *Phys. Rev.* **A42** (1990) 1650-1655.
- [135] H. Paul and Th. Richter, “*Bunching and Antibunching of De-Excited Atoms Leaving a Micromaser*”, *Opt. Commun.* **85** (1991) 508-519.
- [136] G. Rempe, F. Schmidt-Kaler and H. Walther, “*Observation of Sub-Poissonian Photon Statistics in a Micromaser*”, *Phys. Rev. Lett.* **64** (1990) 2783-2786.
- [137] H.-J. Briegel, B.-G. Englert, N. Sterpi and H. Walther, “*One-Atom Maser: Statistics of Detector Clicks*”, *Phys. Rev.* **49** (1994) 2962-2985.
- [138] C. Wagner, A. Schezle and H. Walther, “*Atomic Waiting-Time and Correlation Functions*”, *Opt. Commun.* **107** (1994) 318-326.
- [139] U. Herzog, “*Statistics of Photons and De-Excited Atoms in a Micromaser With Poissonian Pumping*”, *Phys. Rev.* **A50** (1994) 783-786.
- [140] E. Fermi, “*Quantum Theory of Radiation*”, *Rev. Mod. Phys.* **4** (1932) 87-102.
- [141] P. L. Knight and P. W. Milonni, “*The Rabi Frequency in Optical Spectra*”, *Phys. Rep.* **66** (1980) 21-107.
- [142] I. Sh. Averbukh and N. F. Perelman, “*Fractional Regenerations of Wave Packets in the Course of Long-Term Evolution of Highly Excited Quantum Systems*”, *Sov. Phys. JETP* **69** (1989) 464-469.
- [143] I. Sh. Averbukh and N. F. Perelman, “*Fractional Revivals: Universality in the Long-Term Evolution of Quantum Wave Packets Beyond the Correspondence Principle Dynamics*”, *Phys. Lett.* **A139** (1989) 449-453.
- [144] I. Sh. Averbukh and N. F. Perelman, “*The Dynamics of Wave Packets of Highly-Excited States of Atoms and Molecules*”, *Sov. Phys. Usp.* **34** (1991) 572-591.
- [145] M. Fleischhauer and W. Schleich, “*Revivals Made Simple: Poisson Summation Formula as a Key to the Revivals in the Jaynes-Cummings Model*”, *Phys. Rev.* **A47** (1993) 4258-4269.
- [146] M. Brune, E. Hagerly, J. Dreyer, X. Maitre, A. Maali, C. Wunderlich, J. M. Raimond and S. Haroche, “*Observing the Progressive Decoherence of the “Meter” in a Quantum Measurement*”, *Phys. Rev. Lett.* **77** (1996) 4887-4890; *J. M.*

- Raimond, M. Brune and S. Haroche, “*Reversible Decoherence of a Mesoscopic Superposition of Field States*”, Phys. Rev. Lett. **79** (1997) 1964-1967.
- [147] S. Haroche, “*Entanglement, Mesoscopic Superpositions and Decoherence Studies With Atoms and Photons in a Cavity*”, Physica Scripta **T76** (1998) 159-164.
- [148] C. C. Gerry and P. L. Knight, “*Quantum Superpositions and Schrödinger Cat States in Quantum Optics*”, Am. J. Phys. **65** (1997) 964-974.
- [149] J. Gea-Banacloche, “*Collapse and Revival of the State Vector in the Jaynes-Cummings Model: An Example of State Preparation by a Quantum Apparatus*”, Phys. Rev. Lett. **65** (1990) 3385-3388;
 S. J. D. Phoenix and P. L. Knight, “*Comment on “Collapse and Revival of the State Vector in the Jaynes-Cummings Model: An Example of State Preparation by a Quantum Apparatus”*”, Phys. Rev. Lett. **66** (1991) 2833 and “*Establishment of an Entangled Atom-Field State in the Jaynes-Cummings Model*”, Phys. Rev. **A44** (1991) 6023-6029;
 M. Orzag, J. C. Retamal and C. Saavedra, “*Preparation of a Pure Atomic State*”, Phys. Rev. **A45** (1992) 2118-2120;
 C. A. Arancibia-Bulnes, H. Moya-Cessa and J. J. Sánchez-Mondragón, “*Purifying a Thermal Field in a Lossless Micromaser*”, Phys. Rev. **51** (1995) 5032-5034.
- [150] B.-S. Skagerstam, B.Å. Bergsjordet and P.K. Rekdal “*Macroscopic Interferences in Resonant Cavities*” (in progress).
- [151] E. M. Wright and P. Meystre, “*Collapse and Revival in the Micromaser*”, Opt. Lett. **14** (1989) 177-179.
- [152] A. M. Guzman, P. Meystre and E. M. Wright, “*Semiclassical Theory of the Micromaser*”, Phys. Rev. **A40** (1989) 2471-2478.
- [153] U. Herzog, “*Micromasers With Stationary Non-Poissonian Pumping*”, Phys. Rev. **A52** (1995) 602-618.
- [154] M. Nauenberg, “*Quantum Wave Packets on Kepler Orbits*”, Phys. Rev. **40A** (1989) 1133-1136.
- [155] Z. Dačić and C. R. Stroud, Jr., “*Classical and Quantum-Mechanical Dynamics of a Quasiclassical State of the Hydrogen Atom*”, Phys. Rev. **A42** (1990) 6308-6313.
- [156] J. A. Yeazell, M. Mallalieu and C. R. Stroud, Jr., “*Observation of the Collapse and Revival of a Rydberg Electronic Wave Packet*”, Phys. Rev. Lett. **64** (1990) 2007-2010.
- [157] Z. D. Gaeta, M. W. Noel and C. R. Stroud, Jr., “*Excitation of the Classical-Limit State of an Atom*”, Phys. Rev. Lett. **73** (1994) 636-639 .
- [158] M.W. Noel and C. R. Stroud, Jr., “*Excitation of an Atom Electron to a Coherent Superposition of Macroscopically Distinct States*”, Phys. Rev. Lett. **77** (1996) 1913-1916.

- [159] D. M. Meekhof, C. Monroe, B. E. King, W. I. Itano and D. J. Wineland, “*Generation of Nonclassical Motional States of Trapped Atom*”, Phys. Rev. Lett. **76** (1996) 1796-1799.
- [160] C. Monroe, D. M. Meekhof, B. E. King and D. J. Wineland, “A “*Schrödinger Cat*” Superposition State of an Atom ”, Science **272** (1996) 1131-1136 .
- [161] L. P. Pitaevskii, “*Bose-Einstein Condensation in Magnetic Traps. Introduction to the Theory*”, Sov. Phys. Usp. **41** (1998) 569-580;
Yu. Kagan, G. V. Shlyapnikov and J. T. M. Walraven, “*Bose-Einstein Condensation in Trapped Atomic Gases*”, Phys. Rev. Lett. **76** (1996) 2670-2673.
- [162] R. Bluhm, V. A. Kostelecký and J. A. Porter, “*The Evolution and Revival Structure of Localized Quantum Wave Packets*”, Am. J. Phys. **64** (1996) 944-953.
- [163] M. Brune, F. Schmidt-Kaler, A. Maali, J. Dreyer, E. Hagley, J. M. Raimond and S. Haroche, “*Quantum Rabi Oscillation: A Direct Test of Field Quantization in a Cavity*”, Phys. Rev. Lett. **76** (1996) 1800-1803.
- [164] J. Krause, M. Scully and H. Walther, “*Quantum Theory of the Micromaser: Symmetry Breaking Via Off-Diagonal Atomic Injection*”, Phys. Rev. **A34** (1986) 2032.
- [165] L. Lugiato, M. Scully and H. Walther, “*Connection Between Microscopic and Macroscopic Maser Theory*”, Phys. Rev. **A36** (1987) 740-743.
- [166] K. Zaheer and M. S. Zubairy, “*Phase Sensitivity in Atom-field Interaction Via Coherent Superposition*”, Phys. Rev. **A39** (1989) 2000-2004.
- [167] W. Schleich and J. A. Wheeler, “*Oscillations in Photon Distribution of Squeezed States and Interference in Phase Space*”, Nature **326** (1987) 574-577.
- [168] D. F. Walls, “*Squeezed States of Light*”, Nature **306** (1983) 141-146.
- [169] R. Loudon and P. L. Knight, “*Squeezed Light*”, J. Mod. Opt. **34** (1987) 709-759.
- [170] M. S. Kim, F. A. M. de Oliveira and P. L. Knight, “*Properties of Squeezed Number States and Thermal States*”, Phys. Rev. **A40** (1989) 2494-2503.
- [171] V. P. Bykov, “*Basic Properties of Squeezed Light*”, Sov. Phys. Usp. **34** (1991) 910-924.
- [172] C. Fabre, “*Squeezed States of Light*”, Phys. Rep. **219** (1992) 215-225.
- [173] P. K. Rekdal and B.-S. Skagerstam, “*On the Phase Structure of Micromaser Systems*”, Theoretical Physics Seminar in Trondheim, No.4, 1999 (submitted for publication) and “*Theory of the Micromaser Phase Transitions*” (in progress).
- [174] G. S. Agarwal, “*Master Equation Methods in Quantum Optics*”, in *Progress in Optics XI*, pp. 1-75, Ed. E. Wolf, (North Holland, 1973).

- [175] W. H. Louisell, “*Quantum Statistical Properties of Radiation* ” (John Wiley & Sons, 1990);
D. F. Walls and G. J. Milburn, “*Quantum Optics*” (Springer, 1995);
L. Mandel and E. Wolf, “*Quantum Optics and Coherence*” (Cambridge University Press, 1995);
M. O. Scully and M. S. Zubairy, “*Quantum Optics*” (Cambridge University Press, 1996).
- [176] G. Rempe, M. O. Scully and H. Walther, “*The One-Atom Maser and the Generation of Non-Classical Light* ”, *Physica Scripta* **T34** (1991) 5-13.
- [177] L. Mandel, “*Sub-Poissonian Photon Statistics in Resonance Fluorescence* ”, *Opt. Lett.* **4** (1979) 205-207.
- [178] F.-J. Fritz, B. Huppert and W. Willems, “*Stochastische Matrizen* ”, (Springer-Verlag, 1979).
- [179] P. Meystre, G. Rempe and H. Walther, “*Very-Low-Temperature Behavior of a Micromaser* ”, *Opt. Lett.* **13** (1988) 1078-1080.
- [180] P. Filipowicz, J. Javanainen and P. Meystre, “*Quantum and Semiclassical Steady States of a Kicked Cavity Mode* ”, *J. Opt. Soc. Am.* **B3** (1986) 906-910.
- [181] Z. Schuss, “*Theory and Applications of Stochastic Differential Equations*”, (John Wiley and Sons, 1980).
- [182] P. Bogár, J. A. Bergou and M. Hillery, “*Quantum Island States in the Micromaser* ”, *Phys. Rev.* **A50** (1994) 754-762.
- [183] H.-J. Briegel, B.-G. Englert, C. Ginzel and A. Schenzle, “*One-Atom Maser With a Periodic and Noisy Pump: An Application of Damping Bases* ”, *Phys. Rev.* **A39** (1994) 5019-5041.
- [184] A. Mariyan and J. R. Banavar, “*Chaos, Noise, and Synchronization* ”, *Phys. Rev. Lett.* **72** (1994) 1451-1454.
- [185] A. Buchleitner and R. N. Mantegna, “*Quantum Stochastic Resonance in a Micromaser* ”, *Phys. Rev. Lett.* **80** (1998) 3932-3995.
- [186] M. Weidinger, B.T.H. Varcoe, R. Heerlein and H. Walther, “*Trapping States in the Micromaser* ”, *Phys. Rev. Lett.* **82** (1999) 3795-3798.
- [187] O. Benson, G. Raithel and H. Walther, “*Quantum Jumps of the Micromaser Field: Dynamic Behavior Close to Phase Transition Points* ”, *Phys. Rev. Lett.* **72** (1994) 3506-3509; “*Atomic Interferometry with the Micromaser* ”, *Phys. Rev. Lett.* **75** (1995) 3446-3449 and “*Dynamics of the Micromaser Field* ” in “*Electron Theory and Quantum Electrodynamics; 100 Years Later* ”, pp. 93-110, Ed. J. P. Dowling (Plenum Press, 1997).